Radial astrocytes in the developing retinotectal system promote escape behavior through the detection and modulation of neuronal activity

Nicholas Benfey

Integrated Program in Neuroscience

Department of Neurology and Neurosurgery

McGill University, Montréal

June 2022

A thesis submitted to McGill University in partial fulfillment of the requirements of the degree of Ph.D. Neuroscience-Thesis in the Integrated Program in Neuroscience

Table of Contents

Abstract

Astrocytes exist in close apposition to synapses throughout the vertebrate brain where they both sense and respond to neuronal activity and make important contributions to the development, function, and plasticity of neural circuits. With powerful genetic tools to detect and control the activity of astrocytes *in vivo* now becoming widely available, important new mechanistic insights linking astrocytes to various behaviors continue to accumulate. Using the *Xenopus laevis* retinotectal circuit, a well-established model system for studying the role of neuronal activity in neural circuit development and plasticity *in vivo*, we have demonstrated that radial astrocytes, the predominant glial cell in the optic tectum, are highly responsive to both visually evoked neuronal activity and the neuromodulator norepinephrine. We have shown that radial astrocytes exhibit robust calcium increases several seconds following visual stimulation which depend on the activation of both glutamate transporters and sodium-calcium exchangers and that surprisingly, glial glutamate receptors have no clear role in mediating these visually evoked calcium responses in the glia. Norepinephrine also produces large increases in the activation of the radial astrocytes in the circuit which appear to precede powerful decreases in tectal neuron activity. Similar to what has been shown for astroglia in other vertebrate systems, the activation of radial astrocytes in the optic tectum by norepinephrine involves the alpha-1 adrenergic receptor. We have shown that the modulation of the tectum by norepinephrine is not uniform across all neurons in the circuit but rather involves preferential suppression of tectal neurons which are responsive to moving objects of various sizes, while preserving, or in some cases enhancing, the activity of tectal neurons which are strongly selective for large, looming stimuli. Using a targeted chemogenetic approach to selectively activate radial astrocytes in the optic tectum we have

shown that their activation is sufficient to recapitulate the effects we see in our experiments of norepinephrine on circuit function. Consistent with the effects we observed of norepinephrine on the response profile of neurons in the optic tectum, the targeted activation of radial astrocytes significantly enhances the detection of looming stimuli and boosts the probability of escape behavior in a free-swimming behavioral test. Using pharmacology along with visual stimulation and acute application of norepinephrine to the optic tectum *in vivo* we show that ATP, likely released by radial astrocytes, plays an important role in the neuromodulatory effects of norepinephrine we have observed. Taken together, our data show that radial astrocytes are functionally integrated within the retinotectal circuit where they respond to presynaptic release of glutamate from stimulated retinal ganglion cell axons as well as the vigilance state of the animal through release of norepinephrine, suggesting they play an important role as a complex integrator capable of switching the state of the tectum to improve the encoding of relevant behavioral stimuli.

Résumé

Les astrocytes sont apposées étroitement aux synapses dans tout le cerveau des vertébrés dans lequel ils détectent et répondent à l'activité neuronale et apportent d'importantes contributions au développement, à la fonction et à la plasticité des circuits neuronaux. Avec les puissants outils génétiques fréquemment utilisés aujourd'hui qui permettent la détection et le contrôle de l'activité in vivo des astrocytes, de nouvelles connaissances importantes sur le mécanisme liant les astrocytes à divers comportements continuent de s'accumuler. En utilisant le circuit rétinotectal Xenopus laevis, un système modèle bien réputé pour étudier le rôle de l'activité neuronale dans le développement du circuit neuronal et la plasticité in vivo, nous avons démontré que les astrocytes radiaux, cellules gliale les plus communes dans le tectum optique, sont très sensibles à la fois à l'activité neuronale stimulé visuellement et aux neuromodulateurs de la noradrénaline. Nous avons pu démontrer que plusieurs secondes après une stimulation visuelle, il y a une augmentation de calcium dans les astrocytes radiaux et que celle-ci dépend de l'activité des transporteurs de glutamate et des échangeurs sodium-calcium et que surprenament, les récepteurs gliaux du glutamate n'ont pas de rôle clair dans la médiation de ces réponses calciques stimulées visuellement dans les cellules gliales. La noradrénaline produit également de fortes augmentations de l'activation des astrocytes radiaux dans le circuit qui semblent précéder de fortes diminutions de l'activité des neurones tectaux. Semblable à ce qui a été montré pour les cellules astrogliales dans d'autres systèmes de vertébrés, l'activation des astrocytes radiaux dans le tectum optique par la noradrénaline met en jeu le récepteur adrénergique alpha-1. Nous avons montré que la modulation du tectum par la noradrénaline n'est pas uniforme sur tous les neurones du circuit, mais implique plutôt la suppression préférentielle des neurones tectaux qui réagissent

aux objets en mouvement de différentes tailles, tout en préservant, ou dans certains cas en améliorant, l'activité de neurones tectaux qui sont fortement sélectifs pour les stimuli loom. En utilisant une approche chimiogénétique ciblée pour activer sélectivement les astrocytes radiaux dans le tectum optique, nous avons montré que leur activation est suffisante pour reproduire les effets que nous voyons dans nos expériences de noradrénaline sur la fonction du circuit. Conformément aux effets que nous avons observés de la noradrénaline sur le profil de réponse des neurones dans le tectum optique, l'activation ciblée des astrocytes radiaux améliore considérablement la détection des stimuli loom et augmente la probabilité de comportement de fuite dans un test comportemental de nage libre. En utilisant la pharmacologie avec la stimulation visuelle et l'application aiguë de noradrénaline dans le tectum optique in vivo, nous montrons que l'ATP, probablement libérée par les astrocytes radiaux, joue un rôle important dans les effets neuromodulateurs de la noradrénaline que nous avons observés. Dans son ensemble, nos données montrent que les astrocytes radiaux sont fonctionnellement intégrés dans le circuit rétinotectal où ils répondent à la libération présynaptique de glutamate à partir des axones des cellules ganglionnaires rétiniennes stimulées, ainsi qu'à l'état de vigilance de l'animal par la libération de noradrénaline, suggérant qu'ils jouent un rôle important d’intégrateur complexe capable de changer l'état du tectum pour améliorer l'encodage des stimuli pertinents au comportement de l'animal.

Acknowledgements

I would like to begin by extending my sincerest gratitude to my supervisor Dr. Edward S. Ruthazer for his genuine kindness, unwavering support, and thoughtful attention during my time at McGill. Ed has been an outstanding mentor who's truly gone above and beyond what's expected from a supervisor to help me throughout this entire journey. I very much look forward to finding exciting ways to continue our collaborations into the future. Thank you, Ed for permitting me to really make this project my own and for helping me to traverse efficiently through the all-too-often murky territory of neurodevelopment.

To all the members of the Ruthazer lab, both past and present, a sincere thank you to each and every one of you! I know for a fact that I would not have made it to this point without your kind support and encouragement. A very special thanks goes to Anne Schohl, without your expertise none of the *in vivo* imaging I've been doing would have ever been possible! Another special thank you to Phil Kesner for so warmly welcoming me into community at the Neuro – I owe many of the meaningful friendships I've made here to you.

I would like to kindly thank the members of my advisory committee, Drs. Richard Robitaille and Keith Murai for their years of thoughtful insights into my project which helped me avoid many pitfalls in the field and greatly enhance the quality of my research. I would also like to thank my rotation supervisors Drs. Ed Ruthazer, David Stellwagen and Wayne Sossin for such great introductions into the world of neuroscience. You all made jumping into this new world much easier and enjoyable for me.

I would like to extend my sincere thanks to Drs. Anne McKinney and Matthew Holt for kindly accepting to offer their time to examine this thesis.

I would like to offer my gratitude to Dr. Tyler Dunn for all the years of wonderful friendship and mentorship.

A kind thank you to Drs. Sylvain Baillet and Blake Richards and their lab members, particularly Martin Cousineau, for helping me understand and implement domains of research once impenetrable to me. Your insights greatly enhanced the quality of my analysis methods.

The greatest of thank yous to Drs. Dion Durnford, Bryan Crawford, David MaGee, and Mike Duffy. You are all the reason why I decided to pursue a career in science. You all went above and beyond to offer me such kind support and mentorship from the very outset of my journey into academics.

I was very fortunate to be supported by federal Canadian Graduate Scholarship funds from both CIHR (CGS-M) and NSERC (PGS-D), as well as funds from the McGill Faculty of Medicine Studentships.

And I leave the biggest thank you of all to my friends and family. You never doubted me and always encouraged me even when I doubted myself the most. You helped me to see my potential and to feel safe and excited exploring it. Without you none of this would have been possible. To Cathy and Tillmann Benfey, thank you for raising me to love and see all of the beauty in the

natural world and always encouraging my – often intense - enthusiasm for figuring out how it all works. Thank you to Anton Benfey for being the best brother I could ask for and all the thoughtful hours helping me with your expertise in Python. You are a profound source of inspiration for me, and I have learned a lot from your dedication and perseverance. And finally a heartfelt thank you to Audrey Desaulniers, your loving support and astounding creativity have been instrumental in my successful. I'm very excited to continue our collaborations into the future.

List Of Abbreviations

5HT2B	5-hydroxytryptamine receptor 2B
A1	adenosine A1 receptor
ADHD	attention-Deficit/hyperactivity disorder
ADO	adenosine
AMPA	α- amino-3-hydroxy-5-methyl-4-isoxazolepropionic acid
AMPAR	α- amino-3-hydroxy-5-methyl-4-isoxazolepropionic acid receptor
ANOVA	analysis of variance
aRCA3	amphibian regulator of complement activation 3
ATP	adenosine 5'-triphosphate
C1q	complement component 1q
C3	complement component 3
Ca^{2+}	calcium
CaCl2	calcium chloride
CB1R	cannabinoid receptor type 1
CBX	carbenoxolone
CC-BY	creative commons attribution license
cGMP	cyclic guanosine monophosphate
CHPG	2-chloro-5-hydroxyphenylglycine
CNS	central nervous system
CPCCOEt	7-(hydroxyimino)cyclopropa-chromen-1a-carboxylate ethyl ester
CPP	D-4-[(2*E*)-3-phosphono-2-propenyl]-2-piperazinecarboxylic acid

CSV	comma separated values
CX	connexin
CX3CR1	CX3C chemokine receptor 1
DHPG	(S)-3,5-dihydroxyphenylglycine
DNQX	6,7-dinitroquinoxaline-2,3-dione
DOI	digital object identifier
DPCPX	8-cyclopentyl-1,3-dipropylxanthine
EAAT	excitatory amino acid transporter
eGFP	enhanced green fluorescent protein
GABA	gamma-aminobutyric acid
GFAP	glial fibrillary acidic protein
GLAST	glutamate aspartate transporter
GLT-1	glutamate transporter 1
Glu	glutamate
gluR	glutamate receptor
GUI	graphical user interface
HEPES	4-(2-hydroxyethyl)-1-piperazineethanesulfonic acid
IP3R2	inositol 1,4,5-triphosphate receptor 2
KB-R7943	2-[2-[4-(4-nitrobenzyloxy)phenyl]ethyl]isothiourea
KCl	potassium chloride
LGN	lateral geniculate nucleus
L-NMMA	N^G-methyl-L-arginine acetate
LSD	least significant difference

LY341495	(2S)-2-amino-2[(1S,2S)-2-carboxycycloprop-1-yl]-3-(xanth-9-yl)propanoic acid
mAChR	muscarinic acetylcholine receptor
MBSH	modified barth's solution with HEPES
ME	monocular enucleation
MEGF10	multiple EGF-like domains 10
mEPSC	miniature excitatory postsynaptic current
MERTK	proto-oncogene tyrosine-protein kinase MER
MgCL2	magnesium chloride
mGluR	metabotropic glutamate receptor
MPEP	2-methyl-6-(phenylethynyl)-pyridine
mPTP	mitochondrial permeability transition pore
mRNA	messenger ribonucleic acid
MS-222	tricaine mesylate
NA	numerical aperture
Na^+	sodium
NaCl	sodium chloride
NaV	voltage-gated sodium channel
NCX	sodium-calcium exchanger
NE	norepinephrine
Nlg1	neuroligin 1
NMDAR	n-methyl-d-aspartate receptor
NO	nitric oxide
NPY	neuropeptide Y

Nrx1α	neurexin-1-alpha
P2	type 2 purinergic receptor
PC1	principal component 1
PCA	principal component analysis
PKG	cyclic guanosine monophosphate-dependent protein kinase G
PV	parvalbumin
RGC	retinal ganglion cell
ROI	region of interest
SEM	standard error of the mean
SIN	superficial interneuron
SNARE	soluble n-ethylmaleimide sensitive factor attachment protein receptor
SOM	somatostatin
TFB-TBOA	(3S)-3-[[3-[[4-(Trifluoromethyl)benzoyl]amino]phenyl]methoxy]-L-aspartic acid
TRPV1	transient receptor potential channel vanilloid 1
TTX	tetrodotoxin
TWEAK	tumor necrosis factor ligand superfamily member 12
V1	primary visual cortex

List Of Figures

Chapter 1

Chapter 2

Contributions To Original Knowledge

This thesis makes several contributions to original knowledge. The first major contribution is the demonstration that radial astrocytes in the developing optic tectum respond to visual stimulation through a mechanism independent of glutamate receptor activation. Instead, the mechanism mediating visually-evoked calcium events in radial astrocytes was found to involve the presynaptic release of glutamate from retinal ganglion cell axons, the reuptake of glutamate through glial excitatory amino acid transporters, and importantly, the reversal of sodium-calcium exchangers. An article on this was published in the journal *Cell Reports* in 2021. The second major contribution to original knowledge involves the demonstration that both norepinephrine and chemogenetic activation of radial astrocytes in the optic tectum induces a state change in the visual system which biases the tectum towards the detection of looming stimuli. This state change mediated by radial astrocytes involves the activation of alpha-1-adrenergic receptors, the opening of gap junctions/hemichannels, the release of ATP, and the activation of P2 receptors. This state change also greatly enhances the rate of looming stimulus detection by free swimming animals suggesting that this mechanism is likely to impart an important survival benefit to the animals during early development when they are highly vulnerable to predation.

Author Contributions For Chapter 1

The overall theme and scope of the material presented in this chapter was conceived of by Nicholas Benfey under the supervision of Dr. Edward Ruthazer. Nicholas Benfey carried out an exhaustive search of the existing literature on glial cells in the vertebrate visual system and sorted and assembled this literature into a comprehensive review on the topic. Nicholas Benfey wrote all of the material presented in this chapter. David Foubert, a master's student in the Ruthazer lab, helped to create and assemble the figures used in this chapter. Edward Ruthazer provided meaningful feedback and kindly edited all of the material in this chapter.

Preface To Chapter 1: Introduction And Literature Review Of Glial Cells In The Vertebrate Visual System

Over the last several decades we've witnessed a rapid advance in our understanding of how glial cells functionally integrate into neural circuits throughout the brain. We now know from research in many animal species that glial cells, particularly astrocytes, are important contributors to a host of important neurological functions and behaviors. Throughout the broader history of neuroscience, the vertebrate visual system has been a powerful model to understand how sensory experience influences neural circuit development and function with many of the most significant insights in neuroscience stemming from experiments carried out in these systems. However, despite numerous examples that astrocytes are crucially important for visual system development, function, and plasticity, there remains no comprehensive assemblage of what is known about astroglia across all stages of the vertebrate visual system. In order to draw attention

to this important field of study, I aimed to compile the first comprehensive overview of what is known about the functioning of glial cells throughout each major region of the vertebrate visual system. I also aimed to highlight salient gaps in our current knowledge in order to help researchers in the field develop new hypotheses to advance future research directions.

Rationale And Objectives For Thesis Research

Throughout the central nervous systems of a wide variety of animals, glial cells have been shown to directly mediate crucial steps in brain development from the assembly of neural circuits, to the gating of critical periods of plasticity (Allen and Lyons, 2018; Ribot et al., 2021). Astrocytes, the dominant glial cell found in the animal brain, have been shown to monitor local circuit activity and arousal state through a number of distinct intracellular signaling pathways, ultimately influencing behavior in turn through the modulation of neural circuit function (Nagai et al., 2021). Despites multiple signaling pathways having been shown to mediate neuron-glia communication in culture and systems *in vivo*, we are only starting to discover to what extent, and through what mechanisms, the glial cells in midbrain circuits sense and respond to neural activity during early development in intact animals. The extent to which glial cells influence the function of circuits such as the optic tectum, a structure homologous to the mammalian superior colliculus, remain largely unexplored. Additionally, despite several compelling examples that glial cells in the visual system can detect visually-driven neuronal activity, very little remains known about how their activation alters the encoding of visual information throughout the brain.

Previous work in the Ruthazer lab has implicated radial astrocytes, the principal glial cell in the developing brain of the frog *Xenopus laevis*, as being important contributors to the function and maturation of neural circuits in the optic tectum (Tremblay et al., 2009; Sild et al., 2016). In the developing brain of *X. laevis*, radial astrocytes act as both neural progenitor cells and more mature astrocytes, retaining an elongated radial morphology throughout the life of the animal. These cells are highly structurally dynamic during early wiring of the retinotectal projection and

actively contact retinotectal synapses (Tremblay et al., 2009). Little is known however about the mechanisms mediating their communication with tectal neurons, their functional activity patterns during visual stimulation, and whether their activation alters neural circuit function and visual processing in the optic tectum.

Therefore, my main objectives of this Ph.D. thesis research were threefold. My first objective was to implement robust methods for using genetically-encoded calcium indicators to monitor the functional activity of both radial astrocytes and tectal neurons during visual stimulation in intact living animals. An extension of this objective was to find reliable methods for the quantification and analysis of this functional imaging data. My second objective was to use these calcium imaging methods, along with pharmacological manipulations of the optic tectum, to dissect out the cellular signaling pathways mediating visually-evoked calcium events in radial astrocytes in the optic tectum. My third objective was to implement a method to selectively control the activity of radial astrocytes in the optic tectum and investigate how this glial activation influences the functional activity of neurons in the tectum. An extension of this objective was to investigate what effect, if any, the activation of radial astrocytes in the optic tectum had on the behavior of freely swimming animals.

Chapter 1: Introduction And Literature Review Of Glial Cells In The Vertebrate Visual System

General introduction

Visual experience is mediated through a relay of finely-tuned neural circuits extending from the retina, to retinorecipient nuclei in the midbrain and thalamus, to the cortex which work together to translate light information entering our eyes into a complex and dynamic spatio-temporal representation of the world. The vertebrate visual system has long been used as a highly tractable system in which to study how sensory experience influences the development, function, and plasticity of neurons and neural circuits in the brain. While the experience dependent developmental refinement and mature function of neurons in each major stage of the vertebrate visual system have been extensively characterized, the contributions of the glial cells populating each region are comparatively understudied despite important findings demonstrating that they mediate crucial processes related to the development, function, and plasticity of the system (Allen and Lyons, 2018; Nagai et al., 2021).

Over the past several decades, the development of novel tools and techniques has begun to allow for the precise monitoring and targeted manipulation of glial cells throughout the central nervous system and has led to a series of rapid advances in our understanding of the significant ways in which glia actively contribute to brain development and function, including in multiple areas of the visual system. As a result, glial cells, such as astrocytes and microglia, are now becoming widely accepted as critical regulators of a multitude of behaviourally relevant neural processes.

Throughout all areas of the developing and adult brain, including the visual system, glial cells are found in close apposition to neurons where they contact synapses, influencing their formation, maturation, and function (Allen and Lyons, 2018; Nagai et al., 2021). Throughout this introduction and literature review, I will discuss what is known (and unknown) about the roles of glial cells in shaping the development, function, and plasticity of the vertebrate visual system, focusing on mechanisms mediating neuron-glia communication and their functional roles in each stage of the system from the retina to the primary visual cortex.

This will lead into a discussion of the significant gaps which remain in our understanding of the activity dependent function of glial cells in the visual system, particularly in retinorecipent areas such as the optic tectum. This discussion will prepare the stage for the presentation of the following two manuscripts. These manuscripts outline the mechanisms mediating the transmission of visual information from retinotectal neurons to radial astrocytes in the optic tectum as well as how the activation of radial astrocytes in the tectum shapes local circuit activity and function. They will also show how large increases in the calcium activity of radial astrocytes in the tectum has important effects on the behavior of developing *Xenopus laevis* tadpoles. Taken together, these two manuscripts, and the subsequent general discussion, provide a relatively comprehensive characterization of how radial astrocytes are functionally integrated into the retinotectal circuit, significantly advancing our understanding of how astroglia shape the function of neural circuits during their earliest stages of development.

Introduction to the vertebrate visual system

In the back of each eye, specialized photoreceptive retinal tissue senses and responds to distinct features of light energy relaying detailed information about wavelength, intensity, spatial location, and motion to the brain (Figure 1A). The structure and function of the retina is highly conserved between vertebrate species with the outer layer mediating the majority of photoreception through activation of rod and cone photoreceptor cells and the inner layer predominantly processing and relaying that visual information to the brain through selective activation of bipolar and retinal ganglion cells (RGCs)(Masland, 2012). A parallel light-sensing pathway responsible for entrainment of circadian rhythms and other non-image-forming functions is mediated by melanopsin phototransduction in a class of intrinsically photosensitive RGCs (Hattar et al., 2002; Berson et al., 2002; Lazzerini Ospri et al., 2017). Müller glia are the dominant glial cell in the retina having an elongated radial morphology that spans both the inner and outer layers, extending out numerous filopodial processes into synaptic layers which form contacts with retinal synapses (Wang et al., 2017)(Figure 1B).

The retina connects to the brain through the RGC axons which bundle together within the optic nerve (Figure 1A). In fish and frogs which develop externally and whose behaviors rely on vision throughout early development, the vast majority of RGC axons cross the optic chiasm and project contralaterally, innervating a constellation of midbrain pretectal nuclei and most prominently the optic tectum - a retinotopically organized structure homologous to the mammalian superior colliculus - where they form synapses upon tectal neurons (Baier and Wullimann, 2021). The primary function of the optic tectum or superior colliculus involves

integrating sensory information and correctly orienting an animal's behavioral responses in space (Ito and Feldheim, 2018; Isa et al., 2021). Similar to in the retina, the predominant glial cells in the optic tectum of fish and frogs, radial astrocytes (also referred to as radial glia), have an elongated radial morphology which spans from the ventricular to the pial surfaces of the brain, extending highly dynamic filopodia that contact synapses in the neuropil layer (Tremblay et al., 2009)(Figure 1C).

In the mammalian brain, retinal ganglion cell axons innervate specific laminae within both the superior colliculus and the lateral geniculate nuclei (LGN) of the thalamus, along with the intergeniculate leaflet and pulvinar nucleus, collectively referred to as the visual thalamus, a set of layered relay stations for transmitting visual information to the primary visual cortex that also receives input from a number of other brain areas including both the superior colliculus and layer 6 of the primary visual cortex (Hooks and Chen, 2020). While the LGN is known to communicate eye-specific information related to color and spatio-temporal features of visual information, a complete understanding of the function of the LGN is still being elucidated, with experiments suggesting it plays more nuanced roles than just acting as a simple linear filter (Kerschensteiner and Guido, 2017). The LGN is populated by both astrocytes and microglia, with astrocytes exhibiting mature morphological characteristics by the time of eye opening (Somaiya et al., 2021)(Figure 1D).

Thalamic relay neurons in the LGN receiving input from the retina project their axons as a large fiber tract, called the optic radiation, into the primary visual cortex (V1), as well as some higher cortical areas depending on the species, where they largely innervate layer 4 with a smaller

subset innervating layers 2/3 and 6 while preserving retinotopic spatial organization (Espinosa and Stryker, 2012)(Figure 1A). The topographic organization of the primary visual cortex in large mammals, including most carnivores and primates, is highly structured across its surface with neurons participating in hypercolumns consisting of multiplexed maps of spatial frequency, orientation and ocular dominance where groups of neurons exhibit eye preference and selective responsiveness to diverse stimulus features, for each region of the visual field (Espinosa and Stryker, 2012). The primary visual cortex is largely believed to act as a preliminary feature detector used to create a saliency map of objects in the visual field (Zhang et al., 2012). The layers of the primary visual cortex are extensively populated by both astrocytes and microglia (Parnavelas et al., 1983)(Figure 1E).

As I will discuss in detail in the following sections, in the eye, glia have been found to both respond to and modulate spontaneous retinal waves which are known to be instructive in the refinement of visual connections throughout the developing brain, and contribute to the proper transduction of signals through the retina as well as to direct its repair following injury. In retinorecipient areas such as the optic tectum (superior colliculus) and the LGN, glia respond to sensory stimulation and influence synapse maturation and the segregation of retinal inputs through activity-dependent mechanisms. In the primary visual cortex glia are responsive to both visually-evoked neuronal activity and the release of neuromodulators. They regulate the excitability of cortical neurons and gate the duration of critical periods for plasticity. With defined mechanisms for glial functions at each stage of the visual system starting to be revealed, the potential for synthesizing a preliminary model integrating how glia contribute to visual experience across the visual system is now an emerging possibility. I will begin by highlighting

what is currently known about the activity-dependent functions of glia in each major segment of the visual system and then follow with a discussion of the major outstanding questions remaining in the field and experiments that would help to bridge these important gaps before finishing with a predictive summary model for how glia contribute to the development and function of the visual system.

The adult retina - Müller glia

Müller glia constitute one of the most highly studied glial cell types given the relative ease of access to intact retinal tissue for experimental manipulation. It has long been appreciated that they are responsive to visually evoked activity and mediate diverse roles in retinal development, function, and both degeneration and regeneration.

Early work demonstrated that in the retina the glutamate transporter GLAST (EAAT1) is expressed exclusively by Müller glia and required for proper signal transduction between photoreceptors and bipolar cells, indicating that they actively contribute to the processing of visual information in the circuit (Harada et al., 1998). Shortly thereafter, experiments in isolated retinal preparations demonstrated that Müller glia respond to mechanical stimulation with increases in calcium which propagated between retinal Müller glia by means of the release of extracellular ATP, hinting that glia may also be an active signaling partner capable of influencing retinal function through the release of such compounds during periods of stimulation (Newman, 2001). Later, and again in isolated retinal preparations, Müller glia were found to exhibit spontaneous calcium transients while under constant illumination that could be increased

by either presenting a flickering light stimulus or through antidromic stimulation of RGCs and which are blocked by the purinergic antagonist suramin or the voltage-gated sodium channel blocker tetrodotoxin (TTX), demonstrating that their calcium activity is subject to regulation by sensory-driven neuronal activity and hinting that it may occur physiologically *in vivo* (Newman, 2005). Investigation into the mechanism by which light activates Müller glia found that ectonuclease-mediated breakdown of ATP to adenosine increases their calcium responses, which could be prevented by apyrase, an enzyme that limits availability of ATP for adenosine generation. Conversely, blocking mGluRs, NMDARs, or mAChRs, the main mediators of visually-driven activity in retinal neurons, had no effect on calcium activity in Müller glia (Newman, 2005). Consistent with neuronal activity driving the calcium increases in Müller glia, transients were observed to start in their fine processes in the synaptic layers before traveling to their endfeet at the inner surface of the retina (Newman, 2005). Using novel bioluminescent assays that allowed for the calcium activity of Müller glia to be observed under conditions of darkness, investigators found that Müller glia exhibited temporally-coordinated patterns of spontaneous calcium activity that repeated over time in small networks of glial cells and that this could be blocked by TTX suggesting that spontaneous neural activity drives the activation of Müller glia in structured ways (Agulhon et al., 2007).

The first demonstration that calcium transients occur in Müller glia under physiological conditions *in vivo* also observed that they were mediated through the propagation of extracellular ATP, as treatment with apyrase reduced their occurrence by 95%, confirming that the isolated retina was an informative preparation for investigating the mechanisms mediating the activity of Müller glia (Kurth-Nelson et al., 2009). A luciferin assay was then used to quantitatively monitor

the release of ATP during spontaneous glial calcium waves in the rat retina, and found that ATP release occurred during the increases in calcium activity in Müller glia and that the amount and frequency of its release increased across development (Kurth-Nelson et al., 2009). Importantly, adenosine has been shown to hyperpolarize retinal ganglion cells suggesting that the activity-dependent release of ATP from retinal glia may modulate retinal function under physiological conditions (Clark et al., 2009).

Igniting much interest at the time, the spontaneous calcium waves in Müller glia were observed to co-occur with changes in the diameter of retinal arterioles suggesting the activity of Müller glia may control neurovascular coupling in the retina (Kurth-Nelson et al., 2009). There has been much discussion surrounding the role of astrocytic calcium in mediating blood vessel dilation throughout various areas of the brain (Bazargani and Attwell, 2016), and later experiments in the retina helped to address aspects of this controversy by showing that retinal capillaries, but not arterioles, which were adjacent to glial endfeet, dilate following visually evoked calcium responses and that knockout of IP3R2 (the major mediator of calcium release from internal stores in most glia) prevents light evoked dilation of capillaries but not arterioles (Biesecker et al., 2016).

While a mechanistic understanding of the functions mediated by calcium transients in glia remains an active focus in neuroscience research generally, particularly the activity- and calcium-dependent release of gliotransmitters from various glia throughout the brain, functional manipulations in Müller glial cells have contributed some important insights. The targeted expression of botulinum toxin, a protease that cleaves and inactivates the SNARE proteins

necessary for normal calcium-mediated vesicular release, in Müller glia demonstrated that calcium causes the vesicular release of glutamate, but not ATP from Müller glia (Slezak et al., 2012). Although no differences in retinal structure or visual processing were observed when vesicular release of glutamate from Müller glia was prevented, the authors did suggest that their lack of ability to target all Müller glia with botulinum toxin in their experimental preparations may have prevented any such alterations (Slezak et al., 2012), a suggestion consistent with recent observations that only sparse activation of radial astrocytes in the hindbrain of zebrafish is required to fully mediate behavioral effects (Mu et al., 2019).

Structurally, Müller glia span across the entire width of the retina and there have been several interesting observations suggesting that since most cells and structures in the retina cause light scattering, Müller glia may act as biological optic fibers that can help to guide light to the photoreceptor layer in the retina of adult guinea pigs (Franze et al., 2007). Furthermore, additional experiments showed that Müller glia are capable of acting as wavelength-specific guides for light in the isolated retina, channeling red-green spectrum light to cone photoreceptors while allowing blue-purple spectrum light to bleed into areas populated by rod photoreceptors (Labin et al., 2014). Whether this plays a physiological role in the intact retina *in vivo* has yet to be demonstrated.

In the zebrafish retina Müller glia have become an important subject of study following observations that they are capable of acting as late stage progenitor cells that can functionally repopulate damaged retina in adult fish (Bernardos et al., 2007), something that is not normally possible in the adult mammalian retina despite a high degree of similarity in structure and

function (Karl et al., 2008). This work has started to identify promising avenues for restoring function in the damaged mammalian retina as the transcription factor Ascl1 has been shown to be upregulated in Müller glia in the retina of zebrafish following injury and to mediate the regeneration of retinal tissue; while importantly, no such expression of Ascl1 occurs in mammals following retinal damage (Karl et al., 2008). Encouragingly, it has been shown that when Ascl1 is overexpressed in Müller glia in mice, along with an inhibitor of histone deacetylase, retinal regeneration is possible following injury suggesting a potential avenue to induce retinal regeneration in mammals (Karl et al., 2008).

The interactions between microglia, the resident immune cell in the central nervous system, and Müller glia also appear to mediate important roles in retinal development and repair as the presence of microglia is required for the regenerative potential of Müller glia in the adult zebrafish retina (Conedera et al., 2019). Additionally, endocannabinoids, known to modulate glia throughout the CNS, have also been suggested to play a role in mediating the proliferative function of Müller glia as pharmacological activation of Müller glia endocannabinoid receptors promotes the formation of progenitor cells without having an observable impact on microglial responses in the damaged retina (Campbell et al., 2021).

The developing retina - Müller glia

Much of what is known about the function of Müller glia comes from experiments done in the adult retina; however, more recent work has started to explore their function throughout

development as well, offering important mechanistic insights that complement work done in the mature system.

In the developing mouse retina, Müller glia have been shown to exhibit dynamic calcium waves in response to both cholinergic and glutamatergic retinal waves mediated by mAChRs or AMPARs respectively (Rosa et al., 2015). Interestingly, mAChRs were not observed to regulate the calcium activity of Müller glia in the adult retina (Newman, 2005), suggesting that the mechanisms underlying the responsiveness of Müller glia to neural activity are plastic throughout development. As the retina continues to mature, Müller glia increase their expression of excitatory amino acid transporters leading to a continual decrease in the spillover of synaptic glutamate which results in a corresponding decrease in the activation of glial AMPARs (Rosa et al., 2015). Müller glia in the retina of larval zebrafish have also been shown to exhibit spontaneous electrical and calcium waves mediated by the activation of glial AMPARs, beginning in their fine processes in the synaptic layer before spreading vertically to their cell body and endfoot and then horizontally between other glial cells - likely through the release of ATP - while glial excitatory amino acid transporters were observed to tightly regulate the occurrence and propagation of neuronal retinal waves, suggesting that the activity of Müller glia may play a permissive role in the generation of the spontaneous retinal waves that are known to direct the topographic refinement of RGC axons into retinal recipient areas of the brain (Zhang et al., 2019).

Structurally Müller glia are complex cells with numerous fine filopodial processes extending into the surrounding neural retina which are highly motile throughout development (Tworig et al., 2021). Whether calcium activity in glial cells regulates the structural motility of their processes had remained an open question until recently. Here it was shown that calcium activity is compartmentalized in Müller glial stalks (the elongated radial portion of the cell spanning the width of the retina) and processes, with M1 mAChRs mediating calcium events in Müller glial stalks but not in processes (Tworig et al., 2021). Curiously, acute manipulation of retinal wave activity had no effect on lateral process motility in Müller glia, and chronic manipulation had no impact on the distribution, complexity, or length of glial lateral processes, together suggesting a functional decoupling between structural motility and calcium signaling as wave-associated compartmentalized calcium activity was not required for, nor did it regulate glial process motility (Tworig et al., 2021).

The retina - Microglia

In the embryonic mouse retina, microglia have been found to primarily associate with newly born neurons and the depletion of retinal microglia leads to an increase in the density of retinal ganglion cells without altering the proliferation of progenitor cells or the birth of new RGCs suggesting that microglia actively phagocytose RGCs as a normal part of development in the retina (Anderson et al., 2019). These effects of microglia on prenatal development of neurons have been shown to be mediated through complement proteins, known to mediate neuronal phagocytosis and pruning by microglia in other brain areas (Anderson et al., 2019; Lim and Ruthazer, 2021). In the developing retina, knockout of the cytokine receptor CX3CR1 in

microglia has been shown to lead to retinal dysfunction shortly after eye opening and the eventual loss of cone type photoreceptors expressing its signaling partner fractalkine during postnatal development (Jobling et al., 2018). CX3CR1 knockout produced detectable changes in the morphology of retinal microglia as well as the structural elongation of photoreceptors (Jobling et al., 2018).

In the adult retina, acute depletion of microglia does not appear to impact the structural organization or architecture of the retina nor does it appear to impact the survival of retinal neurons (Wang et al., 2016). However, prolonged depletion of retinal microglia was observed to lead to the degeneration of photoreceptor synapses and causes a progressive loss of proper light induced visual responses in the retina (Wang et al., 2016). Additional work has demonstrated that the Fractalkine-CX3CR1 signaling pathway regulates the repopulation and reestablishment of functional roles of newly born microglia in the retina following depletion (Zhang et al., 2018). Microglia and cytokine signals have also been shown to be required for the formation of Müller glia-derived progenitor cells in response to injury in the mature retina as differentiation does not occur in animals where microglia have been ablated (Fischer et al., 2014).

The lateral geniculate nucleus - Astrocytes

Compared to the retina, the functional roles of glia in the mammalian brain regions that receive retinal input, such as the superior colliculus and LGN, remain less well characterized, especially in intact animals likely due to their relative inaccessibility compared with other regions of the visual system. During development, RGC axons from both eyes topographically innervate the

LGN occupying overlapping territories and synapsing promiscuously with thalamic neurons before patterned neural activity instructs their proper segregation and refinement into tightly organized laminae with the correct postsynaptic partners (Guido, 2008). In the developing LGN, astrocytes are positioned and appear morphologically mature, having ensheathed retinogeniculate synapses and being capable of glutamate uptake, before eye-opening (Somaiya et al., 2021).

Several studies have now demonstrated that astrocytes orchestrate synaptogenesis, axonal segregation, and synaptic refinement in this circuit. An early indication that astrocytes actively promote the generation of functional synapses came from *in vitro* work where purified RGCs were cultured with and without astrocytes. This study found that astrocytes mediate increases in the overall number of synapses per RGC, as well as enhanced vesicular release and synaptic efficacy (Ullian et al., 2001). While these observations were purely made *in vitro*, the authors did mention that the appearance of SV2-positive synaptic puncta occurs at the same time as the appearance of S100β positive astrocytes suggesting their observations are likely to be relevant *in vivo*. Subsequent work identified thrombospondins as the astrocyte-secreted signal responsible for their promotion of synaptogenesis in the CNS (Christopherson et al., 2005). In addition to *in vitro* analyses of synaptogenic effects of thromobspondins on cultured RGCs, they further confirmed the expression of thrombospondins throughout the postnatal visual system and demonstrated that animals deficient in thrombospondins have deficits in synapse formation *in vivo*.

One of the first studies to directly implicate astrocytes in axonal segregation and refinement *in vivo* came from work characterizing the role of the complement protein C1q in synapse

elimination in the developing LGN which found that disruptions in either C1q or its signaling partner C3 lead to the excessive innervation of thalamic neurons by retinal ganglion cell axons (Stevens et al., 2007). Hunting for the source of C1q in the circuit, they discovered that immature astrocytes were necessary for inducing the upregulation of all C1q subunits in retinal ganglion cell axons, ultimately targeting them for elimination.

Further evidence consolidating a role for astrocytes in mediating the activity-dependent segregation of retinal inputs in the LGN came a few years later when it was demonstrated that not only do astrocytes actively tag retinal inputs for elimination but they also directly phagocytose synaptic connections tagged for elimination as well (Chung et al., 2013). The researchers found that the proteins MEGF10 and MERTK were localized to astrocytes and these signaling pathways mediate phagocytic engulfment and pruning of synapses by astrocytes during development. Similar to disruptions in C1q or C3, knockout of MEGF10 or MERTK in astrocytes was also shown to lead to impaired segregation and the accumulation of abnormal weak inputs onto thalamic neurons in the LGN. Interestingly, this pruning of synapses by astrocytes was demonstrated to be neural activity-dependent with astrocytes continuing to engulf synapses in the adult brain suggesting synaptic pruning by astrocytes is not restricted to critical periods of development.

The activity of retinal inputs in the developing LGN has also recently been shown to regulate the recruitment of interneurons into the circuit through the activation of astrocytes (Su et al., 2020). Mechanistically, the activity of RGCs was found to drive the expression of FGF15 in astrocytes

with FGF15 ultimately being shown to be the necessary signal mediating the recruitment of interneurons into the thalamus, a process critical to proper function of the LGN.

The optic tectum - Radial astrocytes

The amphibian retinotectal circuit is a well-characterized model for studying how visual experience regulates neurodevelopment and plasticity in the intact brain of living vertebrates. In the brain of the African claw-toed frog *Xenopus laevis*, RGC axons innervate the optic tectum, an area analogous to the mammalian superior colliculus, forming synaptic connections with the dendrites of tectal neurons. Radial astrocytes are the principal resident glial cell, which form columnar zones tiling the optic tectum where they act as a hybrid cell type mediating the roles of both radial glial progenitor cells and astrocytes (Tremblay et al., 2009).

In *Xenopus laevis,* the regulation of the proliferative roles of radial astrocytes by visual activity has been studied. It was demonstrated that the generation of new radial astrocytes expressing the proliferative marker Musashi1 decreases as the optic tectum matures, and that 48 h of visual deprivation leads to an increase in the number of Musashi1 positive radial astrocytes, enhancing proliferation, while visual stimulation increases their differentiation into new tectal neurons ultimately showing that visual experience tightly regulates the development of the optic tectum through the activation of glia (Sharma and Cline, 2010). The knockdown and overexpression of Musashi1 in radial astrocytes have shown that it is both necessary and sufficient for proliferation of radial astrocytes in the developing amphibian visual system; however, the mechanism through

which these cells detect and process visual information was not investigated in this study (Sharma and Cline, 2010).

Radial astrocytes have been shown to extend hundreds of fine filopodia into both neuropil and cell body layers of the optic tectum that contact synapses between RGC axons and tectal neuron dendrites (Tremblay et al., 2009). Radial astrocyte filopodia are highly motile and exhibit continuous structural remodeling over short timescales. Radial astrocytes also exhibit spontaneous calcium transients and both filopodial motility and calcium fluctuations can be increased through visual stimulation and reduced by blocking neuronal NMDARs or nitric oxide synthase. Additional studies have demonstrated that neuronal NMDAR activation mediated effects on radial astrocyte filopodial motility through signaling by the CyclicGMP-Dependent Protein Kinase 1 (PKG-1) and that the motility of radial astrocyte filopodia decreases throughout development (Sild et al., 2016). Manipulating the PKG-1 signaling pathway through expression of dominant-negative PKG-1 in radial astrocytes led to reductions in the frequency of mEPSCs in neighbouring neurons, indicative of a failure to undergo normal synaptic maturation (Sild et al., 2016). Additionally, when radial astrocyte filopodia were eliminated through the expression of a constitutively active RhoA this led to reductions in the frequency and amplitude of mEPSCs in neighbouring neurons while the expression of a dominant negative Rac1 that reduced the motility of radial astrocyte filopodia resulted in reduced density of synapses onto neighbouring neurons demonstrating that activity-dependent filopodial motility in radial astrocytes is an important contributor to neuronal maturation and function in the optic tectum (Sild et al., 2016).

The roles of gliotransmitter release in shaping neuronal development and function are hotly debated in the neuroscience community. The roles of the NMDAR co-agonist D-serine have been studied in the *Xenopus laevis* optic tectum where it has been found to be present within both neurons and radial astrocytes and to modulate NMDAR-mediated retinotectal synaptic signaling (Van Horn et al., 2017). In the rodent hippocampus, D-serine, thought to undergo vesicular release from astrocytes in response to calcium transients, has been shown to promote synaptic long-term potentiation through its enhancement of NMDAR-mediated currents (Henneberger et al., 2010). Rearing tadpoles in exogenous D-serine promoted the developmental maturation of retinotectal synapses, a process involving the trafficking of AMPA receptors to the synapse through mechanisms akin to LTP (Van Horn et al., 2017). This finding further indicated that under normal physiological conditions D-serine levels are not saturating. Furthermore, degradation of D-serine by the addition of exogenous D-amino acid oxidase enzyme prevented normal synapse maturation in the tectum, findings that implicate gliotransmission as playing a role in normal circuit maturation.

At the structural level, rearing in excess D-serine has been shown to reduce dendritic branch elaboration and growth of tectal neurons (Chorghay et al., 2021), consistent with the idea that NMDAR activation and synaptic potentiation may help stabilize dynamically remodeling dendritic arbors (Wu and Cline, 1998). In addition, enhancement of NMDAR function further leads to the hyperstabilization of retinotectal axonal arbors in the optic tectum, presumably through the action of a retrograde signal (Van Horn et al., 2017). At the functional level, D-serine increases the size of receptive fields for ON visual responses in tectal neurons, further indicating this putative gliotransmitter is important for the functional maturation of the visual

system . Whether and how D-serine is released from radial astrocytes in response to neuronal activity remains an active area of investigation.

The lateral geniculate nucleus and the optic tectum - Microglia

Relatively little is known about the roles of microglia in mediating the development and function of retinal recipient areas such as the geniculate and optic tectum; however, several studies in both mouse, fish and frog have suggested that they are likely to be mediating important effects related to the refinement of synapses in these areas during development .

In the developing LGN, microglial processes have been observed to extend out close to serotonergic axon terminals where they sense and respond to focal serotonin release through 5HT2B receptors (Kolodziejczak et al., 2015). In 5HT2B knockout mice, there are observable alterations in the refinement of ipsilaterally-projecting retinothalamic connections, and markers for microglial activation are also increased; however, given this knockout was not specific to microglia, it remains a possibility these effects are unrelated to their function (Kolodziejczak et al., 2015).

Microglia in the geniculate have also been shown to regulate synapse removal through a non-phagocytic pathway involving fn14 and TWEAK expression in neurons and microglia respectively (Cheadle et al., 2020). Here neuronally-expressed fn14 was found to promote the formation of bulbus spines on thalamic relay neurons thereby strengthening connections between RGCs and the visual thalamus; however, when microglia expressing TWEAK interacted with

fn14 on thalamic neurons, synaptic connections were weakened and ultimately eliminated demonstrating that microglia can mediate the refinement of synaptic connections through mechanisms independent of phagocytosis (Cheadle et al., 2020).

In the *Xenopus laevis* optic tectum, microglia have been observed to surveil the tectal neuropil where they contact and accumulate material from intact RGC axons (Lim and Ruthazer, 2021). Depleting microglia was shown to lead to an increase in the number of branches on RGC axonal arbors, likely through a decrease in pruning, and quite interestingly to an inversion of expected behavioral responses to light and dark looming stimuli suggesting that microglial interactions with RGC axons are critical for the refinement of circuitry responsible for proper execution of important escape behaviors. RGCs in Xenopus tadpoles were shown to express a complement inhibitory protein, amphibian regulator of complement activation 3 (aRCA3), a homolog of mammalian CD46. Overexpression of aRCA3 in RGCs reduced the accumulation of axonal material by microglia and increased the size of RGC axonal arbors while over expression of complement C3 at RGC axon synapses led to a decrease in axonal arbor size, demonstrating that microglial interactions with RGC axons are regulated by complement proteins and appear to participate in developmental structural refinement.

The primary visual cortex - Astrocytes

Consistent with observations from various areas across the cortex, astrocytes in the primary visual cortex (V1) each occupy adjacent territories, tiling the volume of the brain. Whether astrocytes in V1 have overlapping territories with neighboring astrocytes was recently explored

in the visual system of ferrets. Here it was observed that despite clear tiling of astrocytes throughout V1, most of the glia have territories that overlap with their neighbors by about 50% suggesting it may be possible for multiple astrocytes to differentially influence a shared subset of neighbouring neurons (López et al, 2016). Interestingly, a specific subset of astrocytes in layers 3 and 4 that receive thalamic input, referred to as kissing astrocytes, were found to have territories that overlap substantially less than those in other layers of V1 demonstrating that astrocyte tiling does not apply uniformly across the cortex and is likely to have important influences on neuronal function (López et al, 2016). Work by a group using computational models to help understand how the spatial distribution of astrocytes influences the organization of the visual cortex found that when astrocytes were integrated into a model for the formation of orientation preference maps, by simply altering the radius of astrocytes one can alter the radius of lateral excitatory connections ultimately modifying the size and presence of orientation preference maps in the visual cortex (Philips et al., 2017).

In the developing brain, the density of astrocytes increases in the primary visual cortex until around the time of eye opening, and gap junctions between astrocytes appear to be present before birth (Wang et al., 2021). Early research into the development of astrocytes in the visual system observed that dark-rearing can delay their maturation (Müller, 1990). Subsequently, an extensive characterization of astrocyte development and maturation in the visual system observed that only long periods of dark-rearing (a minimum of four weeks) were sufficient to change the membrane properties of astrocytes in the primary visual cortex, specifically through altering the expression of astrocytic potassium channels (Wang et al., 2021). Binocular deprivation was found to

increase gap junctional coupling between astrocytes, and similarly to dark-rearing, it only occurred if it was maintained for at least four weeks.

Another recent study performed in depth characterization of how the transcriptional regulation of astrocytes is influenced by neuronal activity across development of the visual cortex. They observed that significant changes in the transcriptome of astrocytes correlated with changes in the expression of genes associated with the formation of synapses, and that the expression of genes in astrocytes that regulate synapse formation are modulated by both thalamic neuronal activity and calcium activity in the astrocytes (Farhy-Tselnicker et al., 2021). Consistent with the observations discussed above, they also observed that astrocytes exhibit transcriptional heterogeneity in the visual cortex based on spatial location, and, that consistent with the larger literature on astrocytes, both neuronal and astrocytic activity alters the transcriptome of astrocytes in ways that suggest effects beyond just those related to synapse formation.

Astrocytes also appear to contribute to the development of synaptic connections in the cortex. Here astrocytes were shown to help mediate the linkage of presynaptic neurexins and postsynaptic neuroligins between developing thalamocortical synapses in V1 (Singh et al., 2016). Astrocytes released the protein Hevin, which is known to influence the organization of pre- and postsynaptic connections, and directly induced the formation of thalamocortical synapses by acting as a structural bridge linking together neurexin 1α with neuroligin 1. This demonstrated that the recruitment of neuroligin 1 and NMDARs to excitatory synapses *in vivo* also relies on astrocyte released Hevin, and that, as will be relevant to the section of this review on astrocytes

and ocular dominance plasticity, Hevin released from astrocytes is necessary for ocular dominance plasticity in the developing brain.

How astrocytes in the primary visual cortex respond to neuronal activity

Some of the first direct evidence that astrocytes respond to sensory-evoked neuronal activity *in vivo* came from observations in the primary visual cortex of juvenile ferrets (Schummers et al., 2008). Here it was shown that astrocytes reliably respond to visual stimulation with increases in internal calcium levels which were mediated by glial excitatory amino acid transporters and which lagged behind neuronal responses by several seconds. Surprisingly, the visually-evoked calcium responses in astrocytes were found to exhibit highly-refined stimulus-feature selectivity and receptive field properties which were previously only attributed to neurons (Schummers et al., 2008). In fact, it was found that similar to neurons, astrocyte orientation selectivity was finely mapped across the visual cortex and that astrocytes have even sharper tuning for spatial-frequency and orientation than the surrounding neurons.

Several years later astrocytes in the primary visual cortex of mice were also shown to respond to visual stimulation; however, visually-evoked responses in these astrocytes were very weak when animals were immobile and it was only during forced locomotion that visually-evoked responses became robust (Paukert et al., 2014). In fact, forced locomotion was shown to induce coordinated wide-scale activation of calcium transients in astrocytes throughout the mouse brain, with norepinephrine being found to mediate this effect, suggesting that locomotion, (or

norepinephrine) gates the responsiveness of astrocytes to sensory-evoked stimulation in the mouse visual cortex (Paukert et al., 2014).

This dual influence of locomotion and visual stimulation on the activity of astrocytes in the primary visual cortex has been replicated several times now with additional insights into the mechanism having been characterized. Astrocytes in the visual cortex of mice were again shown to respond directly to visual stimulation and also to exhibit high amplitude alpha-1 adrenergic receptor mediated global calcium events throughout the cortex in response to norepinephrine released from the locus coeruleus which tended to mask the lower amplitude visual stimulation induced responses (Sonoda et al., 2018; Slezak et al., 2019). Similar to the kinetics observed in the responses of astrocytes in the primary visual cortex of ferrets, visually-evoked events in astrocytes were delayed by approximately five seconds relative to neuronal responses suggesting the likelihood of a conserved mechanism underlying the responses in both species (Sonoda et al., 2018). Interestingly, they observed distinct patterns of calcium activity in astrocytes in response to locomotion and visual stimulation and that chemical ablation of norepinephrine releasing neurons abolished locomotor but not visually-evoked responses (Slezak et al., 2019). The mechanism mediating visually-evoked events in astrocytes was not explored in this context, however.

Astrocytes in the visual cortex also exhibit extensive spontaneous activity, particularly within small microdomains of their fine processes even in the absence of locomotion or visual stimulation . The signals mediating spontaneous microdomain activity in astrocytes have been hotly debated (Bazargani and Attwell, 2016). Researchers have found that different

neurotransmitters activate distinct microdomains within cortical astrocytes (Agarwal et al., 2017). However, spontaneous calcium events in these microdomains continued to occur when neurotransmitter release was prevented or when the release of calcium from internal stores was blocked pharmacologically or largely abolished in IP3R2 knockout mice (Agarwal et al., 2017). Interestingly, spontaneous events in microdomains of the fine processes of astrocytes were found to colocalize with mitochondria, and ultimately, the mitochondrial membrane permeability transition pore was found to be responsible for generating spontaneous microdomain calcium events that occur in the absence of neurotransmitter release. Thus, astrocytes may exert effects on neural circuits as a consequence of intrinsic metabolic activity (Agarwal et al., 2017), in response to neuromodulatory release during states of heightened arousal (Paukert et al., 2014; Slezak et al., 2019), or as a direct response to sensory-evoked neuronal activity (Schummers et al., 2008; Paukert et al., 2014; Sonoda et al., 2018; Slezak et al., 2019).

Action of astrocytes on visual cortical response properties

Several studies have examined how selectively activating astrocytes in the primary visual cortex using optogenetic tools regulates the firing and response properties of cortical neurons and shapes visual processing. Optogenetic activation of astrocytes in V1 was found to enhance synaptic transmission in layers 2/3 through the activation of presynaptic mGluR1, likely as a consequence of astrocytic glutamate release (Perea et al., 2014). Photoactivation of astrocytes led to increases in mEPSC frequency in both PV+ and SOM+ inhibitory neurons, and modulated their spontaneous activity along with that of excitatory neurons in primary visual cortex *in vivo*. Activation of astrocytes was found to alter both excitatory and inhibitory drive onto neurons

throughout V1. Consequently, visual responses and orientation selectivity of cortical neurons were changed by astrocyte activation, with increasing baseline responsiveness leading to a corresponding decrease in orientation selectivity. Interestingly not all neurons responded identically, with PV+ interneurons uniformly increasing baseline visual responses, while SOM+ interneurons showed bidirectional changes. All of these effects of glial activation could be prevented by systemic blockade of mGluR1a, consistent with a central role for astrocytic glutamate release.

Other studies investigated how the activity of astrocytes influences the firing activity of neurons throughout the layers of the primary visual cortex. Consistent with the findings reported above, the firing activity of neurons in layers 2/3 of the visual cortex was increased following four weeks of dark rearing and, surprisingly, this was found to be linked to increased gap junction coupling between astrocytes (Wang et al., 2021). Another group, using optogenetic activation of astrocytes, observed increases in calcium responses, depolarization, and spiking in layer 5 pyramidal neurons accompanied by potentiation of inputs onto their apical dendrites in layer 1 (Ryczko et al., 2021). Interestingly these effects were found to persist in the presence of blockers for glutamate, GABA and ATP receptors suggesting a non-classical mechanism. Ultimately it was demonstrated that astrocytes mediate these effects by altering extracellular calcium around neurons through the activity-dependent release of the calcium binding protein S100β which increases the firing of distal inputs onto layer 5 pyramidal neurons through activation of Nav1.6 channels, highlighting the remarkable diversity of mechanisms for neuron-glia communication.

Roles of astrocytes in regulating plasticity in the primary visual cortex

The possibility that astrocytes might regulate developmental plasticity in the mammalian visual cortex first attained prominence with the observation that ocular dominance plasticity could be restored after the normal critical period had closed by grafting immature astrocytes cultured from the visual cortex of kittens into the visual cortex of adult cats (Müller, 1989). In line with this observation, dark-rearing, which is known to delay critical period closure in the visual cortex, was demonstrated to lower the levels of astrocytic markers such as GFAP and S-100 compared to normal light-rearing, suggesting both that the maturation of astrocytes is linked to visual experience and that there is an association between the presence of immature astrocytes and the potential for plasticity in the visual cortex (Müller, 1990).

More recently there has been a significant advance in our understanding of how astrocytes regulate ocular dominance plasticity by helping to gate the opening and closure of the critical period. Researchers revisited the early observation that the transplantation of immature astrocytes into adult visual cortex, this time in the mouse, can restore ocular dominance plasticity (Ribot et al., 2021). They first observed that the intrinsic membrane properties of astrocytes mature by postnatal week three, just before the onset of the critical period for ocular dominance plasticity in mice, and additionally, that immature astrocytes undergo a significant shift in transcriptional regulation at this time moving away from the expression of genes regulating cell division and towards the expression of genes regulating cellular communication. Transcripts for proteins involved in the formation of gap junctions were some of the most highly differentially

expressed genes, with CX30 exhibiting the highest representation. They showed that CX30 levels increase throughout development and peak at the time of closure of the critical period of ocular dominance plasticity. Four days of exposure to darkness reduced CX30 expression in V1 and increased plasticity, while knockdown of CX30 in astrocytes in V1 delayed the closure of the critical period significantly from P28 to P50. Additionally, grafting immature astrocytes lacking CX30 reopened the critical period in adult mice. When taken together, these observations demonstrate a critical effect of astrocytic expression of the gap junction protein CX30 in gating plasticity in the visual cortex. The researchers took these observations a step further by investigating the role of CX30 in the maturation of PV+ interneurons in V1, which are known to be important regulators of ocular dominance plasticity. Knockdown of CX30 in astrocytes led to a decreased ratio of inhibition to excitation in the cortex and significant alterations in perineuronal nets, a known marker for the maturation of PV+ interneurons and plasticity. They concluded the study by demonstrating that astrocytic CX30 regulates the formation of perineuronal nets through a pathway involving RhoA and release of the extracellular matrix metalloprotease MMP9. Taken together the results of this study demonstrate a critical role for astrocytes in gating cortical plasticity by regulating that maturation of PV+ interneurons consistent with the larger literature on ocular dominance plasticity.

As discussed above, glutamate transporters have been shown to mediate responsiveness of astrocytes to visual stimulation in the primary visual cortex of ferrets (Schummers et al., 2008); as such, understanding how astrocytic glutamate transporters influence the development of the visual system is of particular interest. GLT-1 (EAAT2) is the dominant glutamate transporter expressed by astrocytes in the visual cortex of mice, and visual experience has been shown to

increase GLT-1 expression levels in V1 astrocytes throughout development (Sipe et al., 2021). In GLT-1 heterozygous (HET) mice, astrocytic levels of GLT-1 are reduced by approximately 50% in the visual cortex. In these mice the normal developmental matching of orientation preferences of the responses or the two eyes in V1 cells is disrupted. Layer 2/3 neurons show increased spine density, suggestive of a reduced amount of developmental synaptic pruning. Furthermore, ocular dominance plasticity is significantly altered by this change in the expression of astrocytic GLT-1, with responses to the non-deprived eye failing to increase, and paradoxically decreasing over time, highlighting the important role played by astrocytic glutamate uptake for normal plasticity in the developing visual cortex.

The neuromodulator acetylcholine has also long been known to play a critical role in cortical plasticity in the visual system (Bear and Singer, 1986). Responses to a visual stimulus can be strongly potentiated in excitatory neurons in the visual cortex of adult mice by pairing the release of acetylcholine by nucleus basalis stimulation with the visual stimulus (Chen et al., 2012). It was determined that this potentiation of visual responses is dependent upon the activation of muscarinic acetylcholine receptors on astrocytes in the visual cortex. Importantly, knockout of IP3R2 in these cells abolished this phenomenon, indicative of a role for astrocytic calcium in mediating the effects of cholinergic-mediated cortical potentiation.

Astrocytes have also been implicated in injury-induced plasticity of the adult visual system which can be induced by monocular enucleation (ME), the surgical removal of one eye, in which, following a period of quiescence in the cortical territory serving the lost eye, gradual functional reorganization restores responsiveness to other inputs (Hennes et al, 2020). ME has

been shown to lead to a rapid increase in the density of astrocytes in primary visual cortex, suggesting they are likely to be contributing to the ability of the cortex to reorganize following ME. This was confirmed by metabolic silencing of astrocytes with fluoroacetate immediately following ME and observing that the functional recovery of neurons in the visual cortex was significantly impaired as a result.

The primary visual cortex - Microglia

In the visual cortex astrocytes are not the only glial cell type that has been shown to respond to visual activity and influence circuit development and function. Microglia are also appreciated to contribute to the function of the visual system in important ways (for a dedicated review on microglia and the development of the visual system see Dixon et al., 2021). Here we have included some of the relevant contributions of microglia to the development and function of the visual cortex.

Several studies have investigated the behavior of microglia in response to normal or restricted visual experience. During normal visual experience microglia in the visual cortex of juvenile mice extend numerous processes that are associated with synapses at small spines and which are surrounded by extracellular space (Tremblay et al., 2010). Following light deprivation and eventual reexposure, microglia can be observed at the ultrastructural level to exhibit alterations in the extracellular space around synapses, increases in phagocytic markers, and enhanced contact with synaptic clefts. Additionally, light deprivation caused microglia to exhibit less motility and shift their contacts to larger spines, while light exposure reversed these effects.

Microglial morphology and process motility have also been shown to change quickly following monocular deprivation and lead to alterations in their interaction with synapses (Sipe et al., 2016). The morphology, territories, and behaviour of microglia in the visual cortex continue to undergo changes as animals age suggesting potential roles across the life span of animals (Tremblay et al., 2012).

Several mechanisms associated with microglial function have been explored in the visual cortex. The purinergic receptor P2Y12 is exclusively expressed by microglia in the visual cortex and has been shown to be required for normal ocular dominance plasticity (Sipe et al., 2016). P2Y12 knockout reduces ramification of microglia but does not affect baseline motility of their processes. It prevents the increase in microglial ramification observed during monocular deprivation which is normally associated with enhanced plasticity. The CX3CR1 receptor too has been shown to play important roles in microglial effects on circuit formation and function in areas of the brain such as the retina, but whether it is a global regulator of microglial function is still being investigated. It was observed that knockout of CX3CR1 in microglia does not impair the segregation of retinal inputs in the thalamus and that visual acuity is normal in these animals. Additionally, the activity-dependent potentiation of synaptic connections is normal in CX3CR1 knockout mice as well as the effects of monocular deprivation on ocular dominance plasticity and thalamocortical and cortical synapse density, together suggesting that CX3CR1 does not play an important role in microglial function in the visual cortex relevant to plasticity (Schecter et al., 2017), observations which have been replicated (Lowery et al., 2017).

Of particular interest given the considerable impact of norepinephrine release on astrocyte function in the visual cortex, norepinephrine has also been shown to act as a potent regulator of microglial function in the visual cortex. The first indication came with the observation that microglial surveillance was significantly increased during anesthesia, and that the alpha-2 adrenergic receptor agonist dexmedetomidine, which reduces norepinephrine release, increased microglial surveillance similarly to anesthesia (Stowell et al., 2019). Further investigation into the signaling pathways regulating these effects found that beta-2 adrenergic receptor activation decreases the motility of microglia, and that blockade of beta-2 adrenergic receptors in awake mice reproduces the effects of anesthesia on increasing microglial surveillance. Importantly, the activation of beta-2 receptors was shown to impair the ability of microglia to respond to injury, and chronic activation of microglial beta-2 receptors impaired ocular dominance plasticity in adolescent mice.

Finally, as discussed above, astrocytes have been found to help close the critical period for plasticity in the visual cortex through the regulation of perineuronal nets (Ribot et al., 2021). Interestingly, the depletion of microglia in the adult mouse brain also leads to an increase in the density of perineuronal nets and produces many of the same effects observed when activating astrocytes in the visual cortex, such as increases the amplitude of EPSCs in excitatory pyramidal neurons, increases in local excitatory connections onto excitatory pyramidal neurons, and increases the number of inputs from PV+ interneurons onto excitatory neurons in V1 which would all be consistent with reduced plasticity in the circuit (Liu et al., 2021). Together this strongly suggests, as has recently been observed in other parts of the cortex (Badimon et al.,

2020), that astrocytes and microglia may signal to each other to mutually alter the functional properties of neurons in the visual cortex.

Future perspectives

Although many outstanding questions remain regarding the functional roles of glia throughout the visual system, particularly in deep brain structures such as the thalamus, a clear picture is starting to emerge from the available literature in which glia, through sensing and responding to visually-evoked neuronal activity, directly influence the connectivity, maturation, function, and plasticity of neuronal circuits in each major station of the visual system. As we continue to refine our mechanistic understanding of how glia shape these processes, important conceptual gaps in our knowledge are becoming apparent and point towards meaningful avenues for future research. In the following section I will highlight what we believe to be the most salient open-ended questions yet to be addressed in the field related to the extended functions of glia across the nuclei of the visual system.

Given that information is relayed through the visual system in stages, and that glial activity influences neuronal function locally within each nucleus of the visual system, the possibility that glial activity at one site might influence neuronal activity in another distal location in the visual system is worth seriously investigating. With new techniques allowing for precise targeting and (in)activation of glial cells in intact behaving animals becoming more prevalent, it should now be possible to study potential long-range influences that glia may exert. For addressing these issues,

there are particular advantages to the use of highly optically accessible model systems such as *Xenopus laevis* and *Danio rerio* where the entire visual system can be imaged at once.

Given that Müller glia have been shown to regulate the excitability of retinal neurons and modulate the retinal waves known to instruct the topographic and eye-specific refinement of axonal inputs in retinorecipient areas, an important open question is whether the modulation of the signaling pathways that act on Müller glia (e.g, excitatory amino acid transporters, AMPARs, mAChRs, calcium) can alter the structural and functional connectivity of retinofugal and thalamocortical projections. In theory it should be possible to precisely manipulate the signaling pathways in Müller glia and investigate whether there are alterations in the retinotopic innervation and structural refinement of axons innervating the tectum (superior colliculus) or the LGN and whether these manipulations significantly influence the functional properties of these circuits by impacting such things as neurotransmitter release from RGCs, receptive field properties of postsynaptic neurons, and the maturation of retinotectal or retinogeniculate synapses during critical periods of development. More nuanced investigation into whether controlling the functional activation of Müller glia can alter the information content of visual signals being relayed from the retina to the tectum (superior colliculus) and thalamus, and from the thalamus to the cortex would also be illuminating. Behavioral testing could also contribute novel information about the extent to which glial function in one region of the nervous system is capable of exerting an influence on sensory processing in developing and mature animals. Whether there is a difference between any such Müller glia-mediated effects in animals such as fish and frogs, where visual experience is instructive throughout their development, and mammals where instead, spontaneous retinal activity before eye-opening is instructive

throughout early development, would be equally interesting to explore (Pratt et al., 2016). The roles of microglia in each of these experimental manipulations should also be characterized given their influence on photoreceptor function and Müller glial maturation. Logically, such investigations should also be extended to glia in retinorecipient areas as well, characterizing their influence on structural and functional connectivity between the tectum (superior colliculus), the LGN, the visual cortex, and perhaps even back onto the retina.

Glia in retinorecipient areas are dramatically understudied in comparison to glia in the retina and visual cortex despite critical activity-dependent roles having been identified for glial function in areas such as the tectum (superior colliculus) and the LGN. As such, an in-depth characterization of the different signaling pathways mediating glial activity in these areas is warranted to better understand what information they are integrating and how they are sensing and responding to visual experience across multiple temporal and spatial scales. Focus should be directed towards characterizing which ion exchangers, neurotransmitter and neuromodulator receptors and transporters are expressed by these glial cells, what heterogeneity exists in their expression across development, and how this correlates with changes in neural circuitry over the same developmental epochs.

Neuromodulators such as norepinephrine and acetylcholine, long implicated in regulating the plasticity of the visual system, are emerging as powerful regulators of glial activity throughout the vertebrate brain in some cases directly mediating their effects on plasticity through the activation of glia (Van Horn et al., 2021). As such, a full characterization of which neuromodulators signal through glia to influence neuronal function in each part of the visual

system may be critically important for a comprehensive understanding of how plasticity is mediated throughout the visual system as a representative example of sensory processing in general. Whether different neuromodulators, such as acetylcholine or norepinephrine, have distinct influences on glial activity and function within and across different segments of the visual system is currently unexplored and may be particularly instructive. During the development of the visual system, glia have been shown to influence the excitability, connectivity, and maturation of both excitatory and inhibitory neurons, but whether this influence also extends to the neuromodulatory axons innervating these areas of the visual system and whether glia may regulate the release of neuromodulators remains an open question. As both neuromodulators and glial gap junctions have been implicated in gating critical periods of plasticity in the visual system, how neuromodulators influence the expression and maturation of glial gap junctions, and whether this relationship is present throughout the visual system, may provide additional insight into the mechanisms by which both influence plasticity in these circuits.

Throughout different regions of the visual system, as has been observed more generally throughout the central nervous system, neural activity elicits responses in glia through a variety of different types of signaling mechanisms at different stages of development which, despite largely converging at the level of intracellular calcium dynamics over distinct spatiotemporal patterns of release, suggests the existence of extensive heterogeneity between glia both within and across different segments of the visual system. This warrants careful attention and extensive characterization in order to better understand the precise ways in which glia respond to and influence neuronal activity in distinct locations and at distinct times throughout development. Of

particular interest is whether all glial cells in each region of the visual system are responsive to both visually-evoked neuronal activity and the release of neuromodulators or whether distinct subpopulations of glia exist, each with unique stimulus sensitives and functional influences on neurons. Whether the activation of glia by sensory-evoked neural activity alone, the release of neuromodulators alone, or through coactivation by both stimuli simultaneously, results in different functional outcomes such as distinct influences on proliferation and neuronal differentiation, as well as the release of specific gliotransmitters over different spatio-temporal scales, has important implications for understanding how glia exert their influences over circuit development, maturation, function, and plasticity.

Given that glia in the visual system are responsive to neuromodulatory signals known to regulate complex processes such as learning, memory, and attention, whether glia in different segments of the visual system play a role in mediating higher order processes such as perceptual learning, metaplasticity, and the encoding of salient visual information remains an interesting avenue for future experimental work. More generally, the information content contained within patterned glial activity within networks of the visual system remains largely unexplored despite early experiments showing that astrocytes in the primary visual cortex of ferrets exhibit highly refined stimulus-feature selectivity and receptive field properties which were even more finely-tuned than those in neurons in some cases suggesting that they may also represent complex information in ways complementary and possibly unique from those used by neurons and across different spatiotemporal scales as well. Whether glia in other areas of the visual system also exhibit refined stimulus-feature selectivity remains to be investigated further.

In each region of the visual system, the activity of astrocytes and microglia are both modulated by largely overlapping signaling pathways often mediating complementary influences on neuronal circuit development and function. Exploring to what extent, and through what means, astrocytes and microglia both independently and mutually influence the developing and mature visual system to regulate neural circuit formation and function will be important to carefully consider in all future investigations.

Conclusions

Despite the extensive heterogeneity in the morphologies of glia (Figure 1B-E) and the host of molecular signaling pathways mediating neuron-glia communication across brain regions and development (Figure 2), there appear to be important evolutionarily conserved functions mediated by glia throughout the visual system which are likely to be of general relevance to other sensory systems in the vertebrate brain. Throughout the visual system, astrocytes and microglia both sense and respond to neural activity through parallel mechanisms, integrating local circuit activity and the release of neuromodulators such as norepinephrine, acetylcholine, serotonin, and ATP/Adenosine in order to instruct the segregation and refinement of afferent axonal projections through both phagocytic and non-phagocytic means, as well as the genesis, maturation, maintenance, and plasticity of synaptic connections through a series of physical and chemical interactions. Taken together this suggests that glia form a complex network of dynamic integrators which actively influence the development and function of the nervous system by linking together bottom-up sensory-evoked neuronal activity, largely through the reuptake of

neurotransmitters, with top-down context-specific neural activity, through their activation by neuromodulators, at the level of intracellular calcium dynamics.

Having largely mapped out what is known and unknown about how glia influence the development and function of the visual system, we will conclude with some speculation as to how visual experience would be altered without functional glia in each segment of the system. Without functional glia in the retina the spontaneous waves of activity that instruct the topographic refinement of retinal inputs into our brains during early development may be considerably dysregulated, possibly leading to imprecise spatial maps of our visual world, and ultimately disrupting how we detect and track the motion of objects across space. Additionally, we would also quickly go blind as we age as a result of rapid deterioration of photoreceptors without glia to maintain their synaptic integrity. Without functional glia in the tectum, we know that synapses will not properly mature, and that receptive fields would be significantly altered, together likely leading to defects in the crucial opto-motor responses necessary to direct our attention as well as detect and orient ourselves towards or away from threats in our environments substantially reducing our ability to properly navigate our environments. In the LGN, without the care glia provide to precisely sculpt and segregate visual connections, visual information entering our brains would likely not be faithfully transmitted to the cortex to be consciously represented leaving us experientially blind at worst or at the very least significantly impaired in terms of correctly identifying salient visual information in our environments, putting us at significant risk for injury. Without functional glia in the visual cortex the connections from the thalamus relaying visual information would not be able to anchor into the correct locations in V1 leading to either conscious blindness or a highly disorganized representation of objects in the

world. Without glia to mediate plasticity and gate critical periods in the visual cortex, visual experience may never or may continually influence the wiring of our brains, leaving us with either impoverished and imprecise representations of our environments which lack the crucial contextual information that allows us to make appropriate perceptual decisions, or perpetually destabilizing our representations of the world and the binocular detection of important objects within it with important consequences for behavior.

In contrast to this, one can't help but speculate as to what the future holds in terms of our ability to capitalize on the targeted manipulation of glial function throughout the visual system once we fully decode the nuances of their activity. Will we be able to fully repair damaged retinas, reversing or preventing blindness through modulating the function of Müller glia? Will we have the possibility of selectively enhancing and focusing our attention towards or away from specific stimuli in order to help accomplish specific goals or facilitate learning through the precise tuning of glial activity in the superior colliculus? Will it be possible to suppress or enhance specific types of visual information from reaching the visual cortex in order to help us selectively increase our ability to detect important visual cues in different environments by controlling the activity of glia in the thalamus? Will controlling glial activation in the visual cortex help us reopen critical periods of plasticity in a way that facilitates the functional reorganization necessary to recover from visual deficits in development or damage in adulthood or in ways that allow us to reformat our visual system on demand to function more optimally in a world continually populated by hyper-normal stimuli? What yet undiscovered possibilities remain to be found as we continue to develop an understanding of glial functions throughout the visual system? While we are only beginning to decode and understand the functional relevance of glial

activity, it is eminently clear that our visual experience of the world is critically dependent on their function and that as research progresses, we are likely to continue to find novel important roles for glia throughout the visual system.

In the following chapters I will present data showing that in the developing optic tectum of *Xenopus laevis*, radial astrocytes are highly responsive to visually driven neuronal activity and that their activation strongly influences the visual response properties of the tectum. Using a systematic combination of visual stimulation and acute pharmacological manipulation of the optic tectum *in vivo,* I will demonstrate that visually driven calcium events in radial astrocytes are mediated through the uptake of glutamate and reversal of sodium calcium exchangers. I will also show that radial astrocytes are potently activated by the neuromodulator norepinephrine through alpha1-adrenergic receptors. This activation of radial astrocytes by norepinephrine appears to lead to ATP release, likely through hemichannels, which acts on postsynaptic P2 receptors to alter the excitability of neurons capable of mediating a state shift in the tectum. I will show that this alteration of network excitability appears to bias the animal towards threat detection, and that the targeted chemogenetic activation of radial astrocytes can reproduce the effects of norepinephrine on tectal function, increasing threat detection in freely swimming animals. Taken together, all of my experimental work attempts to demonstrate that radial astrocytes in the optic tectum are cells of high complexity which are capable of integrating both visually driven local circuit activity and arousal state. This integration appears to compute a threshold that once crossed leads to the rapid recruitment of other radial astrocytes and ultimately a state shift in the tectum. I will finish by suggesting how this state shift induced by radial

astrocytes is likely to have multiple important implications for the survivability of animals in their natural environment.

Figures

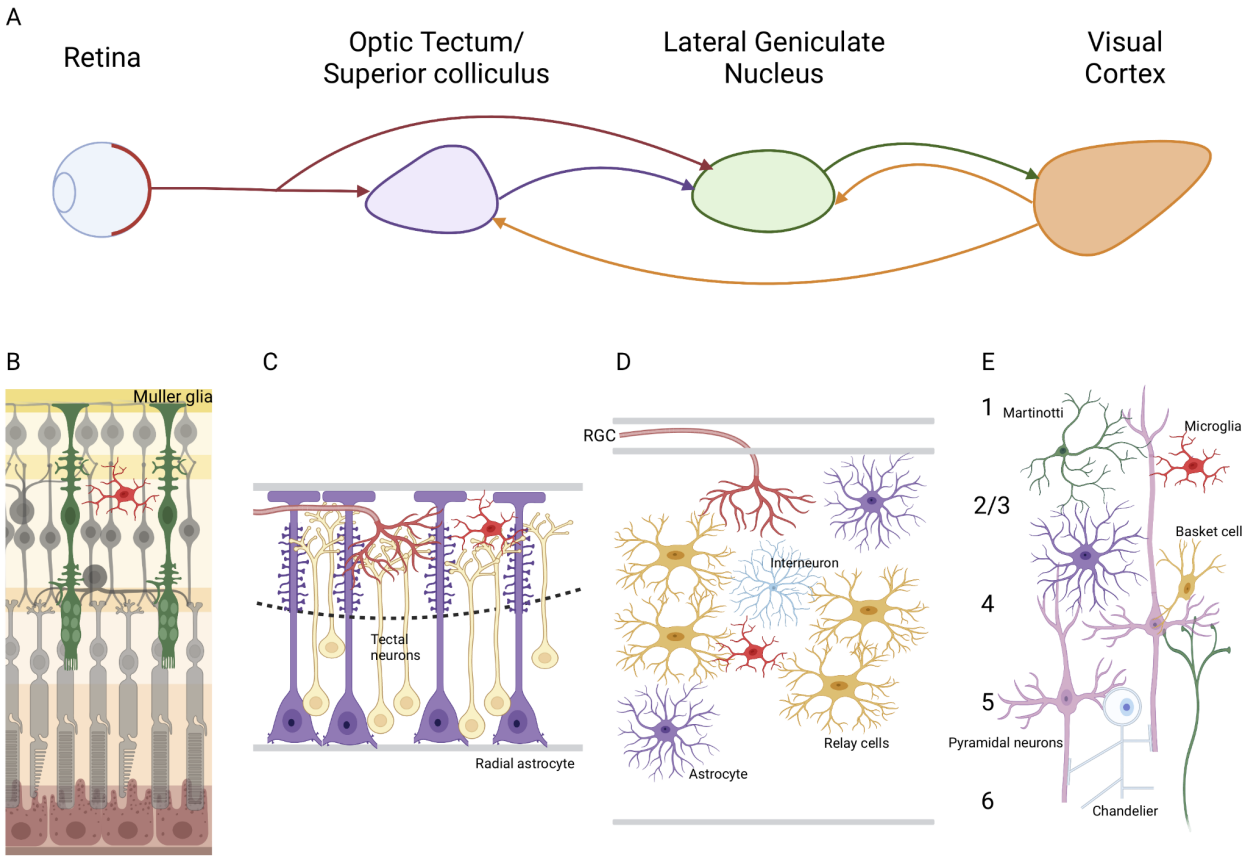

Figure 1. Schematic representation of the vertebrate visual system and the astrocytes and microglia populating each area.

(A) Overview of the vertebrate visual system showing the connectivity between the major areas, the retina, the optic tectum/superior colliculus, the lateral geniculate nucleus, and the primary visual cortex. (B) Cellular organization of the retina showing Müller glia and microglia. (C) Cellular organization of the optic tectum showing radial astrocytes and microglia. (D) Cellular

organization of the lateral geniculate nucleus showing astrocytes and microglia. (E) Cellular organization of the primary visual cortex showing astrocytes and microglia.

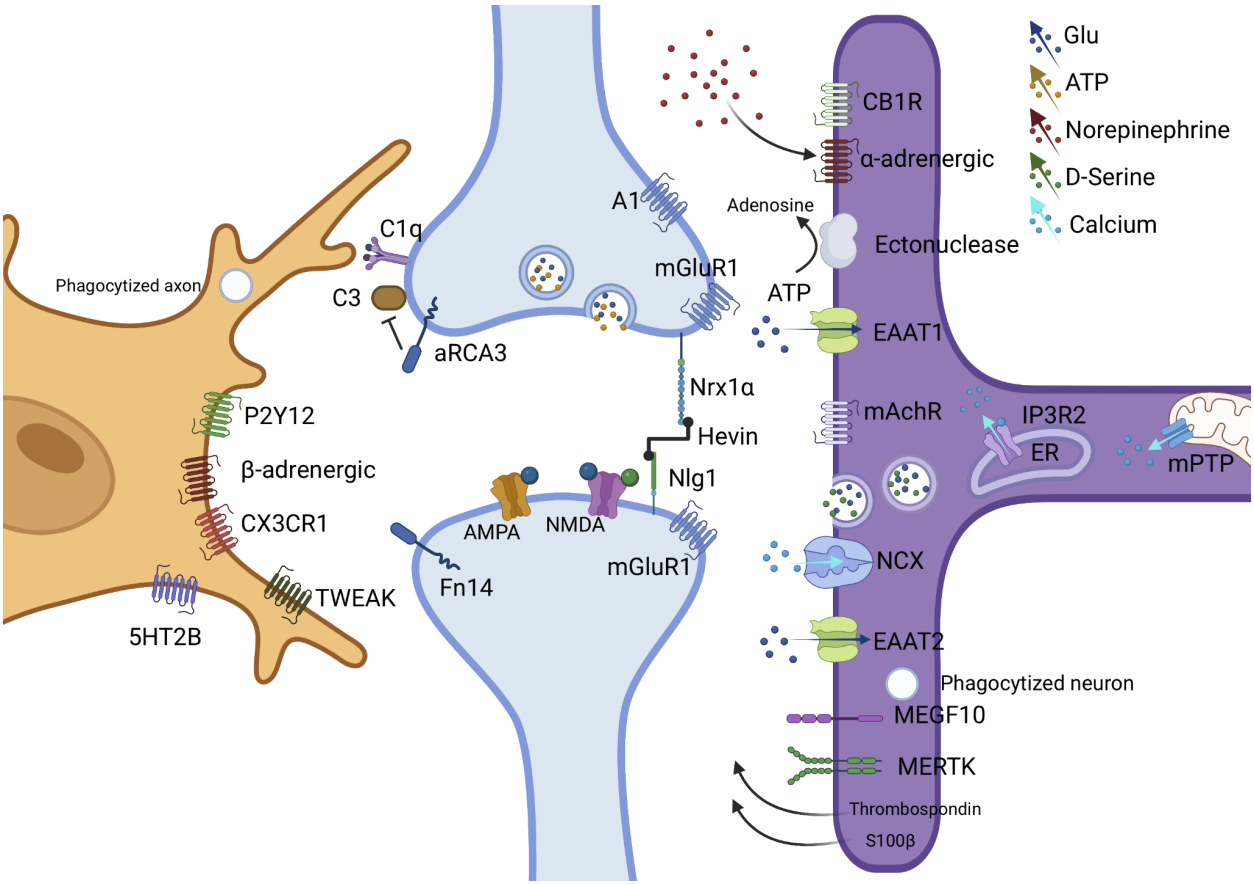

Figure 2. Overview of the signaling mechanisms which have been implicated in mediating neuron-glia communication and interactions throughout the vertebrate visual system.

Representative microglial cell (left, orange), pre- and postsynaptic terminals (middle, blue), and Müller glial cell/radial astrocyte/astrocyte (right, purple) expressing a variety of receptors, transporters, channels, and signaling proteins relevant to their functions across the visual system.

Author Contributions For Chapter 2

The experiments and analysis carried out in this study were conceived of by Nicholas Benfey under the supervision of Dr. Edward Ruthazer. Nicholas Benfey performed all of the experiments and carried out all of the data collection and analysis presented in this manuscript. Nicholas Benfey wrote the manuscript and created the figures. Vanessa Li wrote the original matlab scripts used for the correlation vs. distance analysis carried out in Figure 3 and helped to optimize the calcium imaging methodology used to collect the data for this manuscript. Anne Schohl developed the calcium imaging methodology used to collect the data in this publication and provided general technical support to Nicholas Benfey throughout the process of collecting data for this manuscript. All authors contributed to the editing of this manuscript, particularly Edward Ruthazer. The artwork used in the figures was kindly provided by the scientific illustrator Audrey Desaulniers, Orcéine, Montréal, Canada.

Preface To Chapter 2: Sodium-Calcium Exchanger Mediates Sensory-Evoked Glial Calcium Transients In The Developing Retinotectal System

This chapter presents the experiments I carried out in order to achieve the first and second objectives of my thesis research, namely the implementation of calcium imaging methods to monitor and quantify the functional activity of tectal neurons and radial astrocytes during visual stimulation and the discovery of the molecular signaling mechanisms mediating neuron-glia communication in this system. This study helps to fill important gaps in the field in terms of how glial cells functionally integrate into the midbrain circuits of the vertebrate visual system. Given

changes to published manuscripts is not permitted, references to videos which are not actually included with the thesis, but which may be accessed through the online version of the paper, are still included in the text. This manuscript was published as Benfey, N.J., Li, V.J., Schohl, A., and Ruthazer, E.S. (2021). Sodium-calcium exchanger mediates sensory-evoked glial calcium transients in the developing retinotectal system. *Cell Rep. 37*(1), 109791. doi: 10.1016/j.celrep.2021.109791.

Chapter 2: Sodium-Calcium Exchanger Mediates Sensory-Evoked Glial Calcium Transients In The Developing Retinotectal System

Nicholas J. Benfey, Vanessa J. Li, Anne Schohl, and *Edward S. Ruthazer

Montreal Neurological Institute-Hospital,

Department of Neurology and Neurosurgery,

McGill University,

Montréal, Québec, H3A 2B4 Canada

*Lead Contact: Please address communications to edward.ruthazer@mcgill.ca

Summary

Various types of sensory stimuli have been shown to induce Ca^{2+} elevations in glia. However, a mechanistic understanding of the signaling pathways mediating sensory-evoked activity in glia in intact animals is still emerging. During early development of the *Xenopus laevis* visual system, radial astrocytes in the optic tectum are highly responsive to sensory stimulation. Ca^{2+} transients occur spontaneously in radial astrocytes at rest and are abolished by silencing neuronal activity with tetrodotoxin. Visual stimulation drives temporally correlated increases in the activity patterns of neighboring radial astrocytes. Following blockade of all gluRs, visually-evoked Ca^{2+} activity in radial astrocytes persists, while neuronal activity is suppressed. The additional blockade of either glu transporters or sodium-calcium exchangers (NCX) abolishes visually-evoked responses in glia. Finally, we demonstrate that blockade of NCX alone is

sufficient to prevent visually-evoked responses in radial astrocytes, highlighting a pivotal role for NCX in glia during development.

Introduction

Following the initial discovery that astrocytes in culture respond to glutamate (glu) and neuronal activity through increases in internal Ca^{2+} concentration (Cornell-Bell et al., 1990; Dani et al., 1992; Porter and McCarthy, 1996), there has been an expanding effort to understand glial participation in neural circuits *in vivo* (Allen and Lyons, 2018). Once largely accepted to be passive cells acting principally as scaffolds for neuronal migration and mediators of ionic and metabolic homeostasis (Verkhratsky et al., 2019), glia are now understood to be highly active contributors to neural circuit development (Clarke and Barres, 2013; Van Horn and Ruthazer, 2019), function (Araque and Navarrete, 2010; Perea and Araque, 2010), plasticity (Panatier et al., 2011; Allen and Eroglu, 2017), and behavior (Mu et al., 2019), both in health and disease (Barres, 2008). However, despite experiments performed in adult animals demonstrating that glia respond to physiological stimulation (Wang et al., 2006; Schummers et al., 2008), a comprehensive mechanistic understanding of how glia are recruited by sensory stimulation remains elusive (Bazargani and Attwell, 2016). Additionally, an understanding of how sensory stimulation regulates glial activity during early development remains largely unexplored in intact animals.

Early work on the physiological regulation of glial Ca^{2+} signaling *in vivo* identified multiple mechanisms underlying glutamatergic signaling between neurons and glia. In barrel cortex of

adult mice, the responsiveness of astrocytes to whisker stimulation was shown to depend on type-1 metabotropic glutamate receptors (mGluRs)(Wang et al., 2006), while in the primary visual cortex of adult ferrets, visual responses in astrocytes were reduced following blockade of glu transporters (Schummers et al., 2008). In the cerebellum of adult mice, the response of Bergmann glia to motor activity can be largely abolished by broad spectrum blockade of gluRs (Nimmerjahn et al., 2009), and the Ca^{2+} activity in Müller glia during retinal waves in zebrafish has been shown to involve the activation of Ca^{2+}-permeable AMPA receptors and glu transporters (Zhang et al., 2019). Recent work has also demonstrated that mGluR5 is developmentally regulated, with expression levels in astrocytes decreasing dramatically into adulthood, rendering ambiguous the mechanism by which it influences mature astrocytes (Sun et al., 2013).

Recent work investigating the physiological activation of glia shows that glutamate receptors (gluRs) play a limited role in generating glial Ca^{2+} events suggesting the involvement of additional mechanisms (Zhang et al., 2019; Tang et al., 2015; Shigetomi et al., 2011; Paukert et al., 2014; Bazargani and Attwell, 2017; Stobart et al., 2018; Agarwal et al., 2017). It is also unclear whether glial Ca^{2+} responses result from direct activation of glial gluRs in all cases or indirectly following activation of neuronal receptors and release of diffusible signals, as few experiments have employed simultaneous dual imaging of neurons and glia in their preparations. Recent work both *in vitro* and *ex vivo* has suggested that the rapid entry of Na^{+} via glial glu and GABA transporters may drive extracellular Ca^{2+} entry into glia through reversal of sodium-calcium exchangers (NCX), thereby linking neural activity to glial Ca^{2+} events through a mechanism independent of gluRs (Rojas et al., 2007; Doengi et al., 2009; Shigetomi et al., 2011;

Boddum et al., 2016; Langer et al., 2017; Brazhe et al., 2018; Deemyad et al., 2018). We have therefore investigated the contribution of NCX to physiologically evoked glial Ca^{2+} responses *in vivo*.

The development of genetically-encoded Ca^{2+} indicators has led to significant advances in *in vivo* Ca^{2+} imaging (Chen et al., 2013). As such, we produced GCaMP6s-expressing albino *Xenopus laevis* tadpoles which are easily amenable to acute pharmacological manipulation and allow for the simultaneous imaging of Ca^{2+} activity in neurons and glia in the retinotectal circuit of intact animals during visual stimulation. To dissect the signaling mechanisms by which visual activity regulates Ca^{2+} events occurring in both neurons and glia during early development, we employed a systematic approach involving pharmacological antagonism and activation of glutamate receptors and transporters, and NCX in conjunction with the presentation of a robust and behaviorally relevant visual stimulus to engage presynaptic release from retinal ganglion cell axons while imaging the postsynaptic responses of tectal neurons and radial astrocytes in the optic tectum of GCaMP6s-expressing tadpoles.

We found that visually-evoked activity in radial astrocytes was eliminated following the blockade of excitatory amino acid transporters (EAATs) 1 and 2 or NCX, and that blockade of NCX alone was sufficient to prevent radial astrocytes, but not tectal neurons, from responding to visual stimulation, thereby demonstrating a critical role for NCX in mediating sensory driven Ca^{2+} events in glia during early development.

Results

Radial astrocytes in the developing optic tectum of *Xenopus laevis* exhibit extensive spontaneously occurring Ca^{2+} transients

Radial glia, often called radial astrocytes in fish and frogs where they constitute the main astrocytic cell type in these animals, form the scaffold of the optic tectum in *Xenopus laevis,* having at least one large radial process that extends from the ventricular surface to the pial surface where it forms a broad endfoot. Radial astrocyte endfeet are easily identifiable structures that tile the surface of the brain. Their columnar processes extend numerous fine filopodia into the neuropil that contact the synapses formed between presynaptic retinal ganglion cell (RGC) axons and postsynaptic tectal neuron dendrites (Figures 1A-C) (Tremblay et al., 2009; Sild and Ruthazer, 2011). Thus, in the amphibian optic tectum, radial astrocytes are positioned to serve the roles performed in the mammalian brain by classical astrocytes. To generate tadpoles that express GCaMP6s in all the neurons and radial astrocytes of the optic tectum, allowing for simultaneous monitoring of both neuronal and glial Ca^{2+} activity *in vivo,* we performed microinjection of GCaMP6s mRNA in two-cell stage embryos following *in vitro* fertilization. The dynamic Ca^{2+} fluctuations occurring in tectal neurons and glia were imaged using fast *in vivo* resonance scanning two-photon microscopy of these GCaMP6s-expressing tadpoles at developmental stage 47, when considerable retinotectal circuit remodeling is underway. We found that radial astrocytes exhibit spontaneously occurring Ca^{2+} transients in their processes and endfeet (Figure 1D and Video S1). Ca^{2+} signal in the endfeet of radial astrocytes were highly correlated with their neuropil signal (Figure 1E).

Regions of interest representing individual tectal neuron somata and radial astrocyte endfeet were identified using an automated segmentation algorithm and fluorescence traces were analyzed for neurons and glia (Figures 1F, 1G and Video S2). During resting state in darkness, Ca^{2+} events were common in both cell types. We quantified the spontaneous Ca^{2+} events occurring during 5 min in darkness in 200 radial astrocytes and 390 tectal neurons from 21 animals and found that on average there were 6.00 ± 0.64 (mean ± SEM) active glia and 18.57 ± 2.02 spontaneously active tectal neurons per imaging plane in each tectum, out of a total of approximately 20 glia and 150 neurons in the whole imaging field, on average. Over 5 min of imaging, 3.1 ± 0.3 Ca^{2+} events per active glial cell and 6.4 ± 0.4 Ca^{2+} events per active neuron were observed. Together this demonstrates that Ca^{2+} events occurring spontaneously in radial astrocytes during early development are common and that these events can be monitored in tandem with those in nearby neurons during live imaging *in vivo,* allowing for high temporal and spatial resolution investigation of neuron-glia communication in the developing brain.

Resting state Ca^{2+} activity in radial astrocytes is coupled to neuronal spiking activity

We first sought to determine whether the Ca^{2+} transients that occur spontaneously in radial astrocytes during resting state were coupled to neuronal activity (Figure 2). Tetrodotoxin (TTX) is a potent and selective blocker of the voltage-gated Na^{+} channels (NaVs) that underlie action potential generation in neurons. A thin incision through the skin on the head of the tadpole was made to expose the ventricular space and permit rapid pharmacological manipulation of the optic tectum during live imaging (Figure 2A). After imaging a baseline of Ca^{2+} activity over a 5 min

period in darkness, either vehicle control (Figures 2B and 2D) or TTX (1 μM, Figures 2C, 2E and Video S3) was applied to the brain and a second 5 min period of live imaging was carried out. Application of TTX significantly reduced Ca^{2+} activity in both neurons and radial astrocytes, as revealed by a decreased number of active cells (Figures 2F and 2G), a reduction in integrated Ca^{2+} signal (Figures 2H and 2I), and in the number of events in each cell (Figures 2J and 2K). These results are consistent with the Ca^{2+} transients that occur in radial astrocytes being dependent on spiking activity of neurons, although we cannot entirely rule out the possibility that TTX may also have acted directly on radial glia, should they also express NaVs (Pappalardo et al., 2016).

Visual stimulation drives Ca^{2+} increases in radial astrocytes

Next, we tested whether the presentation of a behaviorally relevant visual stimulus could induce Ca^{2+} transients in radial astrocytes in intact animals by collecting a baseline of spontaneous activity in the circuit and then presenting a looming stimulus every 6 s to the eye of the animal (Figures 3A-C and Video S4). Visual looming stimuli consist of a small dark dot rapidly expanding to fill the field of view which mimics a predator approach event. They encapsulate multiple prominent visual elements detected by the developing eye of aquatic animals such as contrast and motion, and reliably evoke a robust innate behavioral escape response (Temizer et al., 2015; Lim and Ruthazer, 2021). Compared to baseline, visual stimulation significantly increased the number of active glia and tectal neurons (Figures 3D and 3E), while also significantly increasing the integrated Ca^{2+} signal in both cell types (Figures 3F and 3G). The looming stimulus also significantly increased the number of events in each cell for both cell

types (Figures 3H and 3I). This further demonstrates that the Ca^{2+} activity of radial astrocytes in the optic tectum is coupled to afferent inputs and shows that these glia in *Xenopus* respond to visual stimulation during early development in the intact animal.

Visual stimulation enhances correlation between neighboring radial astrocytes

Next, we assessed temporal and spatial correlation of Ca^{2+} responses in both cell types in order to gain information about functional connectivity in the optic tectum. Pearson correlation coefficients were calculated using Brainstorm software (Tadel et al., 2011) for each pairwise combination of Ca^{2+} traces (Figures 3J and 3K). Visual stimulation significantly increased the mean pairwise correlation coefficients between glia and between tectal neurons, but only a trend was observed for an increase in correlation between neurons and glia due to visual stimulation (Figure 3L). To determine whether the correlation between cells was proportional to the distance between them, we pooled the correlation data from 8 animals and then plotted the correlation coefficients against the spatial distance between each corresponding pair of cells (Figures 3M-O, Figure S1A-C). To quantify these relationships, we calculated simple linear regressions of the pairwise correlations, comparing baseline and visual stimulation conditions. Under baseline conditions, glia-glia (Figure 3M, Figure S1A) and neuron-neuron (Figure 3N, Figure S1B), but not neuron-glia (Figure 3O, Figure S1C) correlations, decreased as a function of distance between the cells (as revealed by significantly non-zero negative slopes). During visual stimulation, this relationship between correlated activity and distance persisted for glia-glia and neuron-neuron pairs, and a new relationship of distance to correlation appeared for the neuron-glia pairs (Figure 3O, Figure S1C). Together these data indicate that the spontaneous and evoked

activity of both neurons and glia reflect the topographic organization of the optic tectum and its RGC inputs from the eye; however, the comparative lack of spatial clustering of correlated glia-neuron pairs during baseline conditions suggests that their activity may be independently regulated downstream of visual input from RGCs through separate mechanisms with distinct temporal profiles.

Visually-evoked events in radial astrocytes occur out of phase with those in tectal neurons with a delay of several seconds

To better understand the temporal kinetics underlying visually-evoked responses in the optic tectum and to confirm the presence of visually-evoked events in radial astrocytes, we used cross-correlation analysis to quantify the temporal lag between the onset of each neuronal event and the onset of each glial event with respect to the timing of each visual stimulus presentation in each animal. Because, unlike the neurons, glial events did not occur in tight phase with the visual stimulus frequency and varied significantly in shape, duration, and onset time relative to each stimulus, a simple stimulus triggered average to confirm the presence of visually-evoked events in radial astrocytes has limited use. Instead, we calculated the probability of a glial Ca^{2+} event occurring during specific temporal delay windows after the stimulus onset.

To measure the kinetics of visually-evoked responses in glia, we divided glial and neuronal Ca^{2+} traces into 1 s bins, and then cross-correlated the onset of events in each bin with the start of the preceding looming stimulus in order to plot a probability distribution of events occurring in each post-stimulus time bin (Figures 3P-R). In each case we then compared the resulting distributions

to distributions that would have been generated by an equal number of random chance events. Glial events were significantly enriched with probabilities nearly double that of chance at 2-3 s following each stimulus event (Figure 3P), suggesting that on average, visually-evoked events occurred in glia with a 2-3 s delay relative to the stimulus onset. Comparatively, neuronal events were significantly enriched during the first 1 s post-stimulus onset (Figure 3Q), consistent with their rapid occurrence in phase with the stimulus presentation. Examination of the raw neuronal Ca^{2+} traces suggests an average delay of approximately 200-300 ms for neuronal responses following onset of the visual stimulus (Figure 3C). Because the inter-stimulus interval we used for these analyses was relatively short (6 s), we repeated the experiment in 5 animals with a 20 s inter-stimulus interval and observed a similar enrichment of glial events 1-3 s post-stimulus (Figure 3R) suggesting the results obtained with the higher frequency inter-stimulus interval were accurate and did not mask a longer time lag for visually-evoked events in glia (Figure 3S).

Additionally, we assessed the time it took for both cell types to reach the peak of their Ca^{2+} response and found that in general neurons reached a transient peak in the Ca^{2+} signal following each individual stimulus presentation, suggesting discrete responses to each stimulus, whereas glial responses often peaked only after multiple stimulus events had occurred (average 3.86 ± 0.80 presentations of the looming stimulus). This suggests that the radial astrocytes are in a unique position to integrate sensory information occurring across larger spans of time than tectal neurons.

Blockade of gluRs in the optic tectum suppresses spontaneous and visually-evoked Ca^{2+} activity in tectal neurons but not in radial astrocytes

Given that RGC inputs to the tectum are understood to be exclusively glutamatergic (Zhang et al., 1998), and that gluRs have been shown to mediate Ca^{2+} signalling in glia in a number of other contexts, we next sought to determine whether gluRs mediate the visually-evoked responses we observed in radial astrocytes. To accomplish this, we applied a cocktail of pharmacological agents in the optic tectum to block multiple gluRs (NMDARs - 100 μM R-CPP; AMPA/KainateRs - 50 μM DNQX, group II mGluRs - 100 μM LY341495 (Fitzjohn et al., 1998); mGluR1 - 100 μM CPCCOEt) and effectively drove visually-evoked presynaptic release of glu from RGC axons by presentation of a looming stimulus to the eye every 6 s (Figure 4A). As expected, both spontaneous and visually-evoked Ca^{2+} responses in tectal neurons exposed to this cocktail of inhibitors were suppressed (Figures 4B-G,4I,4K and 4M). The timing of the few remaining residual events was not synchronized to the visual stimuli (Figure 4O). However, surprisingly to us, radial astrocytes continued to exhibit robust spontaneous and visually-evoked Ca^{2+} responses with amplitudes and post-stimulus latencies comparable to those observed in unmanipulated animals (Figure 3) despite this broad spectrum blockade of glutamatergic transmission (Figures 4B-H,4J,4L,4N and Video S5). These results indicate the presence of a signaling pathway mediating visually-evoked Ca^{2+} events in radial astrocytes which is dependent upon presynaptic release from RGC axons but that is independent of ionotropic and metabotropic gluRs.

Pharmacological activation of AMPARs or mGluR1, but not mGluR5, can induce Ca^{2+} increases in tectal neurons and radial astrocytes

Despite our experiments largely ruling out gluRs as major contributors to visually-evoked Ca^{2+} responses in radial astrocytes, we remained curious as to whether these glia might still exhibit basal responsiveness to pharmacological activation of various gluRs, given that these receptors have been implicated in mediating glial Ca^{2+} activity, particularly during early development.

As previous research in our lab has demonstrated that NMDARs are not present on radial astrocytes, at least during these developmental stages (Tremblay et al., 2009; Kesner et al., 2020), we focused on the responses of AMPARs and mGluRs (Figure 5), specifically type-1 mGluRs given the weight of the literature suggesting a role for these receptors during early development (Bazargani and Attwell, 2016). Tectal neurons responded strongly to AMPA (100 μM) (Figures 5B,5E,5H-K and Video S6) and to the mGluR1/5 agonist DHPG (200 μM) (Figures 5C,5F,5H-K and Video S7), while unexpectedly (Panatier and Robitaille, 2016), the mGluR5 agonist CHPG (200 μM) did not elicit any significant responses in the tectum (Figures 5D,5G,5H-K and Video S8). It is worth noting that based on our quantification measures, while both agonists activated tectal neurons and radial astrocytes, AMPA appears to have had a stronger influence on neurons than on glia with the reverse being true for DHPG. Together these data demonstrate that activation of AMPARs or mGluR1, but not mGluR5, can induce Ca^{2+} transients in both tectal neurons and radial astrocytes, despite no clear role for activation of these receptors in mediating spontaneous or visually-evoked responses in radial astrocytes.

GluR agonists may be indirectly activating glial cells

Further observation of the temporal kinetics of the responses of tectal cells to AMPAR and mGluR1 agonists revealed a stark contrast in the time between activation of neurons and glia. It was apparent that neuronal responses preceded responses in adjacent glia by a substantial margin. The first Ca^{2+} responses in glia initiated by AMPA and DHPG wash-on occurred 76.2 ± 7.9 s and 16.0 ± 4.2 s respectively following Ca^{2+} rises in neurons occupying the same spatial regions of the optic tectum (Figures 5E and 5F) whereas the delay between the activation of tectal neurons and glia in response to visual stimulation is only 1-3 s (Figure 3). Taken together, these results suggest that Ca^{2+} increases in radial astrocytes induced by AMPAR or mGluR1 activation are likely to be occurring indirectly, induced by depolarization of tectal neurons and not as a result of direct stimulation of glial receptors. It is important to note that given that radial astrocytes line both the ventricular and pial surfaces of the brain, any pharmacological agents acting upon the optic tectum must first diffuse through layers of glia before reaching tectal neurons; therefore, any delay in the onset of glial activity relative to neuronal activity is even further exaggerated as a result. Additionally, the striking mismatch in temporal kinetics between these agonist-induced responses and those occurring physiologically during visual stimulation, offers further evidence that these receptors are unlikely to be contributing in a significant way to the generation of physiologically relevant Ca^{2+} events in radial astrocytes.

Visually-evoked Ca^{2+} increases in radial astrocytes are prevented following blockade of glu reuptake through EAATs

A number of experiments have suggested a role for EAATs in contributing to Ca^{2+} transients in glia *in vivo* (Schummers et al., 2008; Zhang et al., 2019). Having found that gluR blockade was able to isolate the Ca^{2+} response of glia from any visually-evoked postsynaptic neuronal activity, we again blocked all gluRs in the optic tectum while also testing the effects of blocking the principal routes of glu reuptake by glia through EAAT 1 and 2 by presenting visual stimulation in the presence of TFB-TBOA (500 nM) (Figure 6A and Video S9). In contrast to gluR blockade alone, the additional blockade of EAATs resulted in a quantitative decrease in glial activity during visual stimulation, and a complete loss of the peak at 1-3 s in the post-stimulus time histogram, suggesting that glu transporters are required for the generation of visually-evoked Ca^{2+} transients in radial astrocytes in the tectum, independent of postsynaptic neuronal activation (Figure 6B-I). However, EAATs are not thought to be able to directly import Ca^{2+} into the cell, indicating that the Ca^{2+} response is likely mediated by additional downstream signaling events.

Blockade of the reverse mode of NCX also prevents visually-evoked Ca^{2+} increases in radial astrocytes

EAATs co-transport 3 Na^{+} ions into the cell along with each molecule of glu. A number of studies have demonstrated that, at least *in vitro* or in *ex vivo* preparations, NCX on glia, which under normal circumstances uses electrochemical gradients to export Ca^{2+} and import Na^{+}, reverses direction of ion flow following rapid increases in internal Na^{+} concentration, resulting in

the extrusion of Na^+ ions and import of extracellular Ca^{2+} ions (Rose et al., 2020). To determine whether this mechanism may underlie visually-evoked radial astrocytic Ca^{2+} activity in the developing optic tectum *in vivo*, we again applied our cocktail to block gluRs in the optic tectum while additionally blocking the reverse mode of NCX with 50 μM KB-R7943 (Figure 6J and Video S10). Blockade of the reverse mode of NCX fully prevented any increases in glial activity during visual stimulation (Figures 6K,6M,and 6O) and eliminated the hallmark of visually-evoked events in glia (Figure 6Q). Curiously, both the number of tectal neurons and the change in integrated Ca^{2+} signal in the neurons showed very slight but significant increases with visual stimulation under these conditions (Figures 6L and 6N) despite no increase in the number of events or the presence of any visually-evoked responses (Figure 6P and 6R) in these neurons, suggesting that blockade of NCX may prevent the proper extrusion of Ca^{2+} ions from tectal neurons leading to accumulation of Ca^{2+} across time in these cells. Since no visually-evoked glial Ca^{2+} activity could be elicited in the presence of the NCX blocker, similar to what was observed following EAAT blockade, this suggests that *in vivo* the activity of EAATs and NCX family members may be coupled via internal Na^+ concentration, thereby mediating Ca^{2+} responses in glia during visual stimulation as a result of glu reuptake.

Blockade of NCX alone is sufficient to prevent radial astrocytes from responding to visual stimulation

Given that blockade of NCX prevented radial astrocytes from responding to visual stimulation in the presence of gluR blockers, which significantly reduced postsynaptic activity, we set out to determine whether blocking NCX function alone might be sufficient to prevent radial astrocytes

from responding to visual stimulation in the presence of postsynaptic activity. As such, we treated animals with 50 μM KB-R7943 to block NCX before repeating our visual stimulation protocol (Figure 6S and Video S11). Blockade of reverse mode NCX did not prevent tectal neurons from responding to the looming stimulus (Figures 6U,6W,6Y,6AA) although in some animals it did alter their response properties in such a way as to produce progressively greater responses across time which could be consistent with reduced glu clearance under these conditions. In contrast, radial astrocytes did not exhibit any increases in Ca^{2+} activity during visual stimulation (Figures 6T,6V and 6X) with hallmarks of visually-evoked events absent (Figure 6Z). To determine whether this mechanism is dependent upon the specific stimulus used to evoke activity in the optic tectum, we performed additional experiments using a mixed visual stimulus of dark flashes interleaved with checkerboard patterns presented at the same interval we used for the looming stimulus throughout our experiments (Figure S2A). Here we also observed that visually-evoked increases in neuronal and glial Ca^{2+} events were abrogated in glia but not neurons following the blockade of NCX with KB-R7943 (Figure S2B-J). Taken together with the outcomes of the experiments performed above, this strongly suggests that during early development of the retinotectal circuit, the considerable visually-evoked Ca^{2+} activity in radial astrocytes occurring *in vivo* is largely dependent on glu release from presynaptic RGC axons and Ca^{2+} influx through NCX following reuptake of glu rather than through direct or indirect activation of ionotropic or metabotropic gluRs.

Discussion

We found that Ca^{2+} events are common in both postsynaptic tectal neurons and surrounding radial astrocytes, and that these Ca^{2+} events are greatly attenuated by the voltage-gated Na^{+} channel blocker tetrodotoxin, suggesting that the Ca^{2+} activity of both neurons and astrocytes is coupled to neuronal spiking activity. Indeed, presentation of a range of visual stimuli drove increases in the Ca^{2+} activity of both tectal neurons and radial astrocytes with the onset of glial events occurring several seconds after those in neurons. While broad blockade of gluRs in the optic tectum strongly suppressed spontaneous and visually-evoked Ca^{2+} activity in tectal neurons, surprisingly, visually-evoked activity in radial astrocytes was not reduced by this manipulation. This suggests that visually-evoked activity in radial astrocytes may be directly driven by presynaptic release from retinal ganglion cell axons but that it does not require the activation of gluRs. Additionally, when directly comparing the spontaneous activity occurring during baseline in each of the groups, we did not observe any meaningful differences that could suggest that the basal level of functioning of the glia was being impaired by our manipulations in such a way that could prevent them from being recruited by visual stimulation (Figure S3). Despite gluRs not appearing to play an obvious role in the visually-evoked activity of radial astrocytes, pharmacological activation of tectal AMPA receptors and mGluR1, but not mGluR5, did elevate Ca^{2+} levels in these glia; however, the relative timing between the onset of activity in tectal neurons and radial astrocytes under these conditions (tens of seconds to minutes) was well outside the range occurring under normal physiological conditions (three seconds or less), more consistent with the idea that activation of these receptors can indirectly lead to Ca^{2+} increases in glia in response to the depolarization of nearby neurons. Important to the interpretation of our

manipulations as specifically targeting visually-evoked glial events, opposed to nonspecific increases in glial activity occurring during visual stimulation, we did not observe any meaningful differences between the baseline spontaneous activity of any groups, except in animals where gluRs were blocked (Figure S3A-D)

While early research into glial Ca^{2+} signaling suggested mGluRs might directly mediate glial Ca^{2+} events in response to physiological stimulation (Wang et al., 2006), studies over the last decade have begun to converge on the idea that neurotransmitter transporters such as EAATs and GATs mediate a diversity of glial Ca^{2+} responses (Schummers et al., 2008; Doengi et al., 2009; Murphy-Royal et al., 2015; Boddum et al., 2016; Deemyad et al., 2018). Developing a thorough mechanistic understanding of how glial cells detect and integrate sensory-evoked neurotransmission requires approaches that assess the various contributions of, and interplay between, both receptor and transporter mediated signaling pathways simultaneously in both glia and neurons during sensory processing in awake animals. Such approaches will build on the accumulating literature showing that the activity of neurotransmitter transporters and NCX are functionally connected (Rojas et al., 2007; Rose et al., 2020).

We demonstrated that during early development of the amphibian visual system, radial astrocytes exhibit temporally correlated responses to visual stimulation mediated by glu transporters, and that the temporal correlation of glial activity is highest between neighboring glial cells. This suggests that in the developing optic tectum, glial activity reflects a primitive representation of the topographic spatial organization of the visual system (Figure 7A). Given that these glial responses are mediated by glu reuptake, and that unlike neurons, the responses

only peak following multiple repeated visual events, it suggests that these cells may be processing information related to the total amount of sensory activity occurring over extended intervals of time, a phenomenon which may be important for some forms of homeostatic plasticity. While we believe the visually-evoked glial Ca^{2+} signal is primarily mediated by glial EAAT 1/2, the concentration of TFB-TBOA used prevents us from entirely excluding a potential contribution of neuronal EAAT3. Glia may also refine their processing of higher order visual information through the integration of additional modulatory mechanisms, relating to altered states of attention, sleep, or stress, which may modulate the pathway we have identified here (Paukert et al., 2014). Additionally, in response to being activated by neuronal activity, glia are known to both modulate and negatively regulate neural activity through various mechanisms involving neurotransmitter transporters, neuromodulators, and release of gliotransmitters (Panatier et al., 2011; Shigetomi et al., 2011; Boddum et al., 2016; Deemyad et al., 2018; Mu et al., 2019; Lines et al., 2020). In our visual stimulation experiments, while we cannot entirely rule out non-glial mediated effects of pharmacological blockade of NCX in the optic tectum, when suppressing glial activity by blocking NCX we observed that neuronal responses progressively increased in intensity throughout the period of visual stimulation in a number of animals (Figure 6S), an effect not observed under baseline conditions. This effect could be mediated through multiple mechanisms. For example, it may be consistent with NCX blockade impairing glu reuptake through EAATs leading to the progressive accumulation of glu in the neuropil thereby potentiating neuronal responses. Alternatively, it may be attributable to a downregulation in the release by radial astrocytes of factors that could negatively regulate neural activity as has been shown more recently in zebrafish (Mu et al., 2019). It will be valuable in the future to

mechanistically dissect glia-to-neuron signals occurring in the retinotectal circuit and determine how they modulate visual processing and circuit refinement.

In the visual cortex of adult mammals, mature astrocytes have highly selective receptive fields that reflect the topographic organization of the visual system and exhibit narrow orientation selectivity through a mechanism involving glu transporters (Schummers et al., 2008). The temporal kinetics of the Ca^{2+} responses occurring during visual stimulation in radial astrocytes match closely with those observed in astrocytes in the visual cortex of adult ferrets (Schummers et al., 2008) and more recently in the somatosensory cortex of adult mice (Lines et al., 2020), where sensory-evoked Ca^{2+} responses lag behind neuronal responses by seconds. This suggests the possibility that a shared mechanism may be underlying these responses across development and across species.

Radial astrocytes also exhibited Ca^{2+} rises in response to pharmacological activation of AMPARs and mGluR1, similarly to astrocytes in mammalian systems. These agonist-induced events occurred over timescales more than an order of magnitude longer than the timescales over which Ca^{2+} events occur in response to visual stimulation (Figure 7B). This begs the question as to whether the Ca^{2+} elevations occurring in glia in response to pharmacological activation of gluRs result from direct activation of these receptors on glia, or rather are in response to the release of diffusible signals following activation of tectal neurons. GluR activation has been shown to be coupled to the release of diffusible signals such as nitric oxide and endocannabinoids. Despite our observation that the principal source of glial activation by sensory stimulation is the activation of glutatmate uptake transporters, it remains likely that the

release of diffusible signals following activation of gluRs on neurons may still contribute meaningfully to the modulation of Ca^{2+} signaling in glia.

Glial Ca^{2+} responses in our experiments were often enriched in the first couple of minutes of repeated visual stimulation, and consistent with the mechanism we have proposed above, it has been observed elsewhere that the activity-dependent internalization of the glial glu transporter GLT-1 requires Ca^{2+} entry through NCX (Ibanez et al., 2019). This suggests that visual stimulation may lead to the internalization of glial EAATs here as well. Neuronal nitric oxide and glial cGMP-dependent protein kinase (PKG) signaling, which we have previously demonstrated contribute to Ca^{2+} signaling and to the motility of filopodial processes in radial astrocytes (Tremblay et al., 2009; Sild et al., 2016), have also been shown to promote insertion of EAATs into the plasma membrane of Bergmann glia through a signaling cascade involving NO, cGMP, PKG, and Ca^{2+} entry through NCX (Balderas et al., 2014). As such, the potential exists for intensive postsynaptic activation of tectal neuron gluRs and the ensuing release of nitric oxide to facilitate insertion of EAATs into the glial membrane thereby reducing extracellular glu accumulation. Thus, under conditions of glutamatergic blockade, this homeostasis may become dysregulated, possibly leading to increased extracellular glu and increased frequency of glial transients mediated by NCX activity, as we observed. Whether prolonged alterations in glial NCX activity are capable of influencing neural circuit development remains an interesting open question.

Together our experiments demonstrate that during early development radial astrocytes are highly responsive to sensory stimulation *in vivo*. Mechanistically, visually-evoked Ca^{2+} activity in these

cells is driven by the presynaptic release of glu, activation of EAATs and consequently Ca^{2+} influx through NCX (Figure 7C). Our experiments demonstrate that blockade of NCX alone is sufficient to prevent the visually-evoked increase in Ca^{2+} activity in glia resulting from a variety of visual stimuli, and that the Ca^{2+} events in these glia driven by sensory stimulation were not directly dependent to any significant degree on the activation of ionotropic or metabotropic gluRs. We propose a model that takes into account both the observations in the literature that gluRs can mediate glial Ca^{2+} signaling and our observations of gluR-independent rapid Ca^{2+} events. Our study further suggests that NCX may mediate important downstream contributions of glia to neural circuit development, function, plasticity, and behavior, relevant to neural circuits in both healthy and diseased states.

Figures

Figure 1

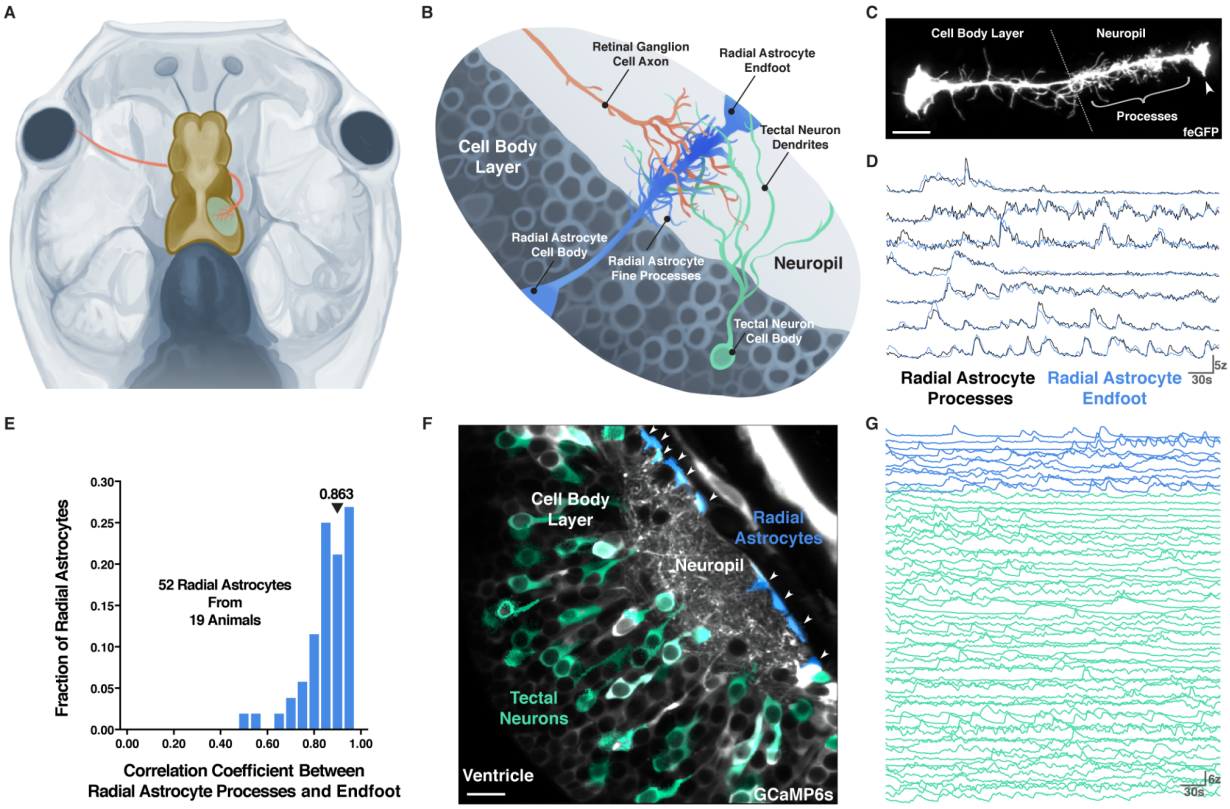

Figure 1: Radial astrocytes in the developing optic tectum of *Xenopus laevis* exhibit extensive spontaneously occurring Ca^{2+} transients.

(A) Retinotectal circuit of a *Xenopus laevis* tadpole highlighted showing a retinal ganglion cell axon (red) innervating the contralateral optic tectum in the brain (yellow).

(B) Cellular organization of the optic tectum showing the spatial relationships between radial astrocytes (blue), presynaptic retinal ganglion cell axons (red), and postsynaptic tectal neuron dendrites (green).

(C) Two-photon z-projection of a radial astrocyte expressing membrane-targeted eGFP, arrowhead indicates the endfoot, scale bar = 10 μm.

(D) Representative traces of resting state Ca^{2+} activity occurring in radial astrocytes where both their processes (black) and endfeet (blue) are visible in the neuropil.

(E) Histogram shows the high degree of correlation between the Ca^{2+} activity in radial astrocyte processes and endfeet, arrowhead at median correlation coefficient.

(F) Averaged temporal projection of 4500 frames (t) from a single optical plane through one hemisphere the optic tectum of a GCaMP6s-expressing tadpole. Regions of interest generated using Suite2p show active tectal neuron cell bodies (green) and radial astrocyte endfeet (blue, arrowheads), scale bar = 25 μm.

(G) Representative traces of resting state Ca^{2+} activity from all active cells in (F), radial astrocyte endfeet (blue), tectal neuron cell bodies (green). Credit: Artwork A. Desaulniers, Orcéine.

Figure 2

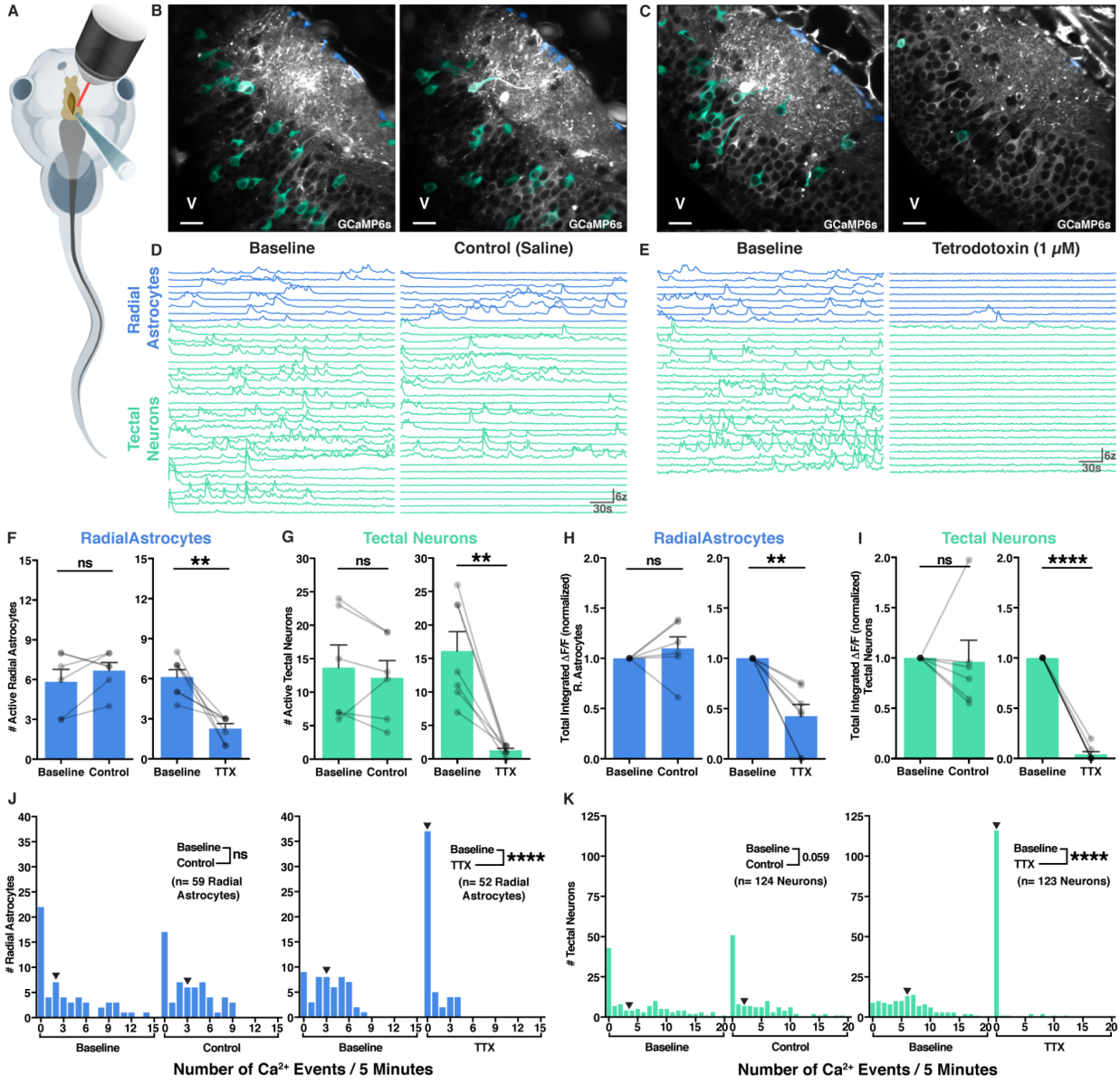

Figure 2: Resting state Ca^{2+} activity in radial astrocytes is coupled to neuronal spiking activity.

(A) Tadpole with a midline slit cut to expose the optic tectum to acute pharmacological manipulation during live imaging.

(B, C) 5 min averaged fields with active ROIs overlaid. In this and subsequent images, radial astrocyte data are presented in blue, neuronal data in green. (B) control group (C) TTX-treated group, V= ventricle, scale bar = 25 μm.

(D, E) Traces of resting state Ca^{2+} activity from (D) control (saline) and (E) TTX-treated animals.

(F, G) Number of active cells during each imaging period. Paired t-tests: control (n=6 animals): $P_{r.astrocytes}$=0.2586, $P_{neurons}$=0.3935. TTX (n=7 animals): **$p_{r.astrocytes}$=0.0041, ** $p_{neurons}$=0.0023.

(H, I) Fold change in integrated DF/F signal for each cell type. Paired t-tests: control (n=6 animals): $p_{r.astrocytes}$=0.4294, $p_{neurons}$=0.8736. TTX (n=7 animals): **$p_{r.astrocytes}$=0.0027, ****$p_{neurons}$<0.0001.

(J, K) Histograms of event counts for each cell during each imaging period. Mann-Whitney tests: control (n=59 r. astrocytes, 124 neurons): $p_{r.astrocytes}$=0.6098, $p_{neurons}$=0.0586. TTX (n=52 r. astrocytes, 123 neurons): ****$p_{r.astrocytes}$<0.0001, ****$p_{neurons}$ <0.0001.

All error bars = standard error of the mean (SEM).

Figure 3

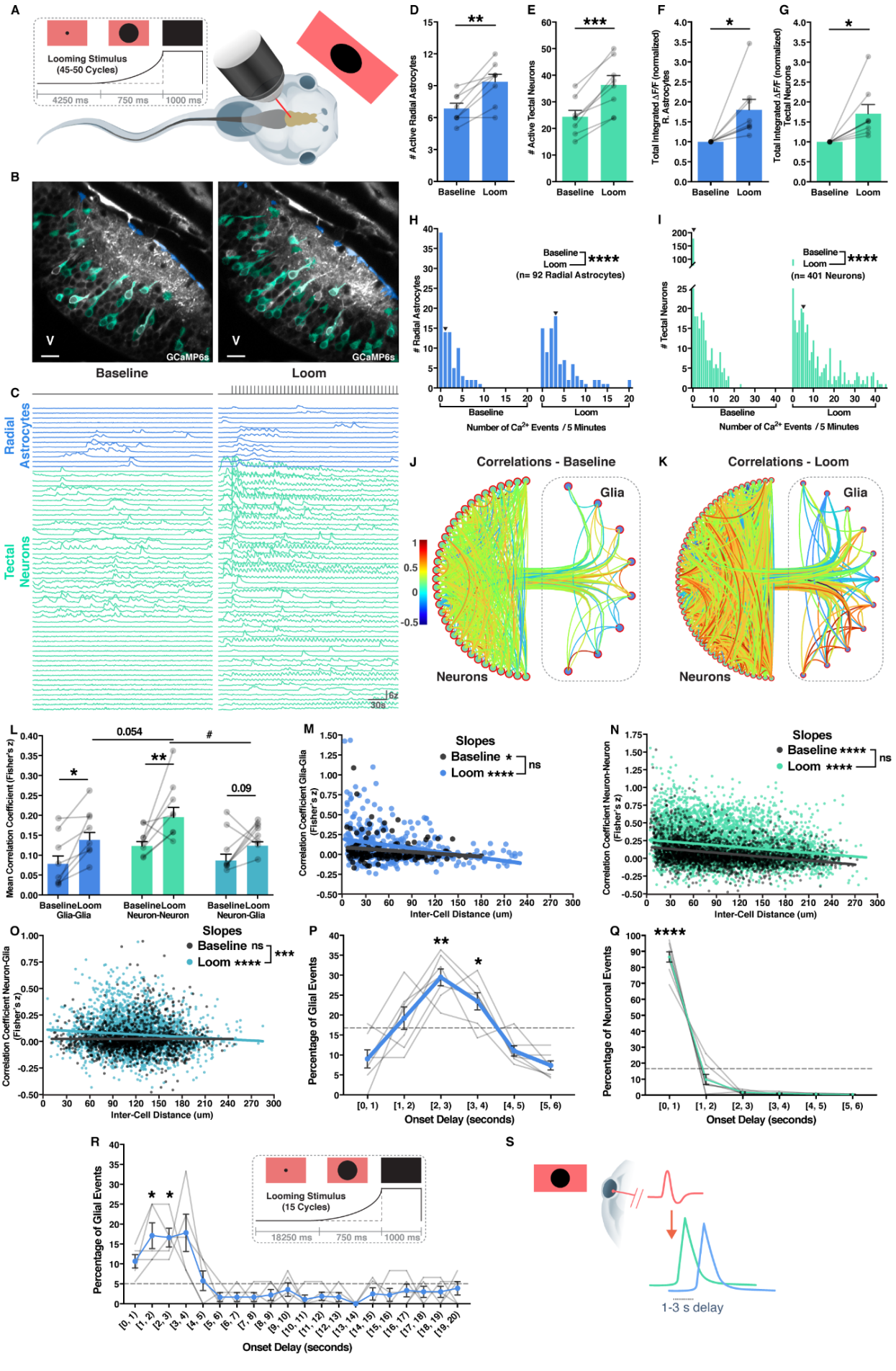
A
Looming Stimulus
(45-50 Cycles)
4250 ms
750 ms
1000 ms
B
V
GCaMP6s
Baseline
Loom
C
Radial Astrocytes
Tectal Neurons
6z
30s
D
Active Radial Astrocytes
Baseline
Loom
E
Active Tectal Neurons
F
Total Integrated ΔF/F (normalized) R. Astrocytes
G
Total Integrated ΔF/F (normalized) Tectal Neurons
H
Radial Astrocytes
(n= 92 Radial Astrocytes)
Number of Ca2+ Events / 5 Minutes
I
Tectal Neurons
(n= 401 Neurons)
J
Correlations - Baseline
Glia
Neurons
K
Correlations - Loom
L
Mean Correlation Coefficient (Fisher's z)
0.054
0.09
Baseline Loom
Glia-Glia
Neuron-Neuron
Neuron-Glia
M
Slopes
Baseline *
Loom ****
ns
Correlation Coefficient Glia-Glia (Fisher's z)
Inter-Cell Distance (um)
N
Slopes
Baseline ****
Loom ****
ns
Correlation Coefficient Neuron-Neuron (Fisher's z)
Inter-Cell Distance (um)
O
Slopes
Baseline ns
Loom ****
***
Correlation Coefficient Neuron-Glia (Fisher's z)
Inter-Cell Distance (um)
P
Percentage of Glial Events
Onset Delay (seconds)
Q
Percentage of Neuronal Events
Onset Delay (seconds)
R
Looming Stimulus
(15 Cycles)
18250 ms
750 ms
1000 ms
Percentage of Glial Events
Onset Delay (seconds)
S
1-3 s delay

Figure 3: Visual stimulation drives correlated-increases in Ca^{2+} activity between neighboring radial astrocytes.

(A) Tadpoles were presented with repeated looming stimuli during live imaging of the optic tectum.

(B) Averaged fields of baseline (left) and stimulus (right) epochs, V= ventricle, scale bar = 25 μm.

(C) Traces of resting state and evoked Ca^{2+} activity during baseline (left) and looming stimulus (right), black lines indicate stimulus presentations.

(D, E) Number of active cells. Paired t-tests (n=8 animals): $^{**}p_{r.astrocytes}=0.0012$, $^{***}p_{neurons}=0.0002$.

(F, G) Fold change in integrated DF/F signal. Paired t-tests (n=8 animals): $^{*}p_{r.astrocytes}=0.0188$, $^{*}p_{neurons}=0.0191$.

(H, I) Event counts. Mann-Whitney tests (n=92 radial astrocytes, 401 neurons): $^{****}p_{r.astrocytes}<0.0001$, $^{****}p_{neurons}<0.0001$.

(J, K) Circular graphs showing correlations between neurons (left), between radial astrocytes (right), and between neurons and astrocytes (linkage between half-circles) in one animal, baseline (J), looming stimulus (K). Cell ordering reflects relative spatial locations of cells.

(L) Mean correlation coefficients between cell types during baseline and looming conditions. Two-way ANOVA (n=8 animals): $F_{stimulation}=22.09$, ***p=0.0002, $F_{celltype}=17.10$, *p=0.0191, Holm-Sidak's tests baseline-loom: $^{*}p_{glia\text{-}glia}=0.0199$, $^{**}p_{neuron\text{-}neuron}=0.0081$, $p_{neuron\text{-}glia}=0.0976$, $p_{neurons\text{-}loom\ vs\ glia\text{-}loom}=0.0516$, $^{\#}p_{neurons\text{-}loom\ vs\ neuron\text{-}glia\text{-}loom}=0.0171$.

(M) Correlation vs. distance plot for radial astrocytes, baseline (black), looming stimulus (blue), n=481 pairs, slopes significantly non-zero: *$p_{baseline}$=0.0413, ****p_{loom}<0.0001, difference between slopes: p=0.1572.

(N) Correlation vs. distance plot for neurons, baseline (black), looming stimulus (green), n=8500 pairs, slopes significantly non-zero: ****$p_{baseline}$<0.0001, ****p_{loom}<0.0001, difference between slopes: p=0.6413.

(O) Correlation vs. distance plot for neuron-radial astrocyte pairs, baseline (black), looming stimulus (turquoise), n=4360 pairs, slopes significantly non-zero: $p_{baseline}$=0.9908, ****p_{loom}<0.0001, difference between slopes: **p=0.0018.

(P, Q) Cross-correlation of glial (P) and neuronal (Q) events to each preceding looming stimulus, onsets binned in 1 s intervals. Horizontal dotted line marks chance distribution. One-way ANOVAs (n=8 animals): (P) r. astrocytes: F=15.46, ****p<0.0001, Holm-Sidak's tests bin-chance: **$p_{[2,3)}$=0.0019, *$p_{[3,4)}$=0.0198, (Q) neurons: F=290, ****p<0.0001, Holm-Sidak's tests bin-chance: ****$p_{[0,1)}$<0.0001.

(R) Cross-correlation of glial events to each preceding looming stimulus (20 s inter-stimulus interval). Horizontal dotted line marks chance distribution. One-way ANOVA (n=8 animals): F=8.315, **p=0.0056, Holm-Sidak's tests: *$p_{[1,2)}$=0.0402, *$p_{[2,3)}$=0.0235, $p_{[3,4)}$=0.0517.

(S) Visually-evoked Ca^{2+} events in radial astrocytes occur with a delay of 1-3 s relative to the looming stimulus.

All error bars = SEM.

See also Figure S1.

Figure 4

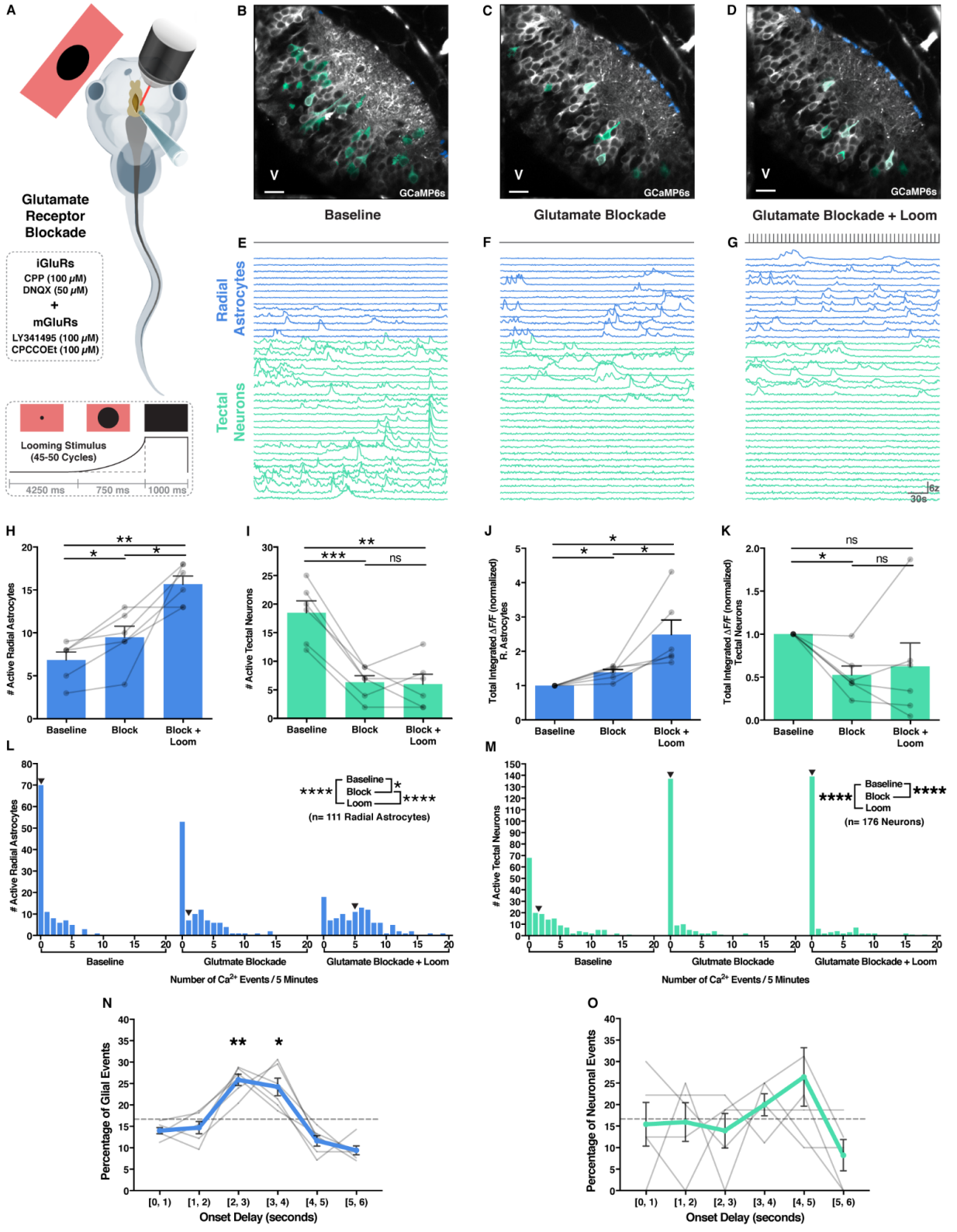
A
Glutamate Receptor Blockade
iGluRs
CPP (100 μM)
DNQX (50 μM)
+
mGluRs
LY341495 (100 μM)
CPCCOEt (100 μM)
Looming Stimulus (45-50 Cycles)
4250 ms
750 ms
1000 ms
B
C
D
V
GCaMP6s
Baseline
Glutamate Blockade
Glutamate Blockade + Loom
E
F
G
Radial Astrocytes
Tectal Neurons
6z
30s
H
Active Radial Astrocytes
I
Active Tectal Neurons
J
Total Integrated ΔF/F (normalized) R. Astrocytes
K
Total Integrated ΔF/F (normalized) Tectal Neurons
Baseline
Block
Block + Loom
ns
L
Active Radial Astrocytes
Baseline
Block
Loom
(n= 111 Radial Astrocytes)
Baseline
Glutmate Blockade
Glutamate Blockade + Loom
Number of Ca2+ Events / 5 Minutes
M
Active Tectal Neurons
(n= 176 Neurons)
N
Percentage of Glial Events
[0, 1)
[1, 2)
[2, 3)
[3, 4)
[4, 5)
[5, 6)
Onset Delay (seconds)
O
Percentage of Neuronal Events

Figure 4: Blockade of ionotropic and metabotropic gluRs in the optic tectum suppresses spontaneous and visually-evoked Ca^{2+} activity in tectal neurons but not in radial astrocytes.

(A) Pharmacological manipulation of tectum was performed along with repeated looming stimulus presentation during live imaging. GluR antagonist cocktail consisted of 100 μM CPP, 50 μM DNQX, 100 μM LY341495, and 100 μM CPPCCOEt.

(B-D) Averaged image fields, (B) baseline, (C) after gluR blockade, (D) plus looming stimulus presentation, V= ventricle, scale bar = 25 μm.

(E-G) Traces of Ca^{2+} activity.

(H, I) Number of active cells. One-way repeated measures ANOVAs (n=6 animals): (H) r. astrocytes: F=20.41, **p=0.0036, Tukey's tests: *$p_{baseline\ vs\ block}$ =0.0382, **$p_{baseline\ vs\ loom}$=0.0034, *$p_{block\ vs\ loom}$ =0.0477, (I) neurons: F=39.76, ****p<0.0001: ***$p_{baseline\ vs\ block}$ =0.0004, **$p_{baseline\ vs\ loom}$ =0.0027, $p_{block\ vs\ loom}$ =0.9778.

(J, K) Fold change in integrated DF/F. One-way repeated measures ANOVAs (n=6 animals): (J) radial astrocytes: F=10.26, *p=0.0215: *$p_{baseline\ vs\ block}$=0.0159, *$p_{baseline\ vs\ loom}$ =0.0338, *$p_{block\ vs\ loom}$ =0.0412, (K) neurons: F=3.254, p=0.1276: *$p_{baseline\ vs\ block}$=0.0143, $p_{baseline\ vs\ loom}$ =0.4149, $p_{block\ vs\ loom}$ =0.8420.

(L, M) Event counts. One-way repeated measures ANOVAs (n=111 radial astrocytes, 176 neurons, from 6 animals): (L) r. astrocytes: F=47.17, ****p<0.0001, Tukey's tests: *$p_{baseline\ vs\ block}$=0.0218, ****$p_{baseline\ vs\ loom}$<0.0001, ****$p_{block\ vs\ loom}$<0.0001, (M) neurons: F=21.35, ****p<0.0001: ****$p_{baseline\ vs\ block}$< 0.0001, ****$p_{baseline\ vs\ loom}$<0.0001, $p_{block\ vs\ loom}$=0.2704.

(N, O) Cross-correlation of glial (N) and neuronal (O) events to each preceding looming stimulus. One-way ANOVAs (n=6 animals): (N) radial astrocytes: F=20.80, ****p<0.0001,

Holm-Sidak's tests vs bin-chance: $^{**}p_{[2,3)}=0.0018$, $^{*}p_{[3,4)}=0.0144$, (O) neurons: $F=1.046$, $p=0.3762$.

All error bars = SEM.

Figure 5

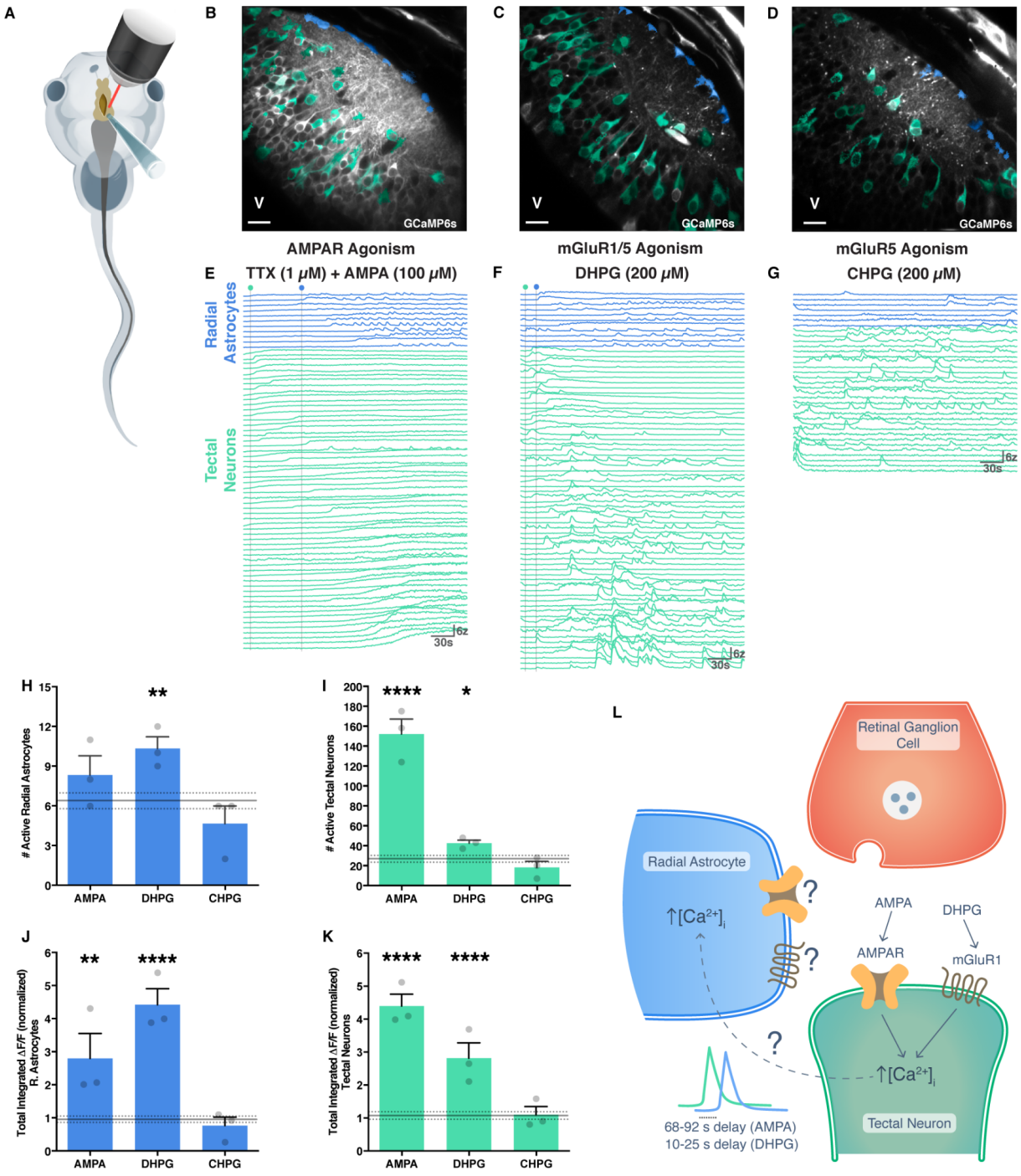

Figure 5: Pharmacological activation of AMPARs or mGluR1, but not mGluR5, can induce Ca^{2+} increases in tectal neurons and radial astrocytes.

(A) Pharmacological manipulation of tectum was performed during live imaging.

(B-D) Averaged imaging fields, (B) 1 μm TTX + 100 μM AMPA, (C) 200 μM DHPG, (D) 200 μM CHPG (V= ventricle, scale bar = 25 μm).

(E-G) Traces of Ca^{2+} activity, (E) 1 μm TTX + 100 μM AMPA, (F) 200 μM DHPG, (G) 200 μM CHPG, vertical lines mark onset of drug effect.

(H, I) Number of active cells, black lines indicate mean ± s.e.m. of baseline data from Figures 3D and 3E. One-way ANOVAs (n=3 animals per treatment group): (H) radial astrocytes: F=5.234 *p=0.0137, Fisher's LSD tests baseline-agonist: p_{AMPA}=0.1557, **p_{DHPG}=0.0094, p_{CHPG}=0.2113, (I) neurons: F=87.67, ****p<0.0001: ****p_{AMPA}<0.0001, *p_{DHPG}=0.0468, p_{CHPG}=0.4805.

(J, K) Fold change in integrated DF/F, black lines indicate mean ± s.e.m. of baseline data from Figures 3F and 3G. One-way ANOVAs (n=3 animals per treatment group): (J) radial astrocytes: F=21.46, ****p<0.0001: **p_{AMPA}=0.0011, ****p_{DHPG}<0.0001, p_{CHPG}=0.5896, (K) neurons: F=52.87, ****p<0.0001: ****p_{AMPA}<0.0001, ****p_{DHPG}<0.0001, p_{CHPG}=0.7356.

(L) Pharmacologically activating AMPAR or mGluR1 leads to Ca^{2+} increases in both neurons and radial astrocytes, but increases in radial astrocytes are delayed by tens of seconds relative to increases in neighboring neurons.

All error bars = SEM.

Figure 6

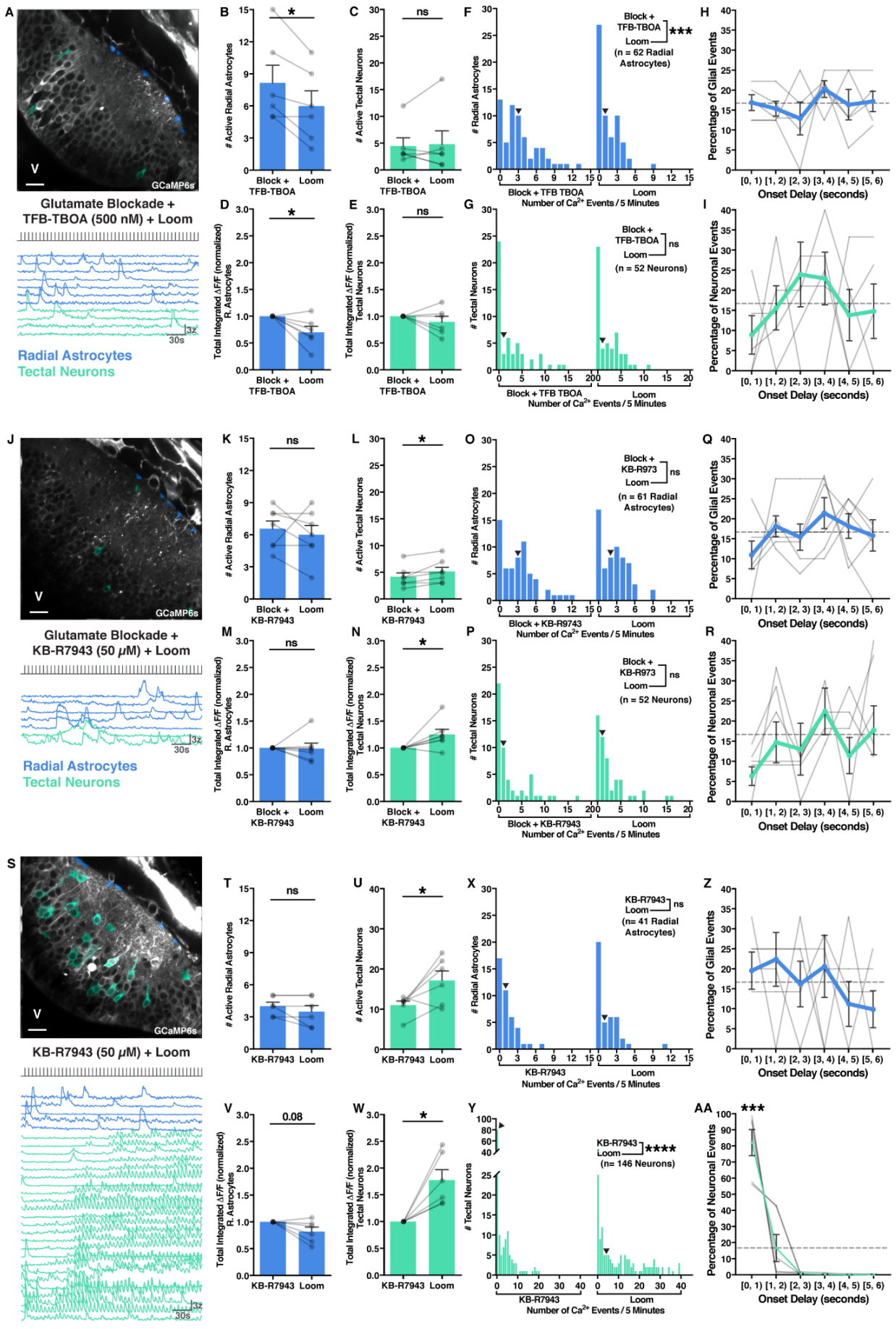
A
V
GCaMP6s
Glutamate Blockade +
TFB-TBOA (500 nM) + Loom
3z
30s
Radial Astrocytes
Tectal Neurons
B
Active Radial Astrocytes
*
Block + TFB-TBOA
Loom
C
Active Tectal Neurons
ns
D
Total Integrated ΔF/F (normalized) R. Astrocytes
E
Total Integrated ΔF/F (normalized) Tectal Neurons
F
Radial Astrocytes
Block + TFB-TBOA
***
(n = 62 Radial Astrocytes)
Block + TFB TBOA
Loom
Number of Ca2+ Events / 5 Minutes
G
Tectal Neurons
ns
(n = 52 Neurons)
H
Percentage of Glial Events
[0, 1) [1, 2) [2, 3) [3, 4) [4, 5) [5, 6)
Onset Delay (seconds)
I
Percentage of Neuronal Events
J
Glutamate Blockade +
KB-R7943 (50 μM) + Loom
Block + KB-R7943
K
L
M
N
O
Block + KB-R973
(n = 61 Radial Astrocytes)
P
(n = 52 Neurons)
Q
R
S
KB-R7943 (50 μM) + Loom
KB-R7943
T
U
V
0.08
W
X
KB-R7943
(n= 41 Radial Astrocytes)
Y
****
(n= 146 Neurons)
Z
AA

Figure 6: Visually-evoked Ca^{2+} increases in radial astrocytes are prevented following blockade of glu reuptake through EAATs or the reverse mode of NCX.

(A) Averaged imaging fields and traces of Ca^{2+} activity during gluR blockade + 500 nM TFB-TBOA with looming stimuli, V= ventricle, scale bar = 25 μm.

(B, C) Number of active cells. Paired t-tests (n=6 animals): $*p_{r.astrocytes}=0.0155$, $p_{neurons}=0.7771$.

(D, E) Fold change in integrated DF/F. Paired t-tests (n=6 animals): $*p_{r.astrocytes}=0.0461$, $p_{neurons}=0.3647$.

(F, G) Event counts. Mann-Whitney tests (n=62 radial astrocytes, 52 neurons, from 6 animals): $***p_{r.astrocytes}=0.0006$, $p_{neurons}=0.9118$.

(H, I) Cross-correlation of glial (H) and neuronal (I) events to each preceding looming stimulus. One-way ANOVAs (n=6 animals): (H) radial astrocytes: F=0.9324, p=0.3902, (I) neurons: F=0.6670, p=0.5150.

(J) Averaged fields and traces of Ca^{2+} activity during gluR blockade + 50 μM KB-R7943 with looming stimulus (V= ventricle, scale bar = 25 μm).

(K, L) Number of active cells. Paired t-tests (n=7 animals): $p_{r.astrocytes}=0.5352$, $*p_{neurons}=0.0382$.

(M, N) Fold change in integrated DF/F. Paired t-tests (n=7 animals): $p_{r.astrocytes}=0.9199$, $*p_{neurons}=0.0459$.

(O, P) Event counts. Mann-Whitney tests (n=61 radial astrocytes, 52 neurons, from 7 animals): $p_{r.astrocytes}=0.3370$, $p_{neurons}=0.5049$.

(Q, R) Cross-correlation of glial (Q) and neuronal (R) events to each preceding looming stimulus. One-way ANOVAs (n=7 animals): (Q) radial astrocytes: F=1.131, p=0.3002, (R) neurons: F=1.161, p=0.3474.

(S) Averaged fields and traces of Ca^{2+} activity during 50 μM KB-R7943 with looming stimulus, V= ventricle, scale bar = 25 μm.

(T, U) Number of active cells. Paired t-tests (n=6 animals): $p_{r.astrocytes}$=0.2031, *$p_{neurons}$=0.0421.

(V, W) Fold change in integrated DF/F. Paired t-tests (n=6 animals): $p_{r.astrocytes}$=0.0868, *$p_{neurons}$=0.0114.

(X, Y) Event counts. Mann-Whitney tests (n=41 radial astrocytes, 146 neurons, from 6 animals): $p_{r.astrocytes}$=0.9902, ****$p_{neurons}$<0.0001.

(Z, AA) Cross-correlation of glial (Z) and neuronal (AA) events to each preceding looming stimulus. One-way ANOVAs (n=6 animals): (Z) r. astrocytes: F=0.6260, p=0.5528, (AA) neurons: F=39.36, **p=0.0015, Holm-Sidak's tests vs bin-chance: ***$p_{[0,1)}$=0.0002.

All error bars = SEM.

See also Figure S2.

Figure 7

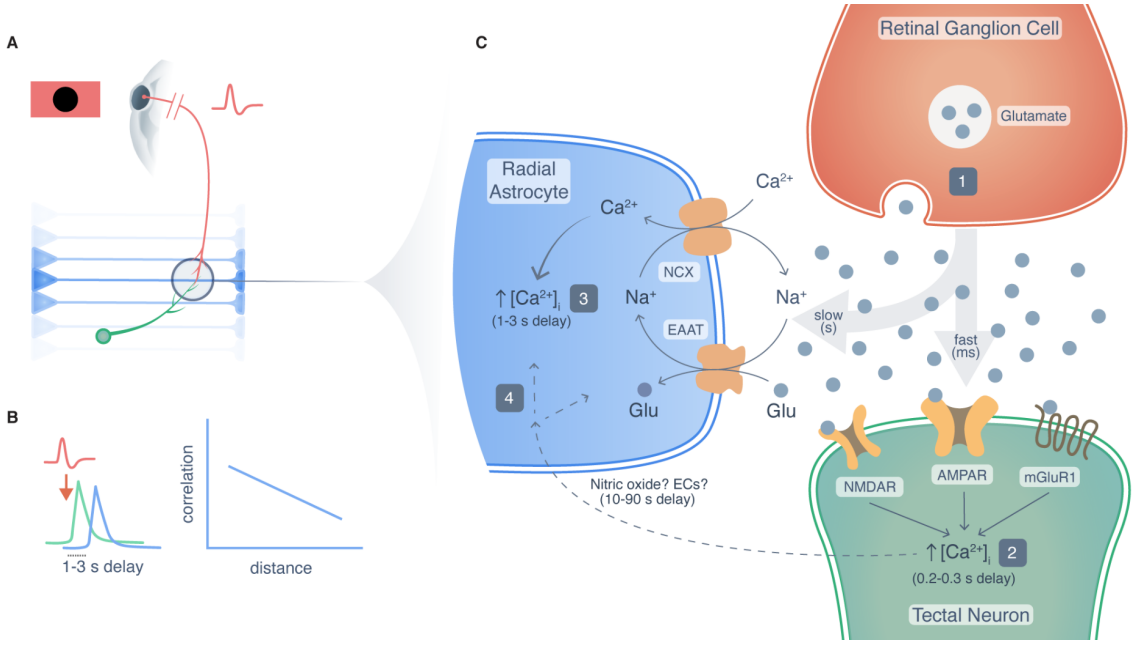

Figure 7: NCX mediates sensory-evoked radial astrocyte Ca^{2+} transients in the developing retinotectal system.

(A) Looming stimuli induce activity in cells converging in the neuropil in the *Xenopus laevis* retinotectal circuit (retinal ganglion cell - red, radial astrocytes - blue, tectal neuron - green).

(B) While visually-evoked Ca^{2+} events occur in tectal neurons within hundreds of milliseconds following retinal ganglion cell activation, visually-evoked Ca^{2+} events occur in radial astrocytes with a delay of multiple seconds. The temporal correlation between Ca^{2+} events in radial astrocytes increases as the inter-cell distance decreases suggesting the activity of radial astrocytes reflects the topographical convergence of retinal inputs in the tectum.

(C) Schematic of the mechanism underlying visually-evoked Ca^{2+} activity in the optic tectum.

(1) Visual stimulation induces release of glu from RGC axons.

(2) Within milliseconds, Ca^{2+} elevations in tectal neurons occur following the activation of gluRs.

(3) Seconds later, Ca^{2+} elevations in radial astrocytes occur through the activation of EAATs, accumulation of intracellular Na^{+}, and reversal of NCX.

(4) Pharmacological activation of gluRs on tectal neurons suggests the release of diffusible signals such as nitric oxide or endocannabinoids may further modulate radial astrocyte Ca^{2+} activity under certain conditions. Credit: Artwork, A. Desaulniers, Orcéine.

Acknowledgements

We thank M.P. Cousineau and S. Baillet (McGill University) for assistance with Brainstorm software. Artwork was kindly provided by Ms. Audrey Desaulniers, Orcéine, Montreal, Canada. This research was supported by Canada Graduate Scholarships - Masters to N.B. and V.L. and a Postgraduate Scholarship - Doctoral to N.B. from the Natural Sciences and Engineering Research Council of Canada. E.S.R. was funded by a grant from the Canadian Institutes of Health Research (FDN-143238) and a Research Chair from the Fonds de recherche santé Québec (31036). A.S. and E.S.R. were also supported by the Brain Canada Canadian Neurophotonics Platform.

Author Contributions

N.B. and E.S.R. conceived and designed the study. N.B. performed all imaging experiments and data analysis. A.S. developed the labeling methodology and provided technical support. V.L. provided analysis software and helped develop labeling methodology. N.B. and E.S.R. drafted the manuscript. All authors provided critical feedback and editing of the final manuscript. E.S.R obtained funding and supervised the research.

Declaration of Interests

The authors declare no competing interests.

STAR Methods

RESOURCE AVAILABILITY

Lead Contact

Further information and requests for resources and reagents should be directed to and will be fulfilled by the lead contact, Edward S. Ruthazer (edward.ruthazer@mcgill.ca).

Materials Availability

Any reagents generated for this study will be made available upon request to the lead contact. Alternatively, the requestor will be directed to a public repository tasked with distributing the reagent.

Data and Code Availability

All data reported in this paper will be shared by the lead contact upon request. DOIs for deposited data are available in the Key Resources Table. All original code has been deposited at Mendeley and is publicly available as of the date of publication. DOIs are listed in the Key Resources Table. Any additional information required to reanalyze the data in this paper is available from the lead contact upon request.

EXPERIMENTAL MODEL AND SUBJECT DETAILS

Adult albino *Xenopus laevis* frogs were housed in the Montreal Neurological Institute-Hospital Centre for Neurological Disease Models animal care facility. All animal use and experiments were approved by the Montreal Neurological Institute-Hospital Animal Care Committee and carried out in accordance with Canadian Council of Animal Care guidelines. The ages of the animals used in our experiments ranged from developmental stage 46 to 48. The sex of the animals used in our experiments was not assessed as sexual characteristics are not present at these early developmental stages.

METHOD DETAILS

Experimental Design

Sample sizes were based on values which had previously been established to produce significant effects on an independent positive control dataset. For all experiments at least 2-3 biological replicates were performed. No data were excluded from analysis in this study. Animals were screened at random for the appropriate expression of GCaMP6s/mCherry and used in the order they were initially identified. Experiments were carried out under conditions blind to experimental manipulation.

GCaMP6s mRNA synthesis

The coding sequence of each GCaMP6s and mCherry were cloned into pCS2+ and the plasmids were linearized with NotI. Capped mRNA of GCaMP6s and mCherry were transcribed with the SP6 mMessage mMachine Kit (Ambion, Thermo Fisher). The GCaMP6s and mCherry mRNA were injected together at the two-cell stage into one blastomere of the embryo.

Generation of GCaMP6s-expressing tadpoles

In vitro fertilization was used to prepare eggs for GCaMP6s mRNA injection. Adult female frogs were primed for egg laying by injection of pregnant mare serum gonadotropin (PMSG, 50UI, Prospec Bio) 4 days before *in vitro* fertilization. In the afternoon preceding *in vitro* fertilization, the frogs previously injected with PMSG were injected with human chorionic gonadotropin (hCG, 400UI, Sigma) to induce egg laying. The following morning an adult male frog was anesthetized by submersion in tricaine mesylate (MS-222, 0.2% w/v, Sigma) until reflexes were unresponsive (approximately 30 minutes). Once anesthetized, the head of the frog was severed and the skin on the belly cut open to expose internal organs. Testis were located and surgically removed and placed in ice chilled 1X Modified Barth's Solution with HEPES (MBSH). Adult female frogs injected with hCG the previous day were then squeezed and eggs were collected in a clean 100 mm petri dish. A testis was placed in a 50 µL drop of 1X MBSH in the petri dish with the unfertilized eggs and then a portion of it was removed and macerated with a razorblade. A pipette tip was then used to mix the eggs with the macerated testis solution. To activate the sperm and initiate *in vitro* fertilization, 750 µL of 0.1X MBSH was added to the eggs and the mixture was kept at room temperature for 5 min before being submerged completely with 0.1X MBSH. After 10 min, embryos were degellied in cysteine (2% w/v in distilled water, pH 8.0,

Sigma), washed twice in distilled water, then washed twice in 0.1X MBSH, and then monitored until they completed their first cell division and reached the two-cell stage. At this point, the embryos were transferred into a petri dish lined with a custom-made grid filled with 2% ficoll in 1X MBSH. Then 500 pg GCaMP6s mRNA along with 250 pg mCherry mRNA, in 2 nL RNAse-free water were pressure injected into one of the two cells of the embryo using a calibrated glass micropipette attached to a PLI-100 picoinjector (Harvard Apparatus). After injection the embryos in 2% ficoll in 1X MBSH were placed in an incubator and kept at 18 degree Celsius for 3 h before being transferred to 1% ficoll in 0.1X MBSH and then kept at 18 degrees Celsius overnight. The next morning embryos were transferred to 0.1X MBSH and raised at 18 degrees Celsius in a biological oxygen demand incubator with a 12 h light / 12 h dark cycle until they reached stage 47.

Tectal electroporation of individual radial astrocytes

To visualize the structure of individual radial astrocytes, the optic tectum of stage 45 tadpoles was electroporated with plasmids encoding EGFP-F following protocols described previously by our lab (Tremblay et al., 2009). Tadpoles were anesthetised in MS-222 (0.02% in 0.1X MBSH), then a brief interventricular injection was performed using a glass micropipette containing 0.5-1 µg/uL pEGFP-F plasmid and the visual indicator fast green. After placing two platinum electrodes on either side of the optic tectum, a Grass Instruments SD9 electrical stimulator outfitted with a 3 µF capacitor was set to 37 V and used to apply three 1.6 ms pulses across the brain in each direction of polarity. Animals recovered in 0.1X MBSH for 48 hours before imaging.

Preparing GCaMP6s-expressing tadpoles for live imaging

Stage 46-47 GCaMP6s-expressing tadpoles were screened for adequate levels of GCaMP6s expression on an Olympus BX-43 epifluorescence microscope prior to imaging. Animals were then immobilized by immersion in a solution of 2 mM pancurionium dibromide (Tocris) in 0.1X MBSH for 2-5 min. Then animals were placed in the middle of a 6 cm diameter petri dish lid and embedded in 0.8% low melting point agarose (Thermo Fisher). To bypass the blood brain barrier and permit for acute pharmacological intervention, a small incision was made into the dorsal surface of the skin of some tadpoles in between the hemispheres of the optic tectum using a 30 ga syringe needle to expose the associated ventricle. After embedding, intact animals were submerged in 9 mL of 0.1X MBSH, while those that underwent incision, were submerged in 9 mL of external saline solution (in mM – 115 NaCl, 2 KCl, 3 CaCl2, 3 MgCl2, 5 HEPES, and 10 glucose, pH 7.20, 250 mOsm).

Two-photon microscope

Live imaging was performed using a Thorlabs multiphoton resonant scanner microscope with a 20X water-immersion objective (1.0 NA) mounted on a piezoelectric focus mount (PI). Fluorescence excitation light was generated using a Spectra-Physics InSight3x infrared femtosecond pulsed laser. Data was collected using ThorImage LS software.

In vivo Ca^{2+} imaging of GCaMP6s-expressing tadpoles

Before imaging, animals were left to settle under the microscope for 15 min to reduce drift in x, y, and z dimensions. Ca^{2+} imaging was then carried out using an excitation wavelength of 910 nm at an approximate power of 125 mW, measured before the scanhead. Each imaging epoch consists of 4500 images collected at 15 frames per second from a single z plane with x-y dimensions of 224.256 μm by 224.256 μm at a resolution of 512 by 512 pixels. Using ImageJ, images were then saved as tiff stacks for further processing.

Baseline timepoints were collected in darkness. For timepoints involving pharmacological treatments, compounds were first dissolved to the appropriate concentration in 1 mL of external saline solution and introduced to the bath in which the animal was embedded via micropipette. Agonists were applied to the bath immediately before an imaging epoch commenced while antagonists were applied immediately following the acquisition of baseline timepoints and allowed to equilibrate for 15 min before imaging. Visual stimuli were presented to the contralateral eye of the animal during treatment timepoints using a flat panel display screen (800 x 480, Adafruit, NY) covered with a red-filter (Wratten #29, Kodak) to prevent activation of the green channel PMT.

Visual stimulation paradigm

For visual stimulation of GCaMP6s-expressing tadpoles, a video of a dark looming stimulus was created using Adobe After Effects. A small dark dot remains stationary in the middle of the screen for 4250 ms before rapidly expanding to fill the visual field over 750 ms; the screen then

remains dark for 1000 ms before resetting and repeating every 6 s during the 5-minute treatment period. A looming stimulus with the same parameters but which repeated only once every 20 s was also used under select conditions. A mixed stimulus consisting of 5000 ms of blank screen followed by either a dark whole field flash lasting 1 s or a checkerboard pattern lasting 1 s was also used under select conditions.

QUANTIFICATION AND STATISTICAL ANALYSIS

Registration and ROI extraction of raw Ca^{2+} imaging data using Suite2p

Suite2p software (https://github.com/MouseLand/suite2p) was run using Python 3. Tiff stacks of raw Ca^{2+} imaging data collected on a two-photon microscope were imported into Suite2p for registration and automated detection of regions of interest (ROIs) based on regions of dynamic Ca^{2+} activity. Both rigid and nonrigid registration were performed using the default configurations of the software. Automated ROI detection used the default parameters of the software except the threshold scaling value was increased to 3.5 to favor detection of structures with a high signal to noise ratio. Then using the software GUI, ROIs were curated by hand to remove those that were neither tectal neuron cell bodies nor radial astrocyte endfeet. Raw fluorescence traces for each ROI were extracted from Suite2p as CSV files and used for further analysis.

Baseline normalization of Ca^{2+} traces and quantification of Ca^{2+} increases and events

To estimate the baseline fluorescence intensity of the Ca^{2+} trace for each ROI, we calculated the bottom 5th percentile of values occurring in the Ca^{2+} trace for that ROI during each 5-minute epoch. Fold change in total Ca^{2+} was calculated by summing the area under the curve of each baseline corrected DF/F Ca^{2+} trace for glia and for neurons in each animal and then normalizing the treatment SUM to the baseline SUM in each case. To quantify the number of Ca^{2+} events occurring in an ROI during each 5 min epoch, we z-scored the Ca^{2+} traces by subtracting the baseline from each value and then dividing by the standard deviation of the values in that trace. Increases in a Ca^{2+} trace were counted as events if they exceeded a z-score of 2. The presence of visually-evoked events was assayed for by first downsampling raw fluorescence traces (15 frames per second) into 1 s bins and then cross-correlating the onset of events in each binned time interval with the onset of the most recent preceding visual stimulus event in order to plot the fraction of events occurring in each binned time interval.

Correlation analysis, quantification, and visualization using Brainstorm

Suite2p files containing the ROIs and fluorescence traces for each experiment were imported into Brainstorm software[38]. Brainstorm was used to assess aspects of temporal correlation and functional connectivity between cells in the network while at rest and during visual stimulation. First, after importing the data, ROIs were annotated by hand as either being tectal neurons or radial astrocytes and segmented into left and right hemispheres respectively for later visualization. Then an N x N correlation matrix of Pearson correlation coefficients was calculated from all the pairwise combinations of ROIs from each animal. For each animal, network connectivity during each imaging epoch was then visualized by plotting the raw

correlation matrix as a circular graph with tectal neuron ROIs along the left side, radial astrocyte ROIs along the right side, and the strength of the correlations between cells as color-coded lines between ROIs.

To quantify the average level of correlation (both positive and negative) that exists between cells of each type in the network for each animal and whether it changes during visual stimulation, raw correlation matrices containing Pearson correlation coefficients for each pair of ROIs were first Fisher's z transformed and converted to absolute values. These matrices of absolute values were then analyzed by looking at each type of possible intercellular correlation (neuron - neuron, glial - glial, and neuron - glial). For each animal the mean Fisher's z transformed Pearson correlation coefficient (absolute value) was calculated between all of its tectal neurons, between all of its radial astrocytes, and between all of its tectal neurons and radial astrocytes. Average correlation coefficients for each animal were then compared between resting state and visual stimulation.

To quantify whether the correlations that exist between cell types in the optic tectum are proportional to the distance between the cells and whether this relationship is influenced by visual stimulation, first we pooled the data from 8 animals into two groups: baseline and visual stimulation. We then extracted the linear distances between each of these pairs of ROIs using a custom Matlab script and matched them to the corresponding Pearson correlation coefficient for that pair. We processed the data in groups based on cell type like above by plotting intercellular distance against Fisher's z transformed Pearson correlation coefficient for each pair of ROIs, and then analyzed the relationships using linear regression analysis.

Statistical Analysis

GraphPad Prism software was used for all statistical analyses. All measurements were taken from distinct samples unless otherwise stated. All data were tested for normality. Pairwise analyses used two-tailed paired t-tests (animal level data, baseline vs. treatment) or Mann-Whitney tests (pooled cell level data, baseline vs. treatment). Group analysis data used two-way ANOVA with Tukey's multiple comparisons tests (correlations between different cell types within group), one-way ANOVA with Dunnett's multiple comparisons tests (cell level data correcting for multiple comparisons), Fisher's LSD tests (animal level data not correcting for multiple comparisons) (comparing different drug treatment groups to the control group), or one-way repeated measures ANOVA with Tukey's multiple comparisons tests (comparing multiple treatments within the same group correcting for multiple comparisons). All regression analysis was performed using simple linear regression. Measures were reported as mean ± standard error of the mean, unless otherwise indicated. Statistical details can be found in the figure legends. Significance was defined as a p-value of 0.05 or less. All p-values can be found along with the relevant statistical information in the figure legends.

Descriptive Titles for Videos

Video S1. Correlated calcium events in radial astrocyte processes and endfeet, Related to Figure 1.

Video S2. Spontaneous calcium activity in all cells of the *Xenopus laevis* optic tectum, Related to Figure 1.

Video S3. Reduction in spontaneous calcium activity following application of TTX, Related to Figure 2.

Video S4. Visually-evoked calcium responses in the *Xenopus laevis* optic tectum, Related to Figure 3.

Video S5. Visually-evoked calcium responses following blockade of glutamate receptors, Related to Figure 4.

Video S6. AMPA induced calcium activity in the TTX treated optic tectum, Related to Figure 5.

Video S7. DHPG induced calcium activity in the optic tectum, Related to Figure 5.

Video S8. Spontaneous calcium activity in the optic tectum following treatment with CHPG, Related to Figure 5.

Video S9. Visually-evoked calcium responses following blockade of glutamate receptors and EAAT 1&2, Related to Figure 6.

Video S10. Visually-evoked calcium responses following blockade of glutamate receptors and sodium-calcium exchangers, Related to Figure 6.

Video S11. Visually-evoked calcium responses following blockade of only sodium-calcium exchangers, Related to Figure 6.

References

Agarwal, A., Wu, P.H., Hughes, E.G., Fukaya, M., Tischfield, M.A., Langseth, A.J., Wirtz, D., and Bergles, D.E. (2017). Transient Opening of the Mitochondrial Permeability Transition Pore Induces Microdomain Calcium Transients in Astrocyte Processes. *Neuron 93*, 587-605.

Allen, N.J., and Eroglu, C. (2017). Cell Biology of Astrocyte-Synapse Interactions. *Neuron 96*, 697-708.

Allen, N.J., and Lyons, D.A. (2018). Glia as architects of central nervous system formation and function. *Science 362*, 181-185.

Araque, A., and Navarrete, M. (2010). Glial cells in neuronal network function. *Philos. Trans. R. Soc. Lond. B. Biol. Sci. 365*, 2375-2381.

Balderas, A., Guillem, A.M., Martinez-Lozada, Z., Hernandez-Kelly, L.C., Aguilera, J., and Ortega, A. (2014). GLAST/EAAT1 regulation in cultured Bergmann glia cells: role of the NO/cGMP signaling pathway. *Neurochem. Int. 73*, 139-145.

Barres, B.A. (2008). The mystery and magic of glia: a perspective on their roles in health and disease. *Neuron 60*, 430-440.

Bazargani, N., and Attwell, D. (2016). Astrocyte calcium signaling: the third wave. *Nat. Neurosci. 19*, 182-189.

Bazargani, N., and Attwell, D. (2017). Amines, Astrocytes, and Arousal. *Neuron 94*, 228-231.

Boddum, K., Jensen, T.P., Magloire, V., Kristiansen, U., Rusakov, D.A., Pavlov, I., and Walker, M.C. (2016). Astrocytic GABA transporter activity modulates excitatory neurotransmission. *Nat. Commun. 7*, 13572.

Brazhe, A.R., Verisokin, A.Y., Verveyko, D.V., and Postnov, D.E. (2018). Sodium-Calcium Exchanger Can Account for Regenerative Ca(2+) Entry in Thin Astrocyte Processes. *Front. Cell. Neurosci. 12*, 250.

Chen, T.W., Wardill, T.J., Sun, Y., Pulver, S.R., Renninger, S.L., Baohan, A., Schreiter, E.R., Kerr, R.A., Orger, M.B., Jayaraman, V., et al. (2013). Ultrasensitive fluorescent proteins for imaging neuronal activity. *Nature 499*, 295-300.

Clarke, L.E., and Barres, B.A. (2013). Emerging roles of astrocytes in neural circuit development. *Nat. Rev. Neurosci. 14*, 311-321.

Cornell-Bell, A.H., Finkbeiner, S.M., Cooper, M.S., and Smith, S.J. (1990). Glutamate induces calcium waves in cultured astrocytes: long-range glial signaling. *Science 247*, 470-473.

Dani, J.W., Chernjavsky, A., and Smith, S.J. (1992). Neuronal activity triggers calcium waves in hippocampal astrocyte networks. *Neuron 8*, 429-440.

Deemyad, T., Luthi, J., and Spruston, N. (2018). Astrocytes integrate and drive action potential firing in inhibitory subnetworks. *Nat. Commun. 9*, 4336.

Doengi, M., Hirnet, D., Coulon, P., Pape, H.C., Deitmer, J.W., and Lohr, C. (2009). GABA uptake-dependent Ca(2+) signaling in developing olfactory bulb astrocytes. *Proc. Natl. Acad. Sci. U.S.A. 106*, 17570-17575.

Fitzjohn, S.M., Bortolotto, Z.A., Palmer, M.J., Doherty, A.J., Ornstein, P.L., Schoepp, D.D., Kingston, A.E., Lodge, D., and Collingridge, G.L. (1998). The potent mGlu receptor antagonist LY341495 identifies roles for both cloned and novel mGlu receptors in hippocampal synaptic plasticity. *Neuropharmacology 37*, 1445-1458.

Ibanez, I., Bartolome-Martin, D., Piniella, D., Gimenez, C., and Zafra, F. (2019). Activity dependent internalization of the glutamate transporter GLT-1 requires calcium entry through the NCX sodium/calcium exchanger. *Neurochem. Int. 123*, 125-132.

Kesner, P., Schohl, A., Warren, E.C., Ma, F., and Ruthazer, E.S. (2020). Postsynaptic and Presynaptic NMDARs Have Distinct Roles in Visual Circuit Development. *Cell Rep. 32*, 107955.

Langer, J., Gerkau, N.J., Derouiche, A., Kleinhans, C., Moshrefi-Ravasdjani, B., Fredrich, M., Kafitz, K.W., Seifert, G., Steinhauser, C., and Rose, C.R. (2017). Rapid sodium signaling couples glutamate uptake to breakdown of ATP in perivascular astrocyte endfeet. *Glia 65*, 293-308.

Lim, T. and Ruthazer, E.S. (2021) Microglial trogocytosis and the complement system regulate axonal pruning in vivo. *Elife 10*, e62167.

Lines, J., Martin, E.D., Kofuji, P., Aguilar, J., and Araque, A. (2020). Astrocytes modulate sensory-evoked neuronal network activity. *Nat. Commun. 11*, 3689.

Mu, Y., Bennett, D.V., Rubinov, M., Narayan, S., Yang, C.T., Tanimoto, M., Mensh, B.D., Looger, L.L., and Ahrens, M.B. (2019). Glia Accumulate Evidence that Actions Are Futile and Suppress Unsuccessful Behavior. *Cell 178*, 27-43.

Murphy-Royal, C., Dupuis, J.P., Varela, J.A., Panatier, A., Pinson, B., Baufreton, J., Groc, L., and Oliet, S.H. (2015). Surface diffusion of astrocytic glutamate transporters shapes synaptic transmission. *Nat. Neurosci. 18*, 219-226.

Nimmerjahn, A., Mukamel, E.A., and Schnitzer, M.J. (2009). Motor behavior activates Bergmann glial networks. *Neuron 62*, 400-412.

Pachitariu, M., Stringer, C., Dipoppa, M., Schroder, S., Rossi, L.F., Dalgleish, H., Carandini, M., and Harris, K.D. (2017). Suite2p: beyond 10,000 neurons with standard two-photon microscopy. *BioRxiv*. doi: 10/1101/061507.

Panatier, A., and Robitaille, R. (2016). Astrocytic mGluR5 and the tripartite synapse. *Neuroscience 323*, 29-34.

Panatier, A., Vallee, J., Haber, M., Murai, K.K., Lacaille, J.C., and Robitaille, R. (2011). Astrocytes are endogenous regulators of basal transmission at central synapses. *Cell 146*, 785-798.

Pappalardo, L.W., Black, J.A., and Waxman, S.G. (2016). Sodium channels in astroglia and microglia. *Glia 64*, 1628-1645.

Paukert, M., Agarwal, A., Cha, J., Doze, V.A., Kang, J.U., and Bergles, D.E. (2014). Norepinephrine controls astroglial responsiveness to local circuit activity. *Neuron 82*, 1263-1270.

Perea, G., and Araque, A. (2010). GLIA modulates synaptic transmission. *Brain Res. Rev. 63*, 93-102.

Porter, J.T., and McCarthy, K.D. (1996). Hippocampal astrocytes in situ respond to glutamate released from synaptic terminals. *J. Neurosci. 16*, 5073-5081.

Rojas, H., Colina, C., Ramos, M., Benaim, G., Jaffe, E.H., Caputo, C., and DiPolo, R. (2007). Na+ entry via glutamate transporter activates the reverse Na+/Ca2+ exchange and triggers Ca(i)2+-induced Ca2+ release in rat cerebellar Type-1 astrocytes. *J. Neurochem. 100*, 1188-1202.

Rose, C.R., Ziemens, D., and Verkhratsky, A. (2020). On the special role of NCX in astrocytes: Translating Na(+)-transients into intracellular Ca(2+) signals. *Cell Calcium 86*, 102154.

Schindelin, J., Arganda-Carreras, I., Frise, E., Kaynig, V., Longair, M., Pietzsch, T., Preibisch, S., Rueden, C., Saalfeld, S., Schmid, B., et al. (2012). Fiji: an open-source platform for biological-image analysis. *Nat. Methods 9*, 676-682.

Schummers, J., Yu, H., and Sur, M. (2008). Tuned responses of astrocytes and their influence on hemodynamic signals in the visual cortex. *Science 320*, 1638-1643.

Shigetomi, E., Tong, X., Kwan, K.Y., Corey, D.P., and Khakh, B.S. (2011). TRPA1 channels regulate astrocyte resting calcium and inhibitory synapse efficacy through GAT-3. *Nat. Neurosci. 15*, 70-80.

Sild, M., and Ruthazer, E.S. (2011). Radial glia: progenitor, pathway, and partner. *Neuroscientist 17*, 288-302.

Sild, M., Van Horn, M.R., Schohl, A., Jia, D., and Ruthazer, E.S. (2016). Neural Activity-Dependent Regulation of Radial Glial Filopodial Motility Is Mediated by Glial cGMP-Dependent Protein Kinase 1 and Contributes to Synapse Maturation in the Developing Visual System. *J. Neurosci. 36*, 5279-5288.

Stobart, J.L., Ferrari, K.D., Barrett, M.J.P., Gluck, C., Stobart, M.J., Zuend, M., and Weber, B. (2018). Cortical Circuit Activity Evokes Rapid Astrocyte Calcium Signals on a Similar Timescale to Neurons. *Neuron 98*, 726-735 e724.

Sun, W., McConnell, E., Pare, J.F., Xu, Q., Chen, M., Peng, W., Lovatt, D., Han, X., Smith, Y., and Nedergaard, M. (2013). Glutamate-dependent neuroglial calcium signaling differs between young and adult brain. *Science 339*, 197-200.

Tadel, F., Baillet, S., Mosher, J.C., Pantazis, D., and Leahy, R.M. (2011). Brainstorm: a user-friendly application for MEG/EEG analysis. *Comput. Intell. Neurosci.* 879716.

Tang, W., Szokol, K., Jensen, V., Enger, R., Trivedi, C.A., Hvalby, O., Helm, P.J., Looger, L.L., Sprengel, R., and Nagelhus, E.A. (2015). Stimulation-evoked Ca2+ signals in astrocytic processes at hippocampal CA3-CA1 synapses of adult mice are modulated by glutamate and ATP. *J. Neurosci. 35*, 3016-3021.

Temizer, I., Donovan, J.C., Baier, H., and Semmelhack, J.L. (2015). A Visual Pathway for Looming-Evoked Escape in Larval Zebrafish. *Curr. Biol. 25*, 1823-1834.

Tremblay, M., Fugere, V., Tsui, J., Schohl, A., Tavakoli, A., Travencolo, B.A., Costa Lda, F., and Ruthazer, E.S. (2009). Regulation of radial glial motility by visual experience. *J. Neurosci. 29*, 14066-14076.

Van Horn, M.R., and Ruthazer, E.S. (2019). Glial regulation of synapse maturation and stabilization in the developing nervous system. *Curr. Opin. Neurobiol. 54*, 113-119.

Verkhratsky, A., Parpura, V., Vardjan, N., and Zorec, R. (2019). Physiology of Astroglia. *Adv. Exp. Med. Biol. 1175*, 45-91.

Wang, X., Lou, N., Xu, Q., Tian, G.F., Peng, W.G., Han, X., Kang, J., Takano, T., and Nedergaard, M. (2006). Astrocytic Ca2+ signaling evoked by sensory stimulation in vivo. *Nat. Neurosci. 9*, 816-823.

Zhang, L.I., Tao, H.W., Holt, C.E., Harris, W.A., and Poo, M. (1998). A critical window for cooperation and competition among developing retinotectal synapses. *Nature 395*, 37-44.

Zhang, R.W., Du, W.J., Prober, D.A., and Du, J.L. (2019). Muller Glial Cells Participate in Retinal Waves via Glutamate Transporters and AMPA Receptors. *Cell Rep 27*, 2871-2880.

Supplementary Materials

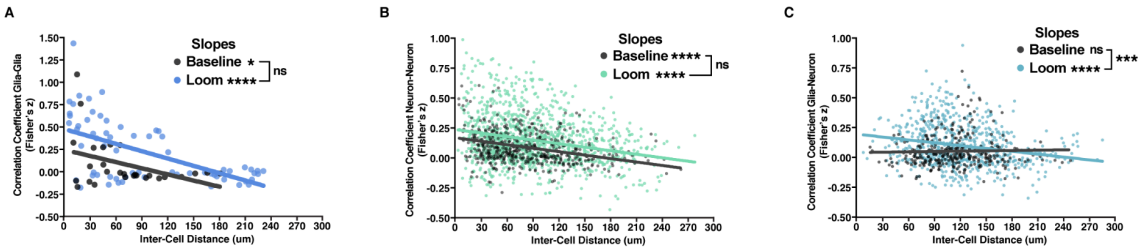

Figure S1, related to Figure 3: Correlation vs. distance analysis for a single animal

(A) Correlation vs. distance plot for radial astrocytes, baseline (black), looming stimulus (blue), n=66 pairs, slopes significantly non-zero: *$p_{baseline}$=0.0401, ****p_{loom}<0.0001, difference between slopes: p=0.7148.

(B) Correlation vs. distance plot for neurons, baseline (black), looming stimulus (green), n=1125 pairs, slopes significantly non-zero: ****$p_{baseline}$<0.0001, ****p_{loom}<0.0001, difference between slopes: p=0.9352.

(C) Correlation vs. distance plot for neuron-radial astrocyte pairs, baseline (black), looming stimulus (turquoise), n=700 pairs, slopes significantly non-zero: $p_{baseline}$=0.5998, ****p_{loom}<0.0001, difference between slopes: **p=0.0009.

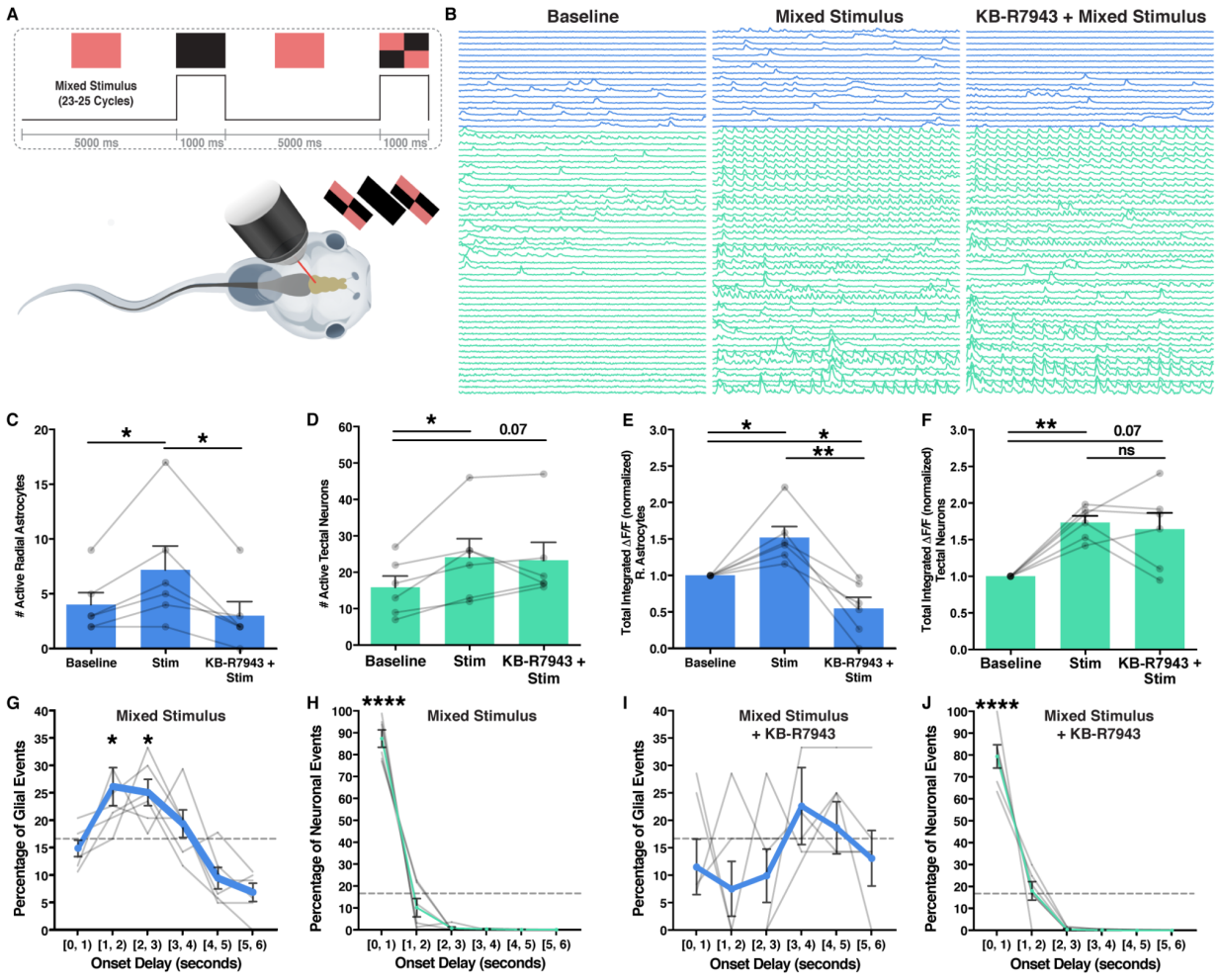

Figure S2, related to Figure 6: NCX-dependent visually-evoked glial calcium activity is present under multiple stimulus conditions.

(A) Tadpoles were presented with a repeating mixed set of visual stimuli during live imaging of the optic tectum.

(B) Traces of resting state (left) and evoked Ca^{2+} activity under normal (middle) and NCX blockade (right) conditions.

(C, D) Number of active cells. One-way repeated measures ANOVAs (n=6 animals): (C) radial astrocytes: F=9.942, *p=0.0121, Fisher's LSD tests: *$p_{\text{baseline vs stim}}$=0.0355, $p_{\text{baseline vs KB stim}}$=0.1438, *$p_{\text{stim vs KB stim}}$=0.0146, (D) neurons: F=5.546, *p=0.0322: *$p_{\text{baseline vs stim}}$=0.0231, $p_{\text{baseline vs KB stim}}$=0.0706, $p_{\text{stim vs KB stim}}$=0.7352.

(E, F) Fold change in integrated DF/F. One-way repeated measures ANOVAs (n=6 animals): (E) radial astrocytes: F=21.17, ***p=0.0003, Holm-Sidak's tests: *$p_{\text{baseline vs stim}}$=0.0359, *$p_{\text{baseline vs KB stim}}$=0.0359, **$p_{\text{stim vs KB stim}}$=0.0036, (F) neurons: F=10.44, *p=0.0146: **$p_{\text{baseline vs stim}}$=0.0011, $p_{\text{baseline vs KB stim}}$=0.0726, $p_{\text{stim vs KB stim}}$=0.8838.

(G-J) Cross-correlation of glial (G,I) and neuronal (H,J) events to each preceding mixed stimulus. One-way ANOVAs mixed stimulus (n=6 animals): (G) radial astrocytes: F=9.749, **p=0.0011, Holm-Sidak's tests vs bin-chance: *$p_{[1,2)}$=0.0424, *$p_{[2,3)}$=0.0349, (H) neurons: F=185.2, ****p<0.0001, Holm-Sidak's tests vs bin-chance: ****$p_{[0,1)}$<0.0001. One-way ANOVAs mixed stimulus + KB-R7943 (n=6 animals): (I) radial astrocytes: F=1.269, p=0.3211, (J) neurons: F=110.6, ***p=0.0001, Holm-Sidak's tests vs bin-chance: ****$p_{[0,1)}$<0.0001.

All error bars = SEM.

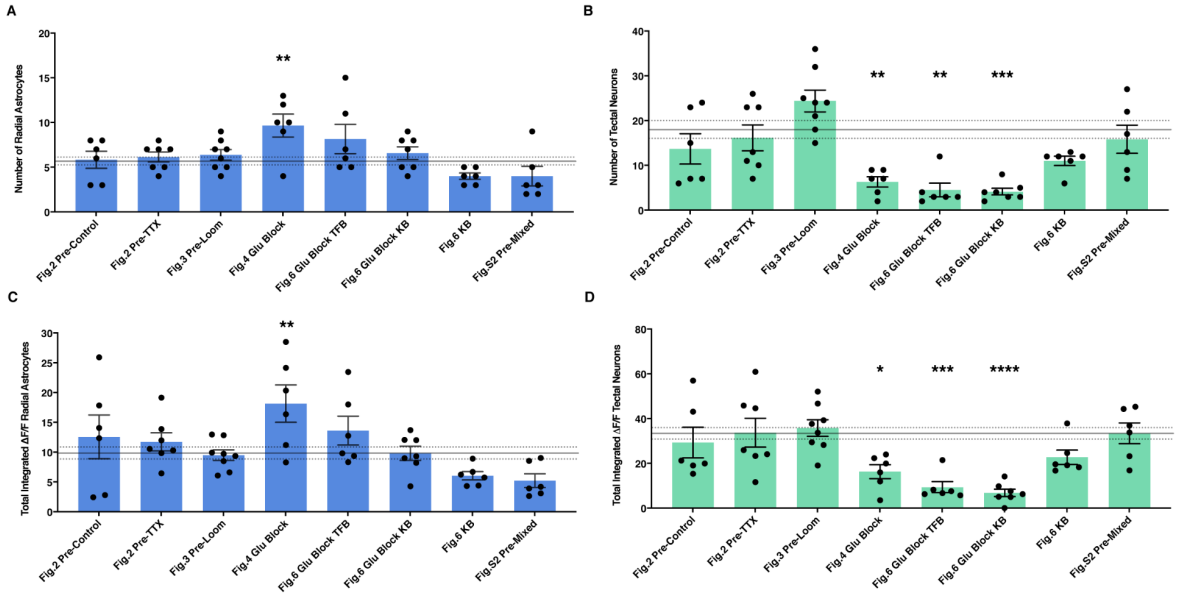

Figure S3, related to Figure 6: Comparison of baseline spontaneous activity between all groups

(A, B) Number of active cells, grey lines mean ± s.e.m. of untreated groups. One-way ANOVAs: 52 animals from 8 groups comparing to mean ± s.e.m. of untreated groups (A) radial astrocytes: F=3.367, **p=0.0025, Dunnett's tests: $^{**}p_{\text{glu block vs. mean untreated}}$=0.0051, all other comparisons ns. (B) neurons: F=6.128, ****p<0.0001: $^{**}p_{\text{glu block vs. mean untreated}}$ =0.0087, $^{**}p_{\text{glu block TFB vs. mean untreated}}$ =0.0023, $^{***}p_{\text{glu block KB vs. mean untreated}}$=0.0007, all other comparisons ns.

(C, D) Fold change in integrated DF/F, grey lines mean ± s.e.m. of untreated groups. One-way ANOVAs: 52 animals from 8 groups comparing to mean ± s.e.m. of untreated groups (C) radial astrocytes: F=3.420, **p=0.0023, Dunnett's tests: $^{**}p_{\text{glu block vs. mean untreated}}$=0.0069, all other comparisons ns. (D) neurons: F=6.738, ****p<0.0001: $^{*}p_{\text{glu block vs. mean untreated}}$ =0.0170, $^{***}p_{\text{glu block TFB vs. mean untreated}}$ =0.0003, $^{****}p_{\text{glu block KB vs. mean untreated}}$<0.0001, all other comparisons ns.

Author Contributions For Chapter 3

The experiments and analysis carried out in this study were conceived of by Nicholas Benfey under the supervision of Dr. Edward Ruthazer. Nicholas Benfey performed all of the experiments and carried out all of the data collection and analysis presented in this manuscript. Nicholas Benfey wrote the manuscript and created the figures. Anton Benfey wrote the original python scripts used for the presentation of visual stimuli as well as the preprocessing and analysis carried out on the data in this manuscript. Anne Schohl developed the calcium imaging methodology used to collect the data in this publication and provided general technical support to Nicholas Benfey throughout the process of collecting data for this manuscript. All authors contributed to the editing of this manuscript. The artwork used in the figures was kindly provided by the scientific illustrator Audrey Desaulniers, Orcéine, Montréal, Canada.

Preface To Chapter 3: Norepinephrine Acts Through Astrocytes In The Developing Optic Tectum To Enhance Threat Detection And Escape Behavior

This chapter presents the experiments I carried out in order to achieve the the final objectives of my thesis research, namely the implementation of a methods to selectively activate radial astrocytes in the intact optic tectum and to assess what effects their activation has on the function of tectal neurons using both calcium imaging and behavioral approaches. The findings presented in these experiments add to the exciting new body of literature demonstrating that glial cells are important mediators of the effects of neuromodulators on neural circuit activity. Taken together with the experimental results of the preceding chapter, this work also suggests that radial

astrocytes are capable of integrating both local circuit activity and arousal state through distinct signaling pathways. This chapter presents a manuscript prepared for publication at the time of the writing of this thesis.

Chapter 3: Norepinephrine Acts Through Astrocytes In The Developing Optic Tectum To Enhance Threat Detection And Escape Behavior

Nicholas J. Benfey[1], Anton T. Benfey[2], Anne Schohl[1], and *Edward S. Ruthazer[1]

[1]Montreal Neurological Institute-Hospital, Department of Neurology and Neurosurgery, McGill University, Montréal, Québec, H3A 2B4, Canada

[2]Information Technology Centre, Department of Computer Science, University of New Brunswick, Fredericton, New Brunswick, E3B 5A3, Canada

*Lead Contact: Please address communications to edward.ruthazer@mcgill.ca

Abstract

The ability to rapidly shift between distinct behavioral states is crucial to the adaptability and fitness of animals. During early development when animals are at their most vulnerable, being able to rapidly and reliably detect and respond to potential threats in the environment is critical for their survival. Across animals, behavioral state switching is known to be regulated by the release of neuromodulators, and more recently has also implicated the activation of astrocytes. Recent studies have also begun to demonstrate that in some neural circuits astrocytes mediate the effects of neuromodulators. Norepinephrine, a neuromodulator known to be associated with attention, learning and memory, as well as heightened states of vigilance and arousal is also a potent activator of astrocytes throughout the vertebrate brain. Here we investigated how the

activation of radial astrocytes in the developing optic tectum of *Xenopus laevis* by norepinephrine alters visual processing in tectal neurons. We found that radial astrocytes are activated by norepinephrine through alpha-1-adrenergic receptors and that norepinephrine shifts the tectum from a state in which diverse visual stimuli are represented into an encoding state that is preferentially responsive to looming stimuli, which are treated as a threat by the animal, inducing escape behavior. We demonstrate that the targeted chemogenetic activation of radial astrocytes in the tectum is sufficient to reproduce the effects of norepinephrine on tectal circuit function and enhances the detection of looming stimuli by freely swimming animals. Taken together our experiments demonstrate that norepinephrine likely acts directly through astrocytes to mediate a state change in the developing visual system which has important implications for processing of sensory information in developing animals.

Introduction

Optimally navigating a complex and constantly changing environment full of resources to exploit and threats to avoid requires the brain to rapidly shift between diverse encoding states in order to carry out the most relevant behavior within a given context. Central to our understanding of the mechanisms mediating state switching in the brain are the neuromodulators, a group of highly conserved neurotransmitters such as serotonin, acetylcholine, dopamine, and norepinephrine, which when released, globally alter the excitability, function, and plasticity of the neural circuits mediating a wide variety of behaviors (Lee and Dan, 2012; Yokogawa et al., 2012; Marques et al., 2019).

Curiously, glial cells, predominantly astrocytes, have also begun to be identified as important mediators of state switching *in vivo* (Poskanzer and Yuste, 2016; Mu et al., 2019; Lines et al., 2020). Evidence is also accumulating which demonstrates that the activation of astrocytes by a range of neuromodulators may in fact be the principal mechanism mediating their effects on neural circuit function. In the visual cortex of mice, the plasticity induced by acetylcholine requires the activation of acetylcholine receptors on astrocytes (Chen et al., 2012), while in the hippocampus, the circadian activation of astrocytes by acetylcholine causes fluctuations in the release of D-serine which gates the function of NMDARs depending on arousal state (Papouin et al., 2017). In both the olfactory bulb and the nucleus accumbens of mice, the actions of dopamine on circuit function have also been found to require the activation of dopamine receptors on astrocytes (Corkrum et al., 2019; Fischer et al., 2020), while perhaps one of the most striking examples of this relationship comes from the amygdala of mice, where oxytocin

mediates a shift between affective states through the direct activation and recruitment of astrocytes (Wahis et al., 2021). This relationship between neuromodulators and astrocytes extends beyond mammals to other animals such as zebrafish and fruit flies where norepinephrine and tyramine/octopamine respectively have been shown to induce behavioral state switching as a consequence of their direct activation of astrocytes (Ma et al., 2016; Mu et al., 2019).

Norepinephrine (NE), one of the principal neuromodulators present in the brains of all vertebrates, is predominantly released by a small group of widely projecting neurons located in the locus coeruleus. NE has many defined effects on neural circuit function ranging from the regulation of sleep/wake cycles, to attention, learning and memory, gating cortical plasticity, enhancing signal-to-noise in neural circuits, and inducing heightened states of vigilance and arousal (Bear and Singer, 1986; Berridge and Waterhouse, 2003). Norepinephrine is also highly implicated in the pathophysiology of human neurodevelopmental disorders such as attention-deficit hyperactivity disorder (ADHD)(Del Campo et al., 2011), and dysfunction of noradrenergic signaling in the mouse superior colliculus has been shown to selectively impair response inhibition and attention, suggesting neuromodulation of this brain center by NE may play an important role in neurodevelopmental disorders (Mathis et al., 2015).

Multiple recent studies have demonstrated that astroglia throughout the vertebrate brain, and particularly within the visual system, are highly responsive to NE, exhibiting large increases in internal calcium concentration often through the activation of alpha1-adrenergic receptors (Giaume et al., 1991; Kulik et al., 1999; Gordon et al., 2005; Bekar et al., 2008; Paukert et al., 2014; Bazargani and Attwell, 2017; Agarwal et al., 2017; Slezak et al., 2019; Mu et al., 2019; Oe

et al., 2020; Ye et al., 2020; Gray et al., 2021; and Wahis et al., 2021). Some of this work even demonstrates that the effects of NE may be mediated predominantly through the activation of glial cells (Mu et al., 2019; Ye et al., 2020). Despite compounding evidence that NE robustly activates astrocytes throughout the vertebrate visual system, the effects this NE-driven glial activation has on the processing of visual information by these neural circuits remains relatively unexplored.

In order to understand how NE and the subsequent activation of astrocytes shapes the processing of behaviorally-relevant visual information during early development of the vertebrate visual system, we used *in vivo* calcium imaging in the developing retinotectal system of albino *Xenopus laevis* tadpoles expressing GCaMP6s. We observed that NE dramatically activates radial astrocytes throughout the optic tectum while simultaneously reducing activity in many postsynaptic tectal neurons, a process that appears to require activation of alpha1-adrenergic receptors, the opening of gap junctions/hemichannels, ATP release, and the activation of P2 receptors. We found that this shifts the visual network in the tectum into a state with robust stimulus encoding properties by suppressing spontaneous activity (Stringer et al., 2019A). Additionally, this state change appears to bias the tectum towards threat detection by preferentially suppressing the activity of tectal neurons which are weakly responsive to multiple visual stimuli while maintaining the activity of tectal neurons which are strongly responsive to looming stimuli, a well characterized visual stimulus which elicits stereotyped escape behavior in animals such as fish and frogs (Barker and Baier, 2015; Temizer et al., 2015; Abbas et al., 2017; Lim and Ruthazer, 2021). The targeted chemogenetic activation of radial astrocytes in the optic tectum was able to replicate the effects we observed of NE on the activity of the tectum and

also significantly increased the rate at which freely swimming animals detected looming stimuli in their environment. Together our results suggest that NE may signal directly through radial astrocytes in the optic tectum to mediate a behavioral state switch which biases the tectum towards threat detection in order to enhance the survivability of the embryo in response to attempted predation.

Results

Radial astrocytes in the optic tectum of *Xenopus laevis* are directly responsive to the neuromodulator norepinephrine during early development

Similar to in other vertebrates, the *Xenopus laevis* optic tectum, the homologue to the mammalian superior colliculus, forms a retinotopic map of the visual environment which is used to orient the animal's behavior in space across time (Isa et al., 2020; Li et al., 2022). The retinotectal circuit is composed of retinal ganglion cell (RGC) axons which project from each eye to the contralateral optic tectum forming synapses with the dendrites of tectal neurons and communicating visual information to the brain (Figure 1A and 1B). In the optic tectum, radial astrocytes are the dominant type of glial cell (Tremblay et al., 2009). They have a distinct elongated radial morphology which spans from the ventricular surface (soma) to the pial surface (endfoot) where they tile the surface of the brain (Figure 1B and 1D). Radial astrocytes are a hybrid cell type that actively contact retinotectal synapses and fulfill the role of both classical radial glial progenitor cell and that of a more mature astrocytes (Tremblay et al., 2009; Sharma and Cline, 2010; Sild et al., 2016; Benfey et al., 2021). Previous work from our lab has

demonstrated that these radial astrocytes are highly structurally and functionally dynamic cells which actively respond to presynaptic release of glutamate from RGC axons during visual stimulation and contribute significantly to the maturation of the network (Tremblay et al., 2009; Sild et al., 2016; Benfey et al., 2021). Using a systematic combination of visual stimulation and acute pharmacological manipulation of the optic tectum in albino GCaMP6s expressing tadpoles, alongside semi-automated ROI extraction using Suite2p, we have shown that it is possible to dissect out the signaling pathways mediating neuron-glia communication in the optic tectum *in vivo* using a single optical indicator (Benfey et al., 2021). This is due to the fact that radial astrocyte endfeet are easily identifiable structures in the combined calcium signal (Figure 1E-G) and serve as reliable proxies for the overall calcium activity in radial astrocytes during early development (Benfey et al., 2021).

To test whether radial astrocytes in the *X. laevis* optic tectum are directly activated by NE *in vivo*, we performed resting state calcium imaging in the tectum of immobilized tadpoles expressing GCaMP6s in both postsynaptic tectal neurons and radial astrocytes. To allow for direct access of small molecules into the optic tectum during the following live imaging experiments, a small incision was cut through the dorsal skin of each tadpole above the optic tectum 30 minutes prior to imaging (Figure 1C). After allowing the animals to settle under the microscope for a half hour to reduce drift while imaging, a 5 min baseline of spontaneous calcium activity was collected simultaneously in both tectal neurons and radial astrocytes. This was then followed by treatment of the optic tectum with tetrodotoxin (TTX)(1 μM) to silence neuronal spiking activity, a manipulation we have previously shown to largely abolish the activity of both tectal neurons and radial astrocytes (Benfey et al., 2021). After collecting another

5 min of spontaneous calcium activity post-TTX, we applied NE (200 μM) to the optic tectum and observed a dramatic elevation in calcium in all radial astrocytes but not tectal neurons (Figure 1E). This strongly suggests that the calcium elevations induced in radial astrocytes by NE are likely to be occurring through direct action of NE on the glial cells given that they occurred in the absence of increases in neuronal spiking activity.

Norepinephrine shifts the optic tectum into a less active state which may enhance the robustness of visual stimulus encoding

Given that NE potently activated radial astrocytes throughout the optic tectum we next wanted to assess what effect NE and the accompanying glial activation had on the processing of visual information by tectal neurons. To do so, we presented immobilized animals with a repeating looming stimulus while performing calcium imaging in the optic tectum over a 5 min baseline followed by another 5 min post-application of NE (Figure 1F and 1G). We observed a dramatic recruitment of radial astrocytes following the application of NE, occurring at the same time as a significant reduction in the number of active tectal neurons compared to baseline (Figure 1H), an effect consistent with recent observations in the zebrafish hindbrain (Mu et al., 2019). Curiously, NE/glial activation appeared to preferentially suppress the recruitment of non-loom and weakly-loom responsive neurons leading to a significant increase in the average loom response amplitude of active neurons in the tectum as a result (Figures 1F, 1G, and 1J). This suggested that NE may enhance the signal-to-noise ratio for the detection of a particular stimulus, in this case loom, by suppressing spontaneous activity and the activity of less robustly activated neurons being trained in the network.

Using the dimensionality reduction technique of principal component analysis (PCA) to assess how the network of tectal neurons represents the looming stimulus across time (Pang et al., 2016; Stringer et al., 2019A; Stringer et al., 2019B), we consistently observed that the looming stimulus-evoked neuronal activity was captured by the first principal component (PC1) and accounts for the vast majority of the response variance in the network activity in nearly all animals (Figure 1I). Interestingly, NE application to the tectum caused a significant increase in the amount of variance captured by PC1 in each animal suggesting it shifts the tectum into a more robust state which may facilitate the detection of a particular stimuli by reducing the overall amount of spontaneous activity in the network (Figure 1I)(Stringer et al., 2019A).

Norepinephrine shifts the tectum into a state biased towards loom detection

In order to assess how the effects we observed of NE/glial activation on stimulus-driven network activity in the tectum apply to more complex representations of stimuli, we next visually stimulated the animals with two contrasting, yet both behaviorally relevant stimuli. We started by presenting small black moving dots (~10° in size) which appear and move across the screen in different directions with no coherence in order to mimic non-threatening debris or prey in the animal's environment (Barker and Baier, 2015; Förster et al., 2020). We would then present a looming stimulus and alternate between the presentation of the two stimuli every 20 s, applying NE after recording baseline activity (Figure 2A, Figure S1A and S1B). Sorting neuronal traces by PC1 allowed us to observe a gradient of neuronal responses in the network, which neatly captures the encoding of the two stimuli (Figure 2A). On one end of the gradient we observed

moving dots-selective neurons which were largely unresponsive to the looming stimulus (top row of traces), and on the other end of the gradient we observed loom selective neurons which were largely unresponsive to the moving dots (bottom row of traces)(Figure 2A). We decided to bin neurons based on their average loom preference by taking each cell's average response to the looming stimulus and normalizing that to the same cell's average response to the moving dots stimulus in order to characterize the effects of NE on groups of neurons across the stimulus gradients (Figure 2B).

Consistent with our previous observations, NE potently activated radial astrocytes while at the same time reducing the activity in a large number of neurons in the tectum (Figure 2C). When comparing neuronal response amplitudes to the moving dots and to the looming stimulus it was clearly apparent that the effects of NE on the two stimuli were asymmetrical as in 4 out of the 5 animals NE caused a reduction in the mean response amplitude to the dots due to a suppression of the strongest dots-detecting cells while causing an increase in the mean response amplitude to the loom due to a drop-out of the weakest loom detecting cells (Figure 2F and 2G). Further analysis using PCA was also strongly suggestive of an asymmetry in the effects of NE on the encoding of both stimuli by the network. Under baseline conditions both stimuli are represented along different PC dimensions with roughly equal weights, with the looming stimulus-driven activity being the primary feature captured by PC1 and the moving dots stimulus-driven activity being the secondary feature captured in the network (Figure 2D). In the NE state, encoding of the looming stimulus was enhanced while the encoding of the moving dots stimulus was profoundly decreased as demonstrated by the significant increase in the weight of PC1 in the NE induced state (Figure 2D and 2E). This asymmetry is perhaps most clearly demonstrated when the effects

of NE are quantified across loom preference bins where we see a significant decrease in the number of active neurons in the network which have a weak preference for the loom over the dots (loom:dot response ratio ≥ 1 > 2) and a large but non-significant decrease in the number of neurons with a slight preference for the dots stimulus (≥ 0.5 > 1) while cells with a strong preference for the loom (≥ 4) are comparatively unaffected by NE (Figure 2B and 2H). Taken together these observations suggest that, at least during early development, the baseline state of the optic tectum has a higher dimensional neural representation of the visual environment which encodes disparate features while still slightly favoring detection of looming threats as would be adaptive to survival; however, in the NE state the optic tectum shifts to a lower dimensional neural representation of the visual environment which primarily encodes looming threats at the expense of other features in the environment which is consistent with a general understanding of heightened states of vigilance.

The state change induced in the optic tectum by norepinephrine requires the activation of alpha1-adrenergic receptors

Across multiple vertebrate species, the alpha1-adrenergic receptor has been found to mediate the majority of the calcium elevations observed in astrocytes resulting from their stimulation with NE (See review by Wahis and Holt, 2021), so we decided to assess the role of this receptor in mediating the effects of NE that we observed on radial astrocytes and tectal network activity. To assess the role of alpha1 in shifting the tectum into a state biased towards loom detection, we pretreated animals with the alpha1 antagonist/inverse agonist prazosin (50 μM) 30 min prior to collecting our initial baseline pre-application of NE. We then repeated the alternating

presentation of both small randomly moving dots and the looming stimulus under both baseline and NE conditions as described above (Figure S1C). On average, the group of animals pretreated with prazosin no longer showed significant increases in the recruitment of radial astrocytes or decreases in the number of active tectal neurons following treatment with NE (Figure 2I). Interestingly, there were significantly more tectal neurons active at baseline in this prazosin treated group which is consistent with either the blockade of endogenous NE which could be mediating a form of tonic inhibition/filtering in the tectum, or simply, the inverse agonism of the alpha1 receptor artificially reversing the direction of the effect we are observing (Figure 2I). NE also no longer induced a consistent shift in the mean response amplitude for either the moving dots stimulus or the looming stimulus (Figure 2L and 2M), nor did NE induce a shift in the dimensionality the tectal network as we have previously observed following the addition of NE (Figure 2J and 2K). Curiously, in a number of animals, the moving dots driven activity actually became the dominant feature in a number of animals in this group (Figures 2J and S1C). When assessing the effects of NE on neurons across loom preference bins the previously observed asymmetry in the suppression of tectal neurons induced by NE appeared to be abolished by prazosin (Figure 2N). Taken together these results strongly suggest that alpha1-adrenergic receptor activation is important for inducing the state changes we have characterized so far in the tectum and suggests that the relationship between NE, alpha1-adrenergic receptors, and astroglia observed elsewhere may be a conserved mechanism in *Xenopus laevis* as well. However, our experiments cannot rule out the possibility that neuronal alpha1 receptors may also contribute to the phenotype we observe (Wahis and Holt, 2021); although, calcium mobilization was not observed in the tectal neurons of animals pretreated with TTX potentially suggesting an absence of alpha1-adrenergic receptors on neurons in the tectum.

Blockade of P2 receptors implicates ATP release in the network alterations induced by norepinephrine

Understanding the signaling pathways downstream of alpha1/radial astrocyte activation is important for understanding how networks flexibly encode visual information and dynamically change state. Extensive work in other systems has implicated ATP release from astrocytes (including following their activation by NE) in their ability to regulate the function of a wide variety of neural circuits (Pascual et al., 2005; Gourine et al., 2010; Boddum et al., 2016; Fujii et al., 2017; Tan et al., 2017; Covelo and Araque, 2018; Eersapah et al., 2019; Agostinho et al., 2020; Corkrum et al., 2020). Common to many of these mechanisms is the activation of postsynaptic neuronal P2 receptors by astrocyte-released ATP, which is often associated with increased inhibition in local networks (Gordon et al., 2005; Lalo et al., 2014; Boué-Grabot and Pankratov, 2017; Tan et al., 2017).

To test whether ATP release is involved in the NE-mediated state switch, we pretreated animals with the broad-spectrum P2 purinergic receptor antagonist suramin (100 μM) 30 min before imaging a baseline and applying NE (Figure S1D). Blockade of P2 receptors did not prevent radial astrocytes from being recruited by NE nor did it prevent the number of active tectal neurons from decreasing following application of NE (Figure 3A). In animals pretreated with suramin, NE no longer caused an increase in the mean loom response amplitude and actually lead to a decrease in both the mean dots response amplitude and the mean loom response amplitude suggesting that activation of P2 receptors by ATP is necessary to boost or maintain

heightened loom responsiveness in the NE state (Figure 3D and 3E). Consistent with these observations, there was no change in the amount of variance captured by PC1 following NE application in suramin-treated animals suggesting that P2 activation, likely on a specific population of neurons, is required to shift the network into a lower dimensional state biased towards loom detection (Figure 3B and 3C). When assessing the effects of NE across loom preference bins we observed a significant main effect of suramin but no interaction which suggests that the inhibitory effect of NE on tectal neurons was more general under conditions where P2 receptors are blocked and not limited to neurons with weak dots or loom preferences as is normally the case (Figure 3F). These observations are consistent with the excitability of a population of loom selective neurons being enhanced through P2 activation, possibly following the release of ATP from radial astrocytes, in the NE state.

Blockade of gap junctions/hemichannels prevents the network alterations induced by norepinephrine

Despite numerous studies demonstrating that ATP is released from astrocytes following elevations in their internal calcium levels, there remains much debate as to the mechanism underlying the release of ATP from astrocytes. Multiple pathways have been suggested ranging from vesicular release, to release via large pore ion channels, and release through hemichannels, and pannexins, often with conflicting results (Lalo et al., 2014; Bazargani and Attwell, 2016; Agostinho et al., 2020); however, recent work appears to be converging on a role for hemichannels in mediating ATP release (Bennett et al., 2003; Orellana and Stehberg, 2014; Roux et al., 2015; Meunier et al., 2017; Fukuyama et al., 2020). Given the relative ease through which

they can be blocked pharmacologically in our system, we decided to probe their role in mediating the NE induced state change in the optic tectum. To do so we pretreated animals with carbenoxolone (CBX) (100 μM) 30 minutes prior to imaging which blocks both gap junctions and hemichannels. Similarly to pretreatment with the P2 receptor antagonist suramin, CBX did not prevent the activation of radial astrocytes nor the deactivation of tectal neurons by NE (Figure 3G); however, CBX did prevent changes in the mean response amplitude for both stimuli (Figure 3J and 3K) as well as changes in the dimensionality of the network (Figure 3H and 3I). Similar to what was observed for P2 receptor blockade with suramin, CBX also led to a more generalized deactivation of neurons across loom preference bins (Figure 3L). While this experiment doesn't directly demonstrate ATP release through hemichannels following activation of radial astrocytes with NE, the results are consistent with such a potential conclusion. Some potential important caveats are presented in the discussion.

Preference for moving dots with coherent motion in the norepinephrine state

In the wild, both tadpoles and many fishes exhibit schooling behavior in which large numbers of animals quickly coalesce to navigate their environment as a group in response to the presence of predators; a behavior which is believed to enhance the odds of survival for any given animal in the group. Such schooling behavior is likely to represent a heightened state of vigilance for both prey and predators alike as looming stimuli have been shown to elevate norepinephrine levels in the optic tectum of zebrafish (Feng et al., 2019). For the animals that commonly initiate schooling following detection of a threat, the rapid detection of a group of coherently moving objects is likely to enhance their survivability should they be able to sync up with the group. For

the predatory animal in a heightened state of vigilance, a group of coherently moving objects may be erroneously perceived as a large object presenting a counter threat. To begin to investigate this line of reasoning, we sought to determine how the optic tectum processes groups of small moving objects in the NE-modulated state by presenting two alternating moving dots stimuli, one with no coherence between the motion of the dots (Dots 0/Coherence=0) and one with full coherence between the moving dots (Dots 1/Coherence=1)(Figure 4A and 4B). Similarly to in our experiments using alternating moving dots stimuli and looming stimuli, we also observed neurons with distinct preferences for moving dots with no coherence and neurons that preferred moving dots with full coherence, suggesting at the circuit level the tectum is able to distinguish between the two stimuli (Figure 4C).

Again, the NE state was characterized by the rapid recruitment of radial astrocytes and a large decrease in the number of active neurons (Figure 4D). Looking at the mean response amplitude of tectal neurons to each of the stimuli we observed reductions for the Dots 0 stimulus in 4 out of 5 animals with the opposite being true for the Dots 1 stimulus (Figure 4F and 4G). Consistent with NE reducing the dimensionality of network activity in the tectum, again we observed that in 4 out of the 5 animals there was a lower dimensional neural code in the NE state which could suggest enhanced encoding of the coherent motion stimulus (Figure 4E). Similar to our observations of an asymmetrical reduction in population of tectal neurons across loom preference bins we also observed significant reductions in the number of active neurons with a preference for Dots 0 or a mild preference for Dots 1 while the neurons with a strong preference for Dots 1 were unaffected by NE (Figure 4H). Most striking is the shift in mean coherence preference (ratio of mean C=1 response amplitude divided by the mean C=0 response amplitude) in these

animals where we see an approximately 40% increase in the preference for the Dots 1 stimulus in the tectum in the NE treated state. This finding suggests that NE may serve to shift the attention of *Xenopus laevis* tadpoles towards groups of objects with coherent motion within in their natural environment (Figure 4I).

Direct chemogenetic activation of radial astrocytes recapitulates the effects of NE on looming stimulus detection and enhances loom-evoked escape behavior in freely swimming animals

Implicit in our experiments is the idea that the large calcium increases observed in tectal radial astrocytes following application of NE plays a causal role in the state change observed in the network of tectal neurons. There is precedence in the literature for such a possibility as astrocytes have been observed to mediate state switching in the cortex (Poskanzer and Yuste, 2016), and radial astrocytes in the hindbrain of zebrafish have been observed to integrate noradrenergic signals and trigger a behavioral state switch as well (Mu et al., 2019). To specifically assess the contribution of radial astrocytes to the state change we observed, and to test the behavioral consequence of radial astrocyte activation on stimulus detection by freely swimming animals, we employed a chemogenetic approach involving the transfection of a tagged, mutant mammalian TRPV1(E600K)-tagRFP (mTRPV1), which exhibits enhanced capsaicin sensitivity (Chen et al., 2016) into radial astrocytes in the optic tectum of GCaMP6s-expressing *X. laevis* tadpoles.

Because in both fish and frogs, the endogenous TRPV1 receptor, a non-specific cation channel which detects increases in temperature, is largely insensitive to the small molecule capsaicin

(*Xenopus* TRPV1 ec50 ~ 85.4 μM), a potent activator of mammalian TRPV1 (mTRPV1 ec50 ~ 3 μM)(Ohkita et al., 2012; Chen et al., 2016), mTRPV1 expressed in radial astrocytes can be activated with low doses of capsaicin that have no effect on endogenous TRPV1 activity in these animals (Mu et al., 2019). We were able to successfully utilize this system to target the radial astrocytes of the *X. laevis* optic tectum through targeted electroporation of mTRPV1 plasmid injected into the brain ventricle, which results in the sparse transfection of periventricular radial astrocytes without transfecting neurons, which migrate away from the ventricle in the developing *X. laevis* optic tectum (Figure 5A)(Tremblay et al., 2009; Sild et al., 2016).

We then assessed how the selective activation of radial astrocytes using capsaicin (10 μM) impacted tectal network activity in response to a repeating looming stimulus (Figure 5B and 5C). Similarly to what we observed with application of NE, chemogenetic activation of a subset of radial astrocytes also significantly increased the total number of active radial astrocytes in the tectum while decreasing the number of active tectal neurons (Figure 5D). Interestingly, the activation of radial astrocytes using this chemogenetic method recruited both mTRVP1(+) radial astrocytes and their mTRPV1(-) neighbors suggesting that activated radial astrocytes propagate their activated state to other glial cells either through release of diffusible signals or directly through gap junctions (Fujii et al., 2017). Chemogenetic activation of radial astrocytes also replicated the effects of NE resulting in the biased suppression of tectal neurons with weak, but sparing those with high, loom responsiveness leading to an increase in the mean response amplitude of neurons responding to the looming stimulus in the tectum (Figure 5G and 5H). Most excitingly, the activation of radial astrocytes also induced a switch to a lower dimensional but more robust representation of the looming stimulus in the tectum (Figure 5E and 5F). These

effects were not observed in animals with mTRPV1(+) radial astrocytes in the tectum treated with vehicle nor were they observed in mTRPV1(-) animals treated with 10 μM capsaicin suggesting that these effects, both the suppression of the activity of a population of tectal neurons and the switch to a lower dimensional stimulus encoding state are mediated by the activation of radial astrocytes in the tectum (Figure S2).

All of our experiments with both NE and specific chemogenetic activation of radial astrocytes strongly suggest the likelihood of enhanced loom detection in freely swimming animals in the NE/glial activation state. Therefore we decided to test this using our chemogenetic approach to specifically activate radial astrocytes in the optic tectum of freely swimming animals. To test the effects on behavior, we presented a repeating looming stimulus to freely swimming animals and tracked their escape behavior using previously published techniques from our lab (Figure 5I)(Lim and Ruthazer., 2021). In brief, a looming stimulus was presented to a freely swimming animal 10 times with a 20 second interstimulus interval, similar to our calcium imaging experiments (Figures 1 and 5). An average loom response rate was calculated for each animal by taking the average number of loom-evoked escapes an animal initiated during the 10 trials. Under baseline conditions, mTRPV1(+) animals treated with vehicle and mTRPV1(-) animals treated with capsaicin (10 μM) both detected the looming stimulus in their environment approximately 30% of the time (Figure 5J). In the group of mTRPV1(+) animals where radial astrocytes in the optic tectum were activated by capsaicin (10 μM) prior to behavioral testing, the average loom detection rate jumped to approximately 60% (Figure 5J).

This strongly suggests that the state change induced by the direct activation of tectal radial astrocytes, as well as the state change induced by NE, are likely to impart a strong survival benefit to animals during predation events by enhancing the prominence of looming features in their visual environment. While we cannot rule out direct effects of NE on neurons throughout the optic tectum, our experiments using chemogenetic activation of radial astrocytes are consistent with the predominant effects of NE on circuit function in our system being directly mediated through the recruitment of radial astrocytes.

Discussion

To understand the neural circuit mechanisms that mediate sensory-motor decision making in aquatic vertebrates such as *Xenopus laevis*, it is useful to draw from the emerging literature in the zebrafish model organism, where the optic tectum has been conclusively identified as the principal brain area involved in representing looming stimuli and driving escape behavior (Temizer et al., 2015; Dunn et al., 2016). Other regions such as the thalamus have been observed to contribute to the processing of the luminance changes that occur during looming stimulus events in order to correctly direct escape away from predators (Heap et al., 2018). The optic tectum has been found to mediate the decision between approaching and avoiding objects in the environment based on the size of the stimulus relative to the eye of the animal (Barker and Baier, 2015). Small objects represented in the tectum tend to trigger approach behavior, however, once a critical image size has been reached, the tectum begins to engage avoidance behaviors instead. This processing of critical image size has been found to be distributed across the entire network of tectal neurons rather than being localized to a specific subpopulation of "loom-detector"

neurons, largely consistent with our observations (Dunn et al., 2016). While our experiments do suggest that there may be a group of loom-responsive neurons which are enhanced by the activation of P2 receptors in the superficial layers of the tectum, on a whole, loom processing remains distributed across the tectum. We did however tend to observe an anterior to posterior gradient for loom responsiveness within the tectum with more anterior regions being more responsive to loom than posterior regions in most animals; this is consistent with what has been observed in the zebrafish brain (Förster et al., 2020). The zebrafish tectum has also been crucially implicated in prey capture with small objects being preferentially represented in more posterior regions of the tectum (Förster et al., 2020). In our experiments the representation of moving dots was not consistently located to any particular region within the tectum, likely due to the fact that we presented many moving dots across the whole visual field. Receptive field mapping with dots presented one at a time across the visual space would likely clarify these observations.

Models of the neural networks processing visual information in the *Xenopus* tectum have also implicated high levels of recurrent network activity in the process of detecting looming stimuli (Jang et al., 2016). Curiously, a group of neurons in the superficial layers of the tectum which exhibit high levels of gap junctional coupling have been found to control recurrent network activity in the *Xenopus* tectum (Liu et al., 2016). Additionally, the authors suggest that these neurons may boost the reliability of signals in the deep layers of the tectum which are known to be involved with mediating escape behavior. This is particularly relevant to our observations as in the both the NE state, and when we chemogenetically activated radial astrocytes in the tectum, we consistently saw a group of neurons in the superficial and neuropil layers which exhibited

calcium increases at the same time that most other tectal neurons in the cell body layer show significant decreases. While the most parsimonious explanation for why carbenoxolone prevented the network changes we typically observed following NE application remains the prevention of ATP release through hemichannels, we cannot rule out the possibility that the blockade of the gap junctional coupling between these superficial layer neurons is also relevant to the state switch. In fact, these superficial layer neurons could be the population of cells being boosted through the activation of postsynaptic P2 receptors downstream of the activation of radial astrocytes and important for our overall understanding of the mechanism underlying the state switching being induced.

Circuit models of tectal function have also implicated a population of superficial interneurons (SINs) primarily found embedded within the synaptic neuropil region of the optic tectum as being critically important for the processing and filtering of size related visual information transmitted between RGCs and the tectal neurons in the deeper layers of the tectum (Del Bene et al., 2010; Barker and Baier, 2013; Temizer et al., 2015; Dunn et al., 2016; Abbas et al., 2017). These SINs extend widely branching dendrites throughout the majority of the tectal neuropil and contribute to the computations that drive the initiation of escape behaviors (Barker and Baier, 2013; Temizer et al., 2015; Dunn et al., 2016; Barker et al., 2021). It has been shown that SINs enhance the detection of visual stimuli, likely by suppressing smaller distractions in the environment or by enhancing the ability to distinguish between objects of different sizes in the environment, thereby facilitating the initiation of specific sensory-motor behaviors such as loom-evoked escapes (Barker and Baier, 2015). In both *Xenopus laevis* and zebrafish the vast majority of SINs are GABAergic (Miraucourt et al., 2012; Barker et al., 2021; Mu et al., 2019). SINs are

highly responsive to the looming stimulus in our experiments and are often highly active in the NE state when many neurons in the cell body layers of the tectum are being suppressed (Figure 1G). Occasionally we observe persistent calcium elevations in these neurons lasting tens of seconds following either the addition of NE or chemogenetic activation of radial astrocytes which strongly suggests that these neurons are likely to play an important role in mediating the state switching and enhanced loom detection that we observe in freely swimming animals. Consistent with this suggestion, the recruitment of radial astrocytes by NE or direct chemogenetic activation has been found to lead to the downstream activation of SINs in the hindbrain of zebrafish and the initiation of behavioral state switching (Mu et al., 2019); optogenetic activation of these SINs was sufficient to mediate the shift in swimming behavior they observed following the activation of radial astrocytes. Further experiments aimed at dissecting the circuit mechanisms mediating NE driven state switching in the tectum will require careful investigation of the relationship between radial astrocytes and SIN function.

Close relationships between astrocytes and inhibitory neurons have been observed in many vertebrate neural circuits. The optogenetic activation of astrocytes in the primary visual cortex has a pronounced effect on the excitability of local GABAergic interneurons leading to significant alterations in visual tuning properties, however recent advances introduce caveats into the mechanistic interpretation of experiences utilizing optogenetic methods to activate astrocytes given it causes changes in extracellular potassium which has an important influence on neuronal excitability (Perea et al., 2014, Octeau et al., 2019). In the neocortex the activation of astrocytes has been shown to cause ATP release through exocytosis which regulates inhibition through the activation of P2X4 receptors (Lalo et al., 2014). In the hippocampus there are numerous

examples of astrocytes enhancing local circuit inhibition. Optogenetic activation of astrocytes in this brain region leads to enhanced inhibition through release of ATP and the activation of P2Y1 receptors on NPY interneurons (Tan et al., 2017). The reuptake of GABA from the synaptic cleft by astrocytes has been shown to lead to the activation of sodium-calcium exchangers (NCX) and the release of ATP/ADO which also decreases local excitation (Boddum et al., 2016). GABA reuptake by astrocytes has also been shown to regulate barrage firing in local inhibitory neurons through the calcium dependent release of glutamate and the activation of mGluR1 on local interneurons (Deemyad et al., 2018). Recently experiments employing the chemogenetic activation of astrocytes in the mouse visual cortex have also shown that astrocytes control the formation and function of GABAergic synapses (Takano et al., 2020). A newly characterized form of neuron-glia communication involving local changes in membrane voltage in the fine processes of astrocytes has also been found to regulate synaptic strength through the tight regulation of glutamate clearance from synapses (Armbruster et al., 2022). Our observations are consistent with NE or direct activation of radial astrocytes enhancing inhibition in the optic tectum and is likely to add to the mounting evidence suggesting a conserved relationship between astroglia and inhibition in vertebrates; however, further validation of this relationship is warranted given that our evidence remains correlative at present. Precisely how this relationship functions in the *Xenopus* tectum will be crucial for understanding behavioral state switching in the developing visual system.

Our experimental manipulations implicate the opening of gap junctions or hemichannels in the switch to a lower dimensional encoding state in the tectum in the NE state. NE has been shown to regulate the formation of gap junctions as well as the redistribution of connexin 43 in

astrocytes downstream of alpha1-adrenergic receptor activation (Giaume et al., 1991; Nuriya et al., 2018). Both gap junctions and hemichannels have been consistently observed to mediate important functions in astrocytes (Orellana and Stehberg, 2014). In the barrel cortex of mice, astrocytes form distinct subnetworks through connexin 30/43 mediated gap junctional coupling (Houades et al., 2008). In the primary visual cortex the expression of connexin 30 by astrocytes has been shown mediate critical period plasticity (Ribot et al., 2021), and in the amygdala connexin 30/43 containing gap junctions/hemichannels in astrocytes are important for the release of the NMDAR co-agonist D-serine and the shift between affective states following the release of oxytocin (Wahis et al., 2021). In the olfactory bulb, astrocytes have been shown to form hemichannels using connexin 43 which open following the increases in glial calcium induced by local circuit activity (Orellana and Stehberg, 2014; Roux et al., 2015); this activity-dependent opening of astrocyte hemichannels leads to the release of ATP and the modulation of slow waves in the olfactory bulb. The calcium-dependent opening of connexin 43 hemichannels in astrocytes has also been associated with D-serine release, an important gliotransmitter in the *Xenopus* tectum (Meunier et al., 2017; Van Horn et al., 2017). The gap junction blocker we used in our experiments has also been shown to prevent gliotransmitter release through connexin 43 hemichannels in astrocytes (Fukuyama et al., 2020). Further investigation into the specific connexins expressed by radial astrocytes in the *Xenopus* tectum will be important for understanding how they modulate visual function through the release of gliotransmitters.

An important effect of both NE application and chemogenetic activation of radial astrocytes that we consistently observed in all of our experiments (except in animals treated with prazosin) is the reduced activity in a large number of tectal neurons. While we expected this effect to be

mediated through P2 activation on local inhibitory neurons, we still observed this deactivation of tectal neurons in animals pretreated with both the P2 receptor antagonist suramin and the gap junction/hemichannel blocker carbenoxolone suggesting an alternative mechanism may mediate this effect. A few interesting possibilities are particularly relevant given our previous report on investigating visually-evoked calcium increases in tectal radial astrocytes found that glutamate reuptake is critically important for their detection of visual stimuli (Benfey et al., 2021). Local changes in membrane voltage in astrocyte processes induced by fluctuations in external potassium and calcium levels have been shown to dramatically alter the efficiency of glutamate clearance through glial excitatory amino acid transporters (Armbruster et al., 2022). The activation of alpha1-adrenergic receptors has been shown to potently enhance glutamate clearance by astrocytes in culture (Hansson and Rönnbäck, 1989; Fahrig, 1993).

Additionally, our experiments show that the tectal neurons which are the most likely to have their activity suppressed in the NE/glial activation state are those in the less mature regions of the posterior tectum which are weakly responsive to multiple stimuli. We believe there is a strong possibility that the suppression of tectal neurons in the NE/glial activation state may be the result of enhanced glutamate clearance by radial astrocytes and a floor effect which renders immature neurons with low signal to noise ratios quiescent during visual stimulation in high vigilance states, though this remains challenging to investigate experimentally *in vivo*. Another relevant observation in the literature that remains a possible explanation is the release of GABA from astrocytes which has been demonstrated following activation of alpha2-adrenergic receptors on astrocytes in culture (Gaidin et al., 2020).

Recent advances in neuroengineering have produced robust genetically encoded fluorescent indicators for a wide variety of neuromodulators such as norepinephrine (Feng et al., 2019) and putative gliotransmitters such as ATP (Wu et al., 2022). Successful implementation of these new optical indicators in the *Xenopus* optic tectum will likely lead to significant advances in our understanding of how specific types of visual stimuli evoke the endogenous release of neuromodulators such as NE as well as endogenous release of gliotransmitters such as ATP/ADO with high spatial and temporal precision. Single looming stimuli have been shown to evoke the release of NE in the tectum of larval zebrafish (Feng et al., 2019). Whether radial astrocytes in the optic tectum also sum NE release over short time intervals until a threshold for behavioral state switching is engaged remains an interesting possibility given the high degree of overlap between our observations and those in the hindbrain circuits of zebrafish (Mu et al., 2019). GABA reuptake and calcium entry through astrocyte NCX has also been shown to enhance inhibition in mammalian circuits (Boddum et al., 2016); given that visual stimulation triggers calcium entry through NCX in the *Xenopus* tectum, this remains another interesting possible avenue to explore (Benfey et al., 2021).

While our investigations focused on the role of NE in the activation of radial astrocytes and behavioral state switching in the optic tectum, multiple other important neuromodulators have also been shown to modulate tectal function in a number of different vertebrate species. In zebrafish, serotonin has been shown to regulate sensory processing through modulation of tectal circuits (Yokogawa et al., 2012) and also induce CNS wide alterations in network activity during shifts between exploratory swimming behavior (Marques et al., 2020). RGC axons and local interneurons are also known to express acetylcholine receptors in the tectum and play an

important role in tectal processing, including the modulation of inhibition and visual gain (Henley et al., 1986; Baginskas et al., 2013; Weigel and Luksch, 2014; Baginskas and Kuras, 2016; Asadollahi and Knudsen, 2016; Marques et al., 2020). Dopamine has long been known to alter visual processing (see review by Woolrych et al., 2021) and has been shown to alter visually driven motor activity through modulation of the optic tectum (Pérez-Fernández et al., 2017). Which neuromodulators activate radial astrocytes in the optic tectum, and whether different neuromodulators exert distinct effects on tectal function will be important to explore. How different neuromodulators work in concert with one another to precisely control visual function also remains an interesting avenue for future research.

In summary, we have demonstrated that NE rapidly shifts the optic tectum into a lower dimensional encoding state which biases vision towards detection of looming threats in the environment. We have shown that this state switch involves the activation of alpha1-adrenergic receptors, likely found on radial astrocytes, and is mediated in part by the activation of P2 receptors, possibly downstream of the release of ATP through hemichannels. This state switch can be fully recapitulated by the sparse chemogenetic activation of radial astrocytes in the optic tectum and greatly enhances the ability of freely swimming animals to detect looming stimuli in their environment. Taken together with our previously reported observations that radial astrocytes directly respond to visual stimulation through the reuptake of glutamate released from RGCs (Benfey et al., 2021), these experiments suggest that radial astrocytes are capable of integrating both local circuit activity and the overall arousal state of the animal. How both these mechanisms work together to control sensory-motor decision making in the tectum will be an exciting avenue for future research.

Figures

Figure 1

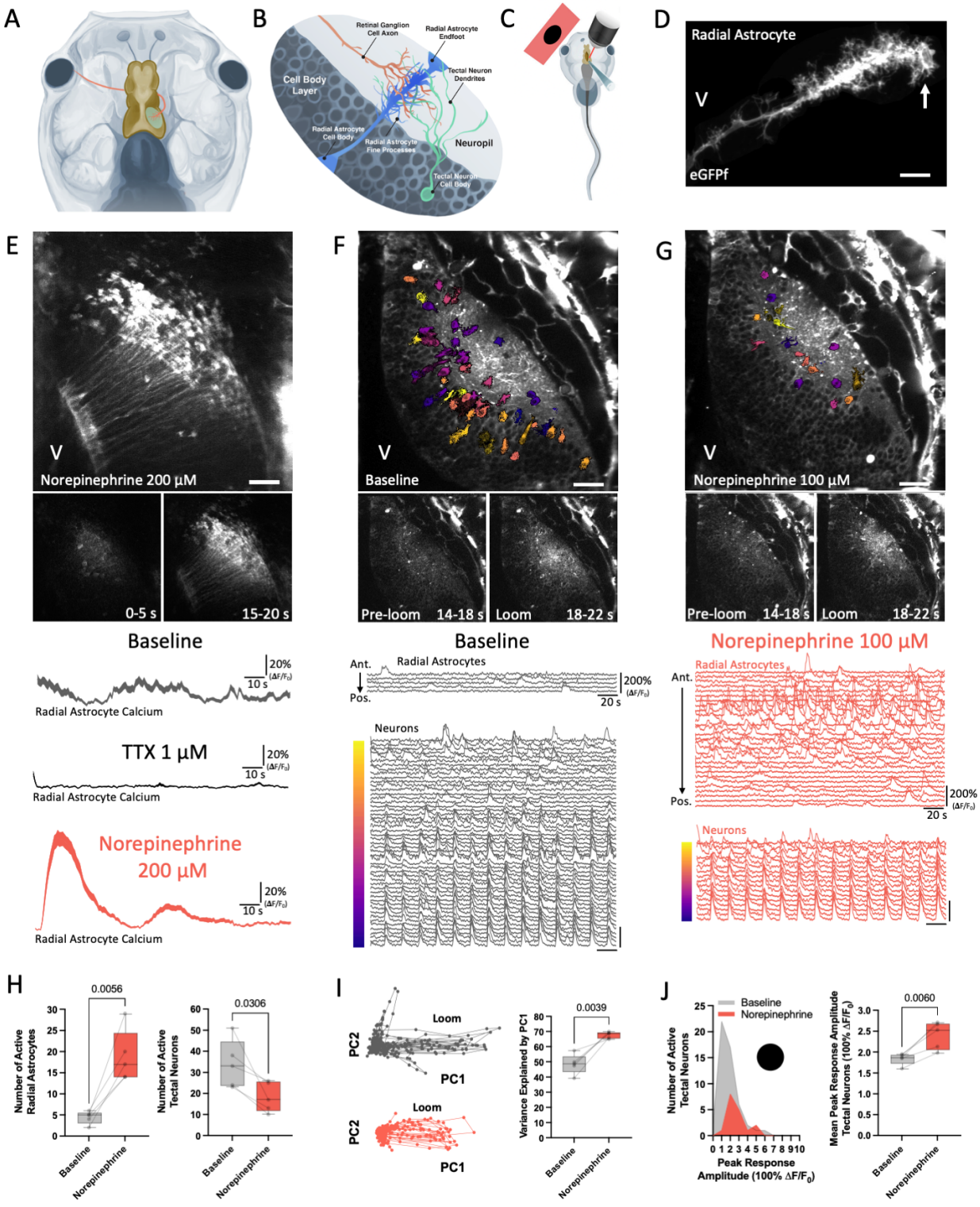
A
B
Retinal Ganglion Cell Axon
Radial Astrocyte Endfoot
Tectal Neuron Dendrites
Cell Body Layer
Radial Astrocyte Cell Body
Radial Astrocyte Fine Processes
Neuropil
Tectal Neuron Cell Body
C
D
Radial Astrocyte
V
eGFPf
E
V
Norepinephrine 200 µM
0-5 s
15-20 s
Baseline
20%
10 s
Radial Astrocyte Calcium
TTX 1 µM
Norepinephrine 200 µM
F
V
Baseline
Pre-loom 14-18 s
Loom 18-22 s
Ant.
Pos.
Radial Astrocytes
200%
20 s
Neurons
G
V
Norepinephrine 100 µM
Pre-loom 14-18 s
Loom 18-22 s
Norepinephrine 100 µM
H
0.0056
0.0306
Number of Active Radial Astrocytes
Number of Active Tectal Neurons
Baseline
Norepinephrine
I
Loom
PC2
PC1
Variance Explained by PC1
0.0039
J
Baseline
Norepinephrine
Number of Active Tectal Neurons
Peak Response Amplitude (100% ΔF/F0)
Mean Peak Response Amplitude Tectal Neurons (100% ΔF/F0)
0.0060

Figure 1. Norepinephrine directly activates radial astrocytes in the developing visual system and reduces the dimensionality of the tectal network

(A) Schematic of the *Xenopus laevis* retinotectal projection showing innervation of the contralateral optic tectum (yellow) by retinal ganglion cell axons (red). Reproduced from Benfey et al., 2021.

(B) Cellular organization of the optic tectum showing an innervating retinal ganglion cell axon (red) forming synapses with the dendrites of a tectal neuron (green) and a neighboring radial astrocyte (blue). Reproduced from Benfey et al., 2021.

(C) Schematic of a tadpole prepared for *in vivo* two-photon calcium imaging showing pharmacological manipulation of the tectum alongside visual stimulation of the animal. Reproduced from Benfey et al., 2021.

(D) Averaged projection of a radial astrocyte expressing membrane-targeted eGFP. Arrow points to the endfoot of the radial astrocyte on the pial surface of the brain. V: ventricle. Scale bar: 10 μm.

(E) Top panel: averaged projection through 140 μm Z of the optic tectum of a GCaMP6s-expressing tadpole showing elevated calcium levels in radial astrocytes following application of norepinephrine to the TTX-treated optic tectum. V: ventricle. Scale bar 25 μm. Subpanels: two time intervals showing the onset and peak of the calcium increases in radial astrocytes. Bottom: average calcium traces of radial astrocyte activity during three sequential 5 minute intervals.

(F) Top panel: averaged projection of the calcium signal from a single optical section of the tectum across 300 s during baseline looming stimulus presentation. ROIs colored to reflect anatomical position of tectal neuron traces plotted below (colored ribbon). V: ventricle. Scale bar

25 μm. Subpanels: two time intervals showing the tectal calcium signal 5 s before loom onset and 5 s following loom onset. Bottom: calcium traces of radial astrocytes sorted from anterior to posterior along the pial surface of the tectum and calcium traces of tectal neurons sorted by the first principal component showing responses to 14 looming stimulus events.

(G) Same as (F) except following NE application to the tectum.

(H) Number of active cells during baseline and NE conditions. Paired t tests (n=5 animals): $p_{\text{Radial Astrocytes}}=0.0056$, $p_{\text{Neurons}}=0.0306$.

(I) PCA plots showing the network activity from the traces in (F) (gray, baseline) and (G) (red, NE) and the percentage of the variance in the network activity explained by the first principal component in each state. Paired t test (n=5 animals): p=0.0039.

(J) Histogram showing the peak looming stimulus response amplitudes of all active tectal neurons during both baseline (gray) and NE (red) states and the mean peak looming stimulus response amplitude of all active tectal neurons during each state. Paired t test (n=5 animals): p=0.0060.

Figure 2

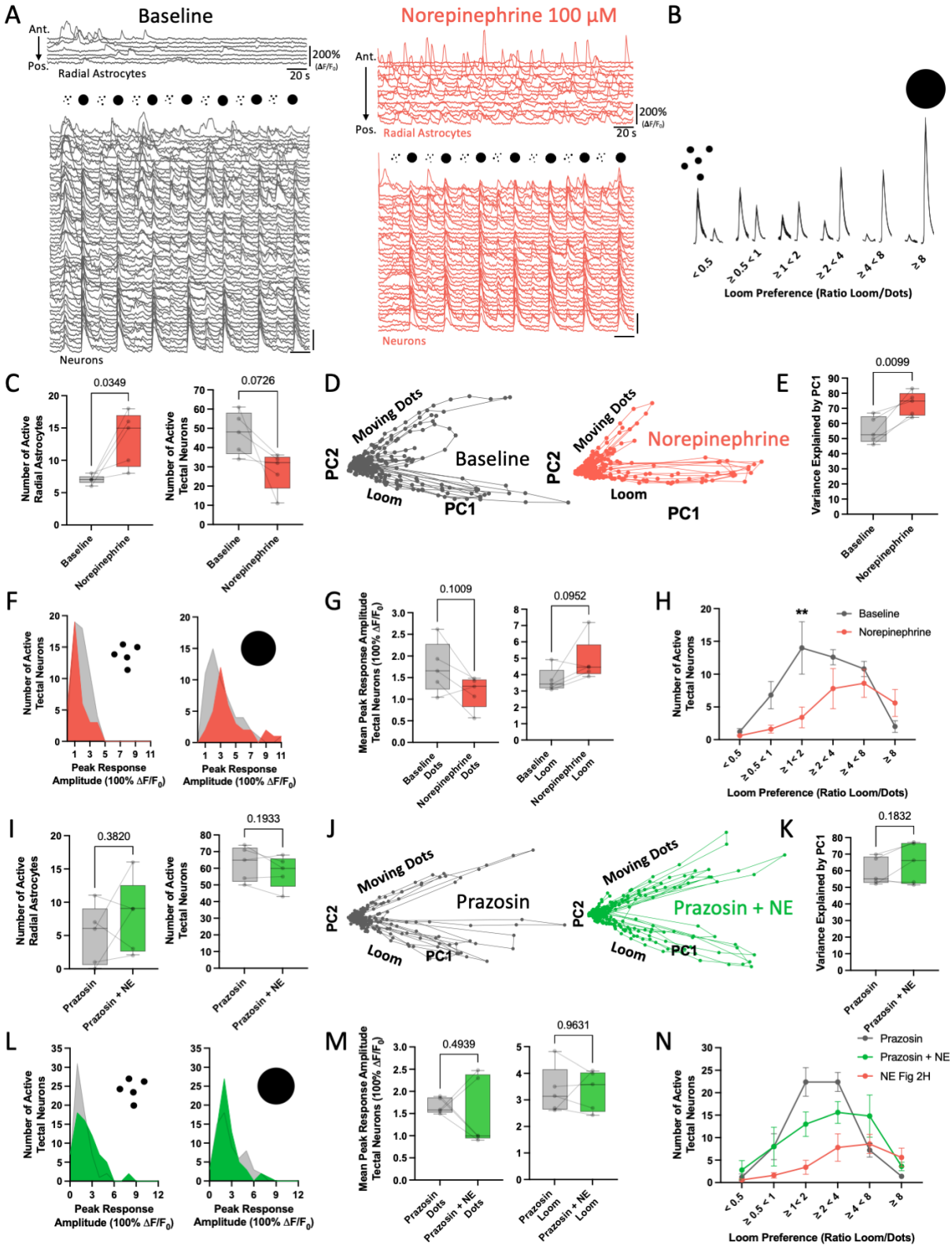
A
Baseline
Ant.
Pos.
Radial Astrocytes
200%
20 s
Neurons
Norepinephrine 100 µM
B
Loom Preference (Ratio Loom/Dots)
C
0.0349
0.0726
Number of Active Radial Astrocytes
Number of Active Tectal Neurons
Baseline
Norepinephrine
D
Moving Dots
Loom
PC1
PC2
Baseline
Norepinephrine
E
0.0099
Variance Explained by PC1
F
Peak Response Amplitude (100% ΔF/F0)
G
0.1009
0.0952
Mean Peak Response Amplitude Tectal Neurons (100% ΔF/F0)
Baseline Dots
Norepinephrine Dots
Baseline Loom
Norepinephrine Loom
H
**
Baseline
Norepinephrine
I
0.3820
0.1933
Prazosin
Prazosin + NE
J
Prazosin
Prazosin + NE
K
0.1832
L
M
0.4939
0.9631
Prazosin Dots
Prazosin + NE Dots
Prazosin Loom
Prazosin + NE Loom
N
Prazosin
Prazosin + NE
NE Fig 2H

Figure 2. The tectum preferentially encodes looming stimulus related information in the NE state

(A) Calcium traces from radial astrocytes (sorted anterior to posterior) and tectal neurons (sorted by PC1) showing responses to the alternating presentation of moving dots and looming stimulus during both baseline (gray) and NE (red) states.

(B) Looming stimulus preference bins showing the gradients between moving dots selective neurons (left to right) and looming stimulus selective neurons (right to left) in the optic tectum.

(C) Number of active cells during baseline and NE conditions. Paired t tests (n=5 animals): $p_{Radial\ Astrocytes}=0.0349$, $p_{Neurons}=0.0726$.

(D and E) (D) PCA plots showing the network activity from the traces in (A) (gray/baseline, red/NE) and (E), the percentage of the variance in the network activity explained by the first principal component in each state. Paired t test (n=5 animals): p=0.0099.

(F and G) (F) Histogram showing the peak dots stimulus response amplitudes of all active tectal neurons (left) and looming stimulus response amplitudes of all active tectal neurons (right) during both baseline (gray) and NE (red) states and (G), the mean peak dots (left) and looming stimulus (right) response amplitudes of all active tectal neurons during each state. Paired t tests (n=5 animals): $p_{Dots}=0.1009$, $p_{Loom}=0.0952$.

(H) Binned histogram showing the number of active neurons in each loom preference bin from (B) during baseline (gray) and NE (red) states. Two-way ANOVA (n=5 animals): $F_{Interaction}=3.072$, p=0.0174, $F_{Loom\ Preference\ Bin}=7.712$, p<0.0001, $F_{State}=8.708$, p=0.0049. Holm-Šidák test baseline-NE: $p_{\geq 1<2}=0.0020$.

(I) Number of active cells during baseline+prazosin (50 μM) and prazosin+NE conditions. Paired t tests (n=5 animals): $p_{\text{Radial Astrocytes}}$=0.3820, p_{Neurons}=0.1933.

(J and K) (J) PCA plots showing the network activity from the traces in (Figure S1C) (gray/baseline+prazosin, green/prazosin+NE) and (K), the percentage of the variance in the network activity explained by the first principal component in each state. Paired t test (n=5 animals): p=0.1832.

(L and M) (L) Histogram showing the peak dots stimulus response amplitudes of all active tectal neurons (left) and looming stimulus response amplitudes of all active tectal neurons (right) during both baseline+prazosin (gray) and prazosin+NE (green) states and (M), the mean peak dots (left) and looming stimulus (right) response amplitudes of all active tectal neurons during each state. Paired t tests (n=5 animals): p_{Dots}=0.4939, p_{Loom}=0.9631.

(N) Binned histogram showing the number of active neurons in each loom preference bin from (B) during baseline+prazosin (gray), prazosin+NE (green), and NE (H)(red) states. Statistical comparison does not include NE (H). Two-way ANOVA (n=5 animals): $F_{\text{Interaction}}$=2.770, p=0.0281, $F_{\text{Loom Preference Bin}}$=15.02, p<0.0001, F_{State}=0.2715, p=0.6047. Holm-Šidák test baseline+prazosin-prazosin+NE: $p_{\geq 1<2}$=0.0917.

Figure 3

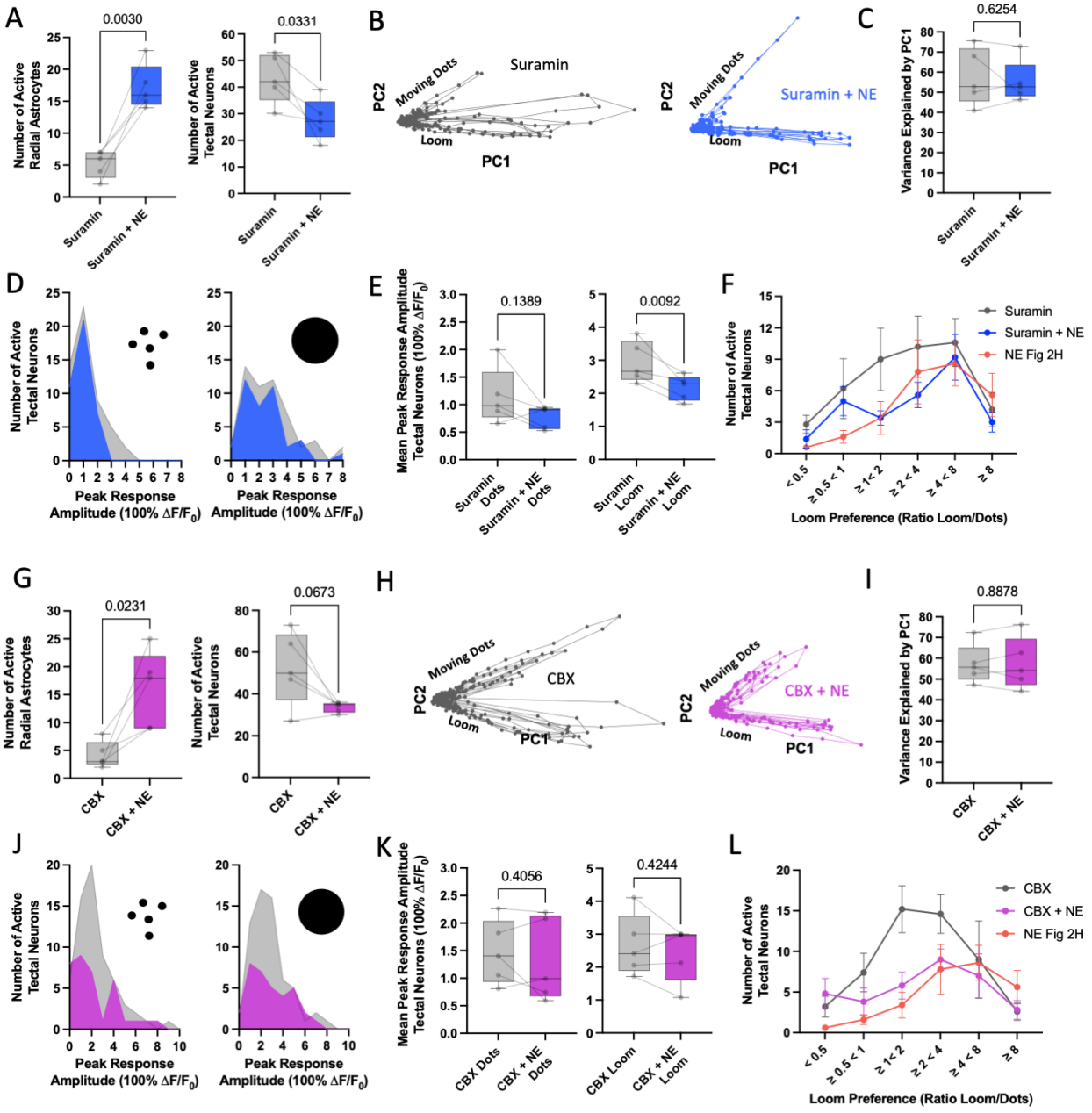
A
0.0030
0.0331
Number of Active Radial Astrocytes
Number of Active Tectal Neurons
Suramin
Suramin + NE
B
Suramin
Suramin + NE
Moving Dots
Loom
PC1
PC2
C
0.6254
Variance Explained by PC1
D
Number of Active Tectal Neurons
Peak Response Amplitude (100% ΔF/F0)
E
0.1389
0.0092
Mean Peak Response Amplitude Tectal Neurons (100% ΔF/F0)
Suramin Dots
Suramin + NE Dots
Suramin Loom
Suramin + NE Loom
F
Suramin
Suramin + NE
NE Fig 2H
Loom Preference (Ratio Loom/Dots)
G
0.0231
0.0673
CBX
CBX + NE
H
CBX
CBX + NE
I
0.8878
J
K
0.4056
0.4244
CBX Dots
CBX + NE Dots
CBX Loom
CBX + NE Loom
L
CBX
CBX + NE
NE Fig 2H

Figure 3. The loom preference state induced by NE involves the activation of P2 receptors and the opening of gap Junctions/hemichannels

(A) Number of active cells during baseline+suramin (100 μM) and suramin+NE conditions. Paired t tests (n=5 animals): $p_{\text{Radial Astrocytes}}$=0.0030, p_{Neurons}=0.0331.

(B and C) (B) PCA plots showing the network activity from the traces in (Figure S1D) (gray/baseline+suramin, blue/suramin+NE) and (C), the percentage of the variance in the network activity explained by the first principal component in each state. Paired t test (n=5 animals): p=0.6254.

(D and E) (D) Histogram showing the peak dots stimulus response amplitudes of all active tectal neurons (left) and looming stimulus response amplitudes of all active tectal neurons (right) during both baseline+suramin (gray) and suramin+NE (blue) states and (E), the mean peak dots (left) and looming stimulus (right) response amplitudes of all active tectal neurons during each state. Paired t tests (n=5 animals): p_{Dots}=0.1389, p_{Loom}=0.0092.

(F) Binned histogram showing the number of active neurons in each loom preference bin during baseline+suramin (gray), suramin+NE (blue), and NE (Figure 2H)(red) states. Statistical comparison does not include NE (Figure 2H). Two-way ANOVA (n=5 animals): $F_{\text{Interaction}}$=0.5345, p=0.7491, $F_{\text{Loom Preference Bin}}$=4.311, p=0.0026, F_{State}=5.337, p=0.0252.

(G) Number of active cells during baseline+carbenoxolone (100 μM) and carbenoxolone+NE conditions. Paired t tests (n=5 animals): $p_{\text{Radial Astrocytes}}$=0.0231, p_{Neurons}=0.0673.

(H and I) (H) PCA plots showing the network activity from the traces in (Figure S1E) (gray/baseline+carbenoxolone, purple/carbenoxolone+NE) and (I), the percentage of the variance

in the network activity explained by the first principal component in each state. Paired t test (n=5 animals): p=0.8878.

(J and K) (J) Histogram showing the peak dots stimulus response amplitudes of all active tectal neurons (left) and looming stimulus response amplitudes of all active tectal neurons (right) during both baseline+carbenoxolone (gray) and carbenoxolone+NE (purple) states and (K), the mean peak dots (left) and looming stimulus (right) response amplitudes of all active tectal neurons during each state. Paired t tests (n=5 animals): p_{Dots}=0.4056, p_{Loom}=0.4244.

(L) Binned histogram showing the number of active neurons in each loom preference bin during baseline+carbenoxolone (gray), carbenoxolone+NE (purple), and NE (Figure 2H)(red) states. Statistical comparison does not include NE (Figure 2H). Two-way ANOVA (n=5 animals): $F_{Interaction}$=1.493, p=0.2099, $F_{Loom\ Preference\ Bin}$=4.879, p=0.0011, F_{State}=5.470, p=0.0236.

Figure 4

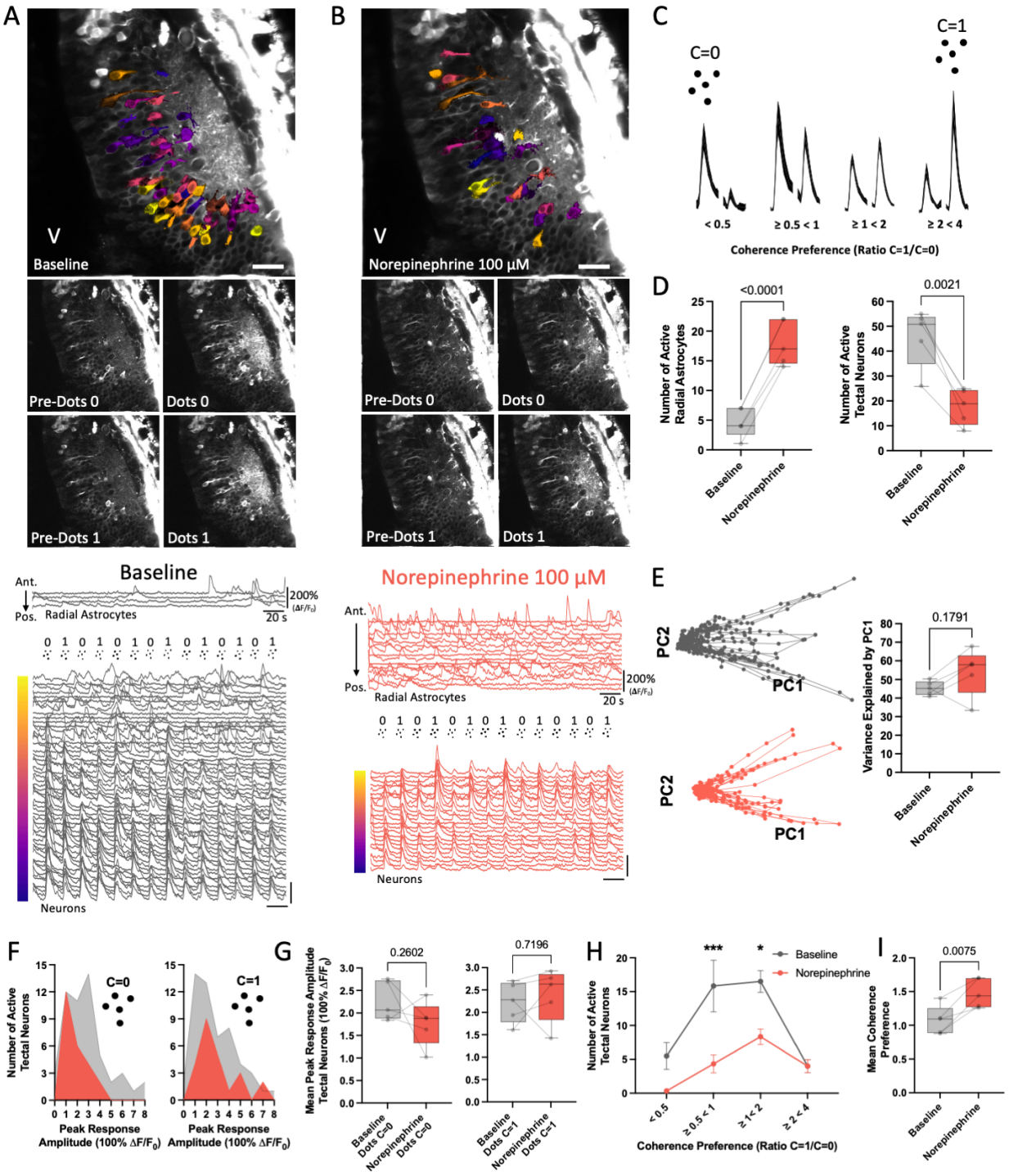
A
V
Baseline
Pre-Dots 0
Dots 0
Pre-Dots 1
Dots 1
B
V
Norepinephrine 100 µM
Pre-Dots 0
Dots 0
Pre-Dots 1
Dots 1
C
C=0
C=1
< 0.5
≥ 0.5 < 1
≥ 1 < 2
≥ 2 < 4
Coherence Preference (Ratio C=1/C=0)
D
<0.0001
Number of Active Radial Astrocytes
Baseline
Norepinephrine
0.0021
Number of Active Tectal Neurons
Baseline
Norepinephrine
Baseline
Ant.
Pos.
Radial Astrocytes
200% (ΔF/F0)
20 s
Neurons
Norepinephrine 100 µM
Ant.
Pos.
Radial Astrocytes
200% (ΔF/F0)
20 s
Neurons
E
PC2
PC1
PC2
PC1
0.1791
Variance Explained by PC1
Baseline
Norepinephrine
F
C=0
C=1
Number of Active Tectal Neurons
Peak Response Amplitude (100% ΔF/F0)
Peak Response Amplitude (100% ΔF/F0)
G
0.2602
Mean Peak Response Amplitude Tectal Neurons (100% ΔF/F0)
Baseline Dots C=0
Norepinephrine Dots C=0
0.7196
Baseline Dots C=1
Norepinephrine Dots C=1
H
***
*
Baseline
Norepinephrine
Number of Active Tectal Neurons
< 0.5
≥ 0.5 < 1
≥ 1 < 2
≥ 2 < 4
Coherence Preference (Ratio C=1/C=0)
I
0.0075
Mean Coherence Preference
Baseline
Norepinephrine

Figure 4. Enhanced preference for groups of moving dots with coherent motion in the NE state

(A) Top panel: averaged projection of the calcium signal from a single optical section of the tectum across 300 s during baseline stimulus presentation. ROIs colored to reflect anatomical position of tectal neuron traces plotted below (colored ribbon). V: ventricle. Scale bar 25 μm. Subpanels: two time intervals showing the tectal calcium signal 5 s before each stimulus onset and 5 s following each stimulus onset. Bottom: calcium traces of radial astrocytes sorted from anterior to posterior along the pial surface of the tectum and calcium traces of tectal neurons sorted by the first principal component showing responses to 14 alternating stimulus events.
(B) Same as (A) except following NE application to the tectum.
(C) Coherence preference bins showing zero coherence selective neurons (left) and full coherence selective neurons (right) in the optic tectum.
(D) Number of active cells during baseline and NE conditions. Paired t tests (n=5 animals): $p_{\text{Radial Astrocytes}}<0.0001$, $p_{\text{Neurons}}=0.0021$.
(E) PCA plots showing the network activity from the traces in (A and B) (gray/baseline, red/NE), and the percentage of the variance in the network activity explained by the first principal component in each state. Paired t test (n=5 animals): p=0.1791.
(F and G) (F) Histogram showing the peak C=0 stimulus response amplitudes of all active tectal neurons (left) and C=1 stimulus response amplitudes of all active tectal neurons (right) during both baseline (gray) and NE (red) states and (G), the mean peak C=0 stimulus (left) and C=1 stimulus (right) response amplitudes of all active tectal neurons during each state. Paired t tests (n=5 animals): $p_{C=0}=0.2602$, $p_{C=1}=0.7196$.

(H) Binned histogram showing the number of active neurons in each coherence preference bin during baseline (gray), and NE (red) states. Two-way ANOVA (n=5 animals): $F_{Interaction}$=3.656, p=0.0202, $F_{Loom\ Preference\ Bin}$=13.10, p<0.0001, F_{State}=23.66, p<0.0001.

(I) Mean C=1 coherence preference of all active tectal neurons during baseline (gray) and NE (red) states. Paired t test (n=5 animals): p=0.0075.

Figure 5

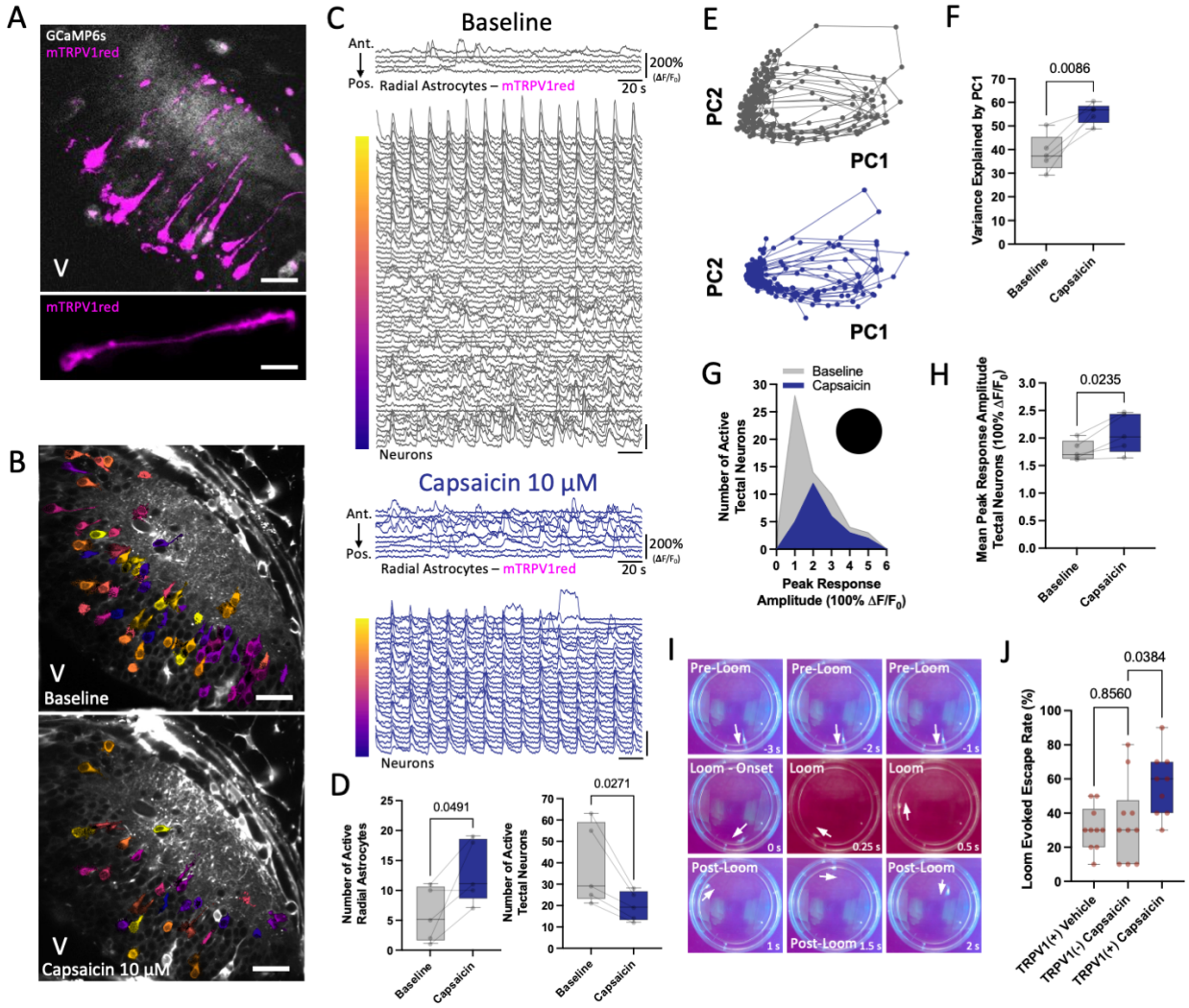
A
GCaMP6s
mTRPV1red
V
mTRPV1red
B
V
Baseline
V
Capsaicin 10 µM
C
Baseline
Ant.
Pos.
Radial Astrocytes – mTRPV1red
200%
20 s
Neurons
Capsaicin 10 µM
Ant.
Pos.
Radial Astrocytes – mTRPV1red
200%
20 s
Neurons
D
0.0491
Number of Active Radial Astrocytes
Baseline
Capsaicin
0.0271
Number of Active Tectal Neurons
Baseline
Capsaicin
E
PC2
PC1
PC2
PC1
F
0.0086
Variance Explained by PC1
Baseline
Capsaicin
G
Baseline
Capsaicin
Number of Active Tectal Neurons
Peak Response Amplitude (100% ΔF/F0)
H
0.0235
Mean Peak Response Amplitude Tectal Neurons (100% ΔF/F0)
Baseline
Capsaicin
I
Pre-Loom
Pre-Loom
Pre-Loom
-3 s
-2 s
-1 s
Loom - Onset
Loom
Loom
0 s
0.25 s
0.5 s
Post-Loom
Post-Loom
Post-Loom
1 s
Post-Loom 1.5 s
2 s
J
0.0384
0.8560
Loom Evoked Escape Rate (%)
TRPV1(+) Vehicle
TRPV1(-) Capsaicin
TRPV1(+) Capsaicin

Figure 5. Chemogenetic activation of radial astrocytes recapitulates the effects of NE on looming stimulus detection and enhances loom-evoked escape behavior in freely swimming animals

(A) Top panel: averaged projection of the calcium signal (gray) and mTRPV1red electroporated radial astrocytes (magenta) in the tectum. Bottom panel: a single mTRPV1red labeled radial astrocyte in the tectum. V: ventricle. Scale bar: 20 μm.

(B) Averaged projection of the calcium signal during baseline (top) and following chemogenetic activation of radial astrocytes (bottom). ROIs colored to reflect anatomical position of tectal neuron traces plotted in (C). V: ventricle. Scale bar 25 μm.

(C) Calcium traces of radial astrocytes sorted from anterior to posterior along the pial surface of the tectum and calcium traces of tectal neurons sorted by the first principal component showing responses to 14 looming stimulus events during baseline (gray) and following chemogenetic activation of radial astrocytes (dark blue).

(D) Number of active cells during baseline and glial activation state. Paired t tests (n=5 animals): $p_{\text{Radial Astrocytes}}=0.0491$, $p_{\text{Neurons}}=0.0271$.

(E and F) (E) PCA plots showing the network activity from the traces in (C) (gray/baseline, dark blue/glial activation states) and (F), the percentage of the variance in the network activity explained by the first principal component in each state. Paired t test (n=5 animals): p=0.0086.

(G and H) (G) Histogram showing the peak looming stimulus response amplitudes of all active tectal neurons during both baseline (gray) and glial activation (dark blue) states and (G), the mean peak looming stimulus response amplitudes of all active tectal neurons during each state. Paired t tests (n=5 animals): p=0.0235.

(I) Images showing a characteristic loom-evoked escape response in a freely swimming tadpole. (J) Loom-evoked escape rate of tadpoles during baseline (gray) and glial activation (dark blue) states. One-way ANOVA (n=10 animals per condition): F=4.846, p=0.0163. Dunnett's test mTRPV1(-)+capsaicin-mTRPV1(+) +capsaicin: p=0.0384.

Acknowledgements

We would like to thank the lab of DA Prober for providing us with the mTRPV1 plasmid we used for our chemogenetic experiments as well as Ms. Audrey Desaulniers, Orcéine, Montréal, Canada, for creating the artwork used in our figures. We would also like to thank Dr. Blake Richards and his lab members for meaningful discussions that helped to inform our dimensionality reduction analysis approach. This research was supported by both Masters and Doctoral Canada Postgraduate Scholarships to N.J.B from the Canadian Institutes of Health Research and the Natural Sciences and Engineering Research Council of Canada. Support was also received through the funding E.S.R. received from the Canadian Institutes of Health Research (FDN-143238) and Fonds de recherche santé Québec (31036). Both A.S. and E.S.R also receive financial support from the Brain Canada Canadian Neurophotonics Platform.

Author Contributions

N.J.B and E.S.R conceived of and designed the study. N.J.B. carried out all imaging experiments and data analysis with the help of custom python scripts written by A.T.B. A.S. developed the methodology for labeling animals with GCaMP6s and provided technical support throughout the development of the techniques used in this study. N.J.B. drafted the manuscript which was subsequently edited by E.S.R. All authors contributed to the editing of the final version of the manuscript. E.S.R obtained the funding and supervised the research.

Declaration of Interests

The authors declare no competing interests.

Methods

Resource availability

Lead Contact

All requests for further information about resources or reagents used in this manuscript can be directed to the lead contact, Edward S. Ruthazer (edward.ruthazer@mcgill.ca).

Materials Availability

Any reagents produced for the experiments carried out in this manuscript will be made accessible upon request to the lead contact or through the relevant public repository responsible for distributing the reagents.

Data and Code Availability

All data included in the publication of this manuscript will be made accessible by the lead contact upon reasonable request. All code written in house for this manuscript has been deposited at Mendeley and is publicly accessible as of the publication of this manuscript. Any additional requests for information relevant for the analysis of the data provided in this manuscript will be made available from the lead contact upon request.

Experimental model and subject details

All experimentation and use of animals was carried out in accordance with the Canadian Council of Animal Care guidelines and received approval from the Montreal Neurological Institute-Hospital Animal Care Committee. All adult *Xenopus laevis* frogs (albino) used to produce *in vitro* born tadpoles were kept in the care of the Montreal Neurological Institute-Hospital Center for Neurological Disease Models animal care facility. All animals used in the experiments outlined in this manuscript ranged in age from developmental stage 45-47. As sexual characteristics are not defined at these early developmental stages, the sex of the animals used in our experiments was not relevant to assess.

GCaMP6s mRNA synthesis and generation of GCaMP6s-expressing tadpoles

GCaMP6s-expressing tadpoles were generated following previously published methods from our lab (see Benfey et al., 2021 for more detail). In brief GCaMP6s mRNA was generated using a SP6 mMessage mMachine Kit (Ambion, Thermo Fisher) to transcribe GCaMP6s mRNA from pCS2+ plasmids. Following *in vitro* fertilization, eggs were monitored until the first cell division commenced and then injected with 500-750 pg of GCaMP6s mRNA using a calibrated glass micropipette and a PLI-100 picoinjector (Harvard Apparatus). Animals were raised under a 12 H light / 12 H dark cycle in an 18°C incubator until they reached stages developmental 45-47.

Tectal electroporation of radial astrocytes

To transfect radial astrocytes with either membrane-targeted eGFPf for structural visualization or mTRPV1red for chemogenetic activation we followed previously published protocols from our lab (Tremblay et al., 2009). In brief, the tectum of anesthetized developmental stage 45 tadpoles (0.02% MS-222 in 0.1X MBSH) was injected with plasmid (0.5-1 µg/µL) encoding the desired construct and using two platinum electrodes placed on either side of the tectum current was passed in both directions of polarity using Grass Instruments SD9 electrical stimulator. Animals were left to recover in 0.1X MBSH for 2 days before chemogenetic activation and imaging was performed.

Preparing GCaMP6s-expressing tadpoles for live imaging

After screening stage 46-47 GCaMP6s-expressing tadpoles for sufficient levels of GCaMP6s expression in the optic tectum using an Olympus BX-43 epifluorescence microscope, animals were treated with 2mM pancuronium dibromide (Tocris) in 0.1X MBSH for several minutes until the onset of paralysis and then embedded in 0.8% low melting point agarose (Thermo Fisher) in a custom made imaging chamber. To circumvent the blood brain barrier and allow for direct acute pharmacological manipulation of the optic tectum during live imaging, a small puncture through the skin covering the tectum was cut using the tip of a 30 ga syringe needle 30 minutes before imaging. Animals were then submerged in 9mL of external saline solution (115mM NaCl, 2mM KCl, 3mM CaCl2, 3mM MgCl2, 5mM HEPES, and 10mM glucose, pH 7.20, 250 mOsm).

Two-photon microscope

All *in vivo* imaging experiments were carried out using a custom built Thorlabs multiphoton resonant scanner microscope with a 20X water-immersion objective (1.0 NA) attached to a piezoelectric focus mount (PI). A Spectra-Physics InSight3x infrared femtosecond pulsed laser was used to generate fluorescence excitation light during live imaging experiments.

***In vivo* calcium imaging of GCaMP6s-expressing tadpoles**

To minimize the occurrence of drift across all three dimensions during imaging sessions, animals were left to settle in the imaging chambers under the microscope for approximately 30 minutes before the onset of imaging. Calcium imaging was then performed in 5 minute intervals using an excitation wavelength of 910 nM and a power of ~ 125 mW (as measured before the scan-head). Each 5 minute imaging period involved the collection of 4500 images at a rate of 15 images per second in a single optical section in the z dimension with x,y dimensions of 224.256 μm^2 at a resolution of 512 $pixels^2$.

All drugs used for pharmacological manipulation of the tectum were dissolved in 1 mL of external saline solution to facilitate rapid diffusion when applied. Agonists were applied immediately following collection of a 5 minute baseline and their effects were imaged after waiting 60 seconds for water soluble drugs such as NE and after 300 seconds for less water soluble drugs like capsaicin in order to allow for adequate diffusion of the agents into the optic tectum. Antagonists were added to the bath of embedded animals immediately following the

creation of the incision above the tectum and allowed to equilibrate for 30 minutes prior to imaging.

Visual stimulation during live imaging experiments was carried out by using a flat panel display screen (800 X 480, Adafruit, NY) covered with a red-filter (Wratten #29, Kodak) to stimulate one eye of the animal while imaging the contralateral optic tectum.

Visual stimulation paradigms

Three different visual stimulation paradigms were used throughout our experiments. All visual stimuli were generated using custom python scripts running the PsychoPy package (https://www.psychopy.org/index.html). All stimuli were presented with an interstimulus interval of 20 s to avoid the habituation that we have observed to occur at faster stimulus presentation frequencies. Looming stimuli consisted of a blank screen for 19 s followed by the appearance of a small black dot which rapidly expands to fill the screen over the following 1 s. The moving dots stimuli used in the moving dots vs loom experiments were presented for 1 s following 19 s of blank screen and consisted of 25 size 25 black dots (~10° in size for the animal) which randomly appear on the screen and move at a speed of 2 units per frame in various directions with no coherence. The moving dots used in the zero coherence versus full coherence experiments persisted for 2 s to exaggerate the motion of the stimulus and again consisted of 25 size 25 black dots (~10°) which randomly appear on the screen and move at a speed of 2 units per frame either with no coherence or with full coherence in a downward direction to enhance visual detection.

Registration and ROI extraction of raw calcium imaging data using Suite2p

Calcium imaging data collected on the two-photon microscope was registered and both neuronal and radial astrocyte ROIs were extracted using Suite2p software (http://github.com/MouseLand/suite2p) running on python 3 as described previously (Benfey et al., 2021). Raw fluorescence traces for each ROI were exported for further analysis.

Baseline normalization and quantification of fluorescence increases

Raw fluorescence traces were normalized to baseline using standard $\Delta F/F_0$ methods. In brief, baseline fluorescence was estimated using a sliding window to calculate the bottom 5th percentile of fluorescence values within a 120 s window centered around each value in the fluorescence trace. For each fluorescence value, we subtracted this baseline and then divided by the baseline value in order to obtain a percent change in the fluorescence signal relative to baseline across time.

Principal component analysis

Principal component analysis of the tectal network activity during each 5 minute imaging epoch was computed using custom made python scripts built using open source modules from both scikit-learn (https://scikit-learn.org/stable/index.html) and SciPy (https://scipy.org/) which we have made available along with this manuscript.

Loom-evoked escape behavior

Loom-evoked escape behavior was assayed in freely swimming stage 47 tadpoles using methods published by Lim and Ruthazer (2021)(https://github.com/tonykylim/XenLoom_beta). Tadpoles are placed in a closed 6 cm diameter petri dish submerged in 0.1X MBSH at the bottom of a large 20 cm glass bowl filled with 0.1X MBSH and allowed to freely navigate this environment. A 2000 lumens projector is used to present 10 looming stimuli (one every 20 s) on a paper screen attached to the side of the bowl while a webcam fixed overtop of the bowl tracks the animal's movement through its environment. A binary assessment of whether a loom-evoked escape response was initiated was carried out for each video while blind to experimental conditions.

Statistical analysis

All statistical analysis was performed using GraphPad's Prism software package. All pairwise analysis was performed using two-tailed paired t tests while group analysis was performed using one-way or two-way ANOVA followed by Dunnett's or Holm-Šidák's tests respectively when appropriate. All relevant statistical information including p values (with significance defined as a p value of 0.05 or less) can be found in the appropriate figure legends.

References

Abbas, F., Triplett, M.A., Goodhill, G.J., and Meyer, M.P. (2017). A Three-Layer Network Model of Direction Selective Circuits in the Optic Tectum. *Front. Neural Circuits 11*, 88. doi: 10.3389/fncir.2017.00088.

Agarwal, A., Wu, P.H., Hughes, E.G., Fukaya, M., Tischfield, M.A., Langseth, A.J., Wirtz, D., and Bergles, D.E. (2017). Transient Opening of the Mitochondrial Permeability Transition Pore Induces Microdomain Calcium Transients in Astrocyte Processes. *Neuron 93*, 587-605. doi: 10.1016/j.neuron.2016.12.034.

Agostinho, P., Madeira, D., Dias, L., Simões, A.P., Cunha, R.A., and Canas, P.M. (2020). Purinergic signaling orchestrating neuron-glia communication. *Pharmacol. Res. 162*, 105253. doi: 10.1016/j.phrs.2020.105253.

Armbruster, M., Naskar, S., Garcia, J.P., Sommer, M., Kim, E., Adam, Y., Haydon, P.G., Boyden, E.S., Cohen, A.E., and Dulla, C.G. (2022). Neuronal activity drives pathway-specific depolarization of peripheral astrocyte processes. *Nat. Neurosci. 25*, 607-616. doi: 10.1038/s41593-022-01049-x.

Asadollahi, A., and Knudsen, E.I. (2016). Spatially precise visual gain control mediated by a cholinergic circuit in the midbrain attention network. *Nat. Commun. 7*, 13472. doi: 10.1038/ncomms13472.

Baginskas, A., Kuraite, V., and Kuras, A. (2013). Phasic nicotinic potentiation of frog retinotectal transmission facilitates eliciting of higher activity level of the tectum column. *Neurosci. Lett*. *554*, 1-5. doi: 10.1016/j.neulet.2013.08.053.

Baginskas, A., and Kuras, A. (2016). Retinal co-mediator acetylcholine evokes muscarinic inhibition of recurrent excitation in frog tectum column. *Neurosci. Lett*. *629*, 137-142. doi: 10.1016/j.neulet.2016.07.005.

Barker, A.J., and Baier, H. (2015). Sensorimotor decision making in the zebrafish tectum. *Curr. Biol. 25*, 2804-2814. doi: 10.1016/j.cub.2015.09.055.

Barker, A.J., and Baier, H. (2013). SINs and SOMs: neural microcircuits for size tuning in the zebrafish and mouse visual pathway. *Front. Neural Circuits. 7*, 89. doi: 10.3389/fncir.2013.00089.

Barker, A.J., Helmbrecht, T.O., Grob, A.A., and Baier, H. (2021). Functional, molecular and morphological heterogeneity of superficial interneurons in the larval zebrafish tectum. *J. Comp. Neurol. 529*, 2159-2175. doi: 10.1002/cne.25082.

Bazargani, N., and Attwell, D. (2016). Astrocyte calcium signaling: the third wave. *Nat. Neurosci*. *19*, 182-189. doi: 10.1038/nn.4201.

Bazargani, N., and Attwell, D. (2017). Amines, Astrocytes, and Arousal. *Neuron 94*, 228-231. doi: 10.1016/j.neuron.2017.03.035.

Bear, M.F., and Singer, W. (1986). Modulation of visual cortical plasticity by acetylcholine and noradrenaline. *Nature 320*, 172-176. doi: 10.1038/320172a0.

Bekar, L.K., He, W., and Nedergaard, M. (2008). Locus coeruleus alpha-adrenergic-mediated activation of cortical astrocytes in vivo. *Cereb. Cortex 18*, 2789-2795. doi: 10.1093/cercor/bhn040.

Benfey, N.J., Li, V.J., Schohl, A., and Ruthazer, E.S. (2021). Sodium-calcium exchanger mediates sensory-evoked glial calcium transients in the developing retinotectal system. *Cell Rep*. *37*, 109791. doi: 10.1016/j.celrep.2021.109791.

Bennett, M.V., Contreras, J.E., Bukauskas, F.F., and Sáez, J.C. (2003). New roles for astrocytes: gap junction hemichannels have something to communicate. *Trends Neurosci. 26*, 610-617. doi: 10.1016/j.tins.2003.09.008.

Berridge, C.W., and Waterhouse, B.D. The locus coeruleus-noradrenergic system: modulation of behavioral state and state-dependent cognitive processes. *Brain Res. Brain Res. Rev. 42*, 33-84. doi: 10.1016/s0165-0173(03)00143-7.

Boddum, K., Jensen, T.P., Magloire, V., Kristiansen, U., Rusakov, D.A., Pavlov, I., and Walker, M.C. (2016). Astrocytic GABA transporter activity modulates excitatory neurotransmission. *Nat. Commun*. *7*, 13572. doi: 10.1038/ncomms13572.

Boué-Grabot, E., and Pankratov, Y. (2017). Modulation of Central Synapses by Astrocyte-Released ATP and Postsynaptic P2X Receptors. *Neural. Plast. 2017*, 9454275. doi: 10.1155/2017/9454275.

Chen, N., Sugihara, H., Sharma, J., Perea, G., Petravicz, J., Le, C., and Sur, M. (2012). Nucleus basalis-enabled stimulus-specific plasticity in the visual cortex is mediated by astrocytes. *Proc. Natl. Acad. Sci. U.S.A*. *109*, E2832-2841. doi: 10.1073/pnas.1206557109.

Chen, S., Chiu, C.N., McArthur, K.L., Fetcho, J.R., and Prober, D.A. (2016). TRP channel mediated neuronal activation and ablation in freely behaving zebrafish. *Nat. Methods*. *13*, 147-150. doi: 10.1038/nmeth.3691.

Corkrum, M., Covelo, A., Lines, J., Bellocchio, L., Pisansky, M., Loke, K., Quintana, R., Rothwell, P.E., Lujan, R., Marsicano, G., Martin, E.D., Thomas, M.J., Kofuji, P., and Araque, A. (2020). Dopamine-Evoked Synaptic Regulation in the Nucleus Accumbens Requires Astrocyte Activity. *Neuron 105*, 1036-1047.e5. doi: 10.1016/j.neuron.2019.12.026.

Covelo, A., and Araque, A. (2018). Neuronal activity determines distinct gliotransmitter release from a single astrocyte. *Elife 7*, e32237. doi: 10.7554/eLife.32237.

Dallérac, G., Zapata, J., and Rouach, N. (2018). Versatile control of synaptic circuits by astrocytes: where, when and how? *Nat. Rev. Neurosci. 19*, 729-743. doi: 10.1038/s41583-018-0080-6.

Deemyad, T., Lüthi, J., and Spruston, N. (2018). Astrocytes integrate and drive action potential firing in inhibitory subnetworks. *Nat. Commun*. *9*, 4336. doi: 10.1038/s41467-018-06338-3.

Del Bene, F., Wyart, C., Robles, E., Tran, A., Looger, L., Scott, E.K., Isacoff, E.Y., and Baier, H. (2010). Filtering of visual information in the tectum by an identified neural circuit. *Science 330*, 669-673. doi: 10.1126/science.1192949.

Del Campo, N., Chamberlain, S.R., Sahakian, B.J., and Robbins, T.W. (2011). The roles of dopamine and noradrenaline in the pathophysiology and treatment of attention-deficit/hyperactivity disorder. *Biol. Psychiatry 69*, e145-157. doi: 10.1016/j.biopsych.2011.02.036.

Dunn, T.W., Gebhardt, C., Naumann, E.A., Riegler, C., Ahrens, M.B., Engert, F., and Del Bene, F. (2016). Neural Circuits Underlying Visually Evoked Escapes in Larval Zebrafish. *Neuron 89*, 613-628. doi: 10.1016/j.neuron.2015.12.021.

Eersapah, V., Hugel, S., and Schlichter, R. (2019). High-resolution detection of ATP release from single cultured mouse dorsal horn spinal cord glial cells and its modulation by noradrenaline. *Purinergic Signal. 15*, 403-420. doi: 10.1007/s11302-019-09673-2.

Fahrig, T. (1993). Receptor subtype involved and mechanism of norepinephrine-induced stimulation of glutamate uptake into primary cultures of rat brain astrocytes. *Glia 7*, 212-218. doi: 10.1002/glia.440070304.

Feng, J., Zhang, C., Lischinsky, J.E., Jing, M., Zhou, J., Wang, H., Zhang, Y., Dong, A., Wu, Z., Wu, H., Chen, W., Zhang, P., Zou, J., Hires, S.A., Zhu, J.J., Cui, G., Lin, D., Du, J., and Li, Y. (2019). A Genetically Encoded Fluorescent Sensor for Rapid and Specific In Vivo Detection of Norepinephrine. *Neuron 102*, 745-761. doi: 10.1016/j.neuron.2019.02.037.

Fischer, T., Scheffler, P., and Lohr, C. (2020). Dopamine-induced calcium signaling in olfactory bulb astrocytes. *Sci. Rep. 10*, 631. doi: 10.1038/s41598-020-57462-4.

Förster, D., Helmbrecht, T.O., Mearns, D.S., Jordan, L., Mokayes, N., and Baier, H. (2020). Retinotectal circuitry of larval zebrafish is adapted to detection and pursuit of prey. *Elife 9*, e58596. doi: 10.7554/eLife.58596.

Fujii, Y., Maekawa, S., and Morita, M. (2017). Astrocyte calcium waves propagate proximally by gap junction and distally by extracellular diffusion of ATP released from volume-regulated anion channels. *Sci. Rep. 7*, 13115. doi: 10.1038/s41598-017-13243-0.

Fukuyama, K., Ueda, Y., and Okada, M. (2020). Effects of Carbamazepine, Lacosamide and Zonisamide on Gliotransmitter Release Associated with Activated Astroglial Hemichannels. *Pharmaceuticals (Basel) 13*, 117. doi: 10.3390/ph13060117.

Gaidin, S.G., Zinchenko, V.P., Sergeev, A.I., Teplov, I.Y., Mal'tseva, V.N., and Kosenkov, A.M. (2020). Activation of alpha-2 adrenergic receptors stimulates GABA release by astrocytes. *Glia 68*, 1114-1130. doi: 10.1002/glia.23763.

Giaume, C., Marin, P., Cordier, J., Glowinski, J., and Premont, J. (1991). Adrenergic regulation of intercellular communications between cultured striatal astrocytes from the mouse. *Proc. Natl. Acad. Sci. U.S.A*. *88*, 5577-81. doi: 10.1073/pnas.88.13.5577.

Gordon, G.R., Baimoukhametova, D.V., Hewitt, S.A., Rajapaksha, W.R., Fisher, T.E., and Bains, J.S. (2005). Norepinephrine triggers release of glial ATP to increase postsynaptic efficacy. *Nat. Neurosci*. *8*, 1078-1086. doi: 10.1038/nn1498.

Gourine, A.V., Kasymov, V., Marina, N., Tang, F., Figueiredo, M.F., Lane, S., Teschemacher, A.G., Spyer, K.M., Deisseroth, K., and Kasparov, S. (2010). Astrocytes control breathing through pH-dependent release of ATP. *Science 329*, 571-575. doi: 10.1126/science.1190721.

Gray, S.R., Ye, L., Ye, J.Y., and Paukert, M. (2021). Noradrenergic terminal short-term potentiation enables modality-selective integration of sensory input and vigilance state. *Sci. Adv*. *7*, 1378. doi: 10.1126/sciadv.abk1378.

Hansson, E., and Rönnbäck, L. (1989). Regulation of glutamate and GABA transport by adrenoceptors in primary astroglial cell cultures. *Life Sci*. *44*, 27-34. doi: 10.1016/0024-3205(89)90214-2.

Heap, L.A.L., Vanwalleghem, G., Thompson, A.W., Favre-Bulle, I.A., and Scott, E.K. (2018). Luminance Changes Drive Directional Startle through a Thalamic Pathway. *Neuron 99*, 293-301 doi: 10.1016/j.neuron.2018.06.013.

Henley, J.M., Lindstrom, J.M., and Oswald, R.E. (1986). Acetylcholine receptor synthesis in retina and transport to optic tectum in goldfish. *Science 232*, 1627-1629. doi: 10.1126/science.3715468.

Houades, V., Koulakoff, A., Ezan, P., Seif, I., and Giaume, C. (2008). Gap junction-mediated astrocytic networks in the mouse barrel cortex. *J. Neurosci. 28*, 5207-5217. doi: 10.1523/JNEUROSCI.5100-07.2008.

Isa, T., Marquez-Legorreta, E., Grillner, S., and Scott, E.K. (2021). The tectum/superior colliculus as the vertebrate solution for spatial sensory integration and action. *Curr. Biol. 31*, 741-762. doi: 10.1016/j.cub.2021.04.001.

Jang, E.V., Ramirez-Vizcarrondo, C., Aizenman, C.D., and Khakhalin, A.S. (2016). Emergence of Selectivity to Looming Stimuli in a Spiking Network Model of the Optic Tectum. *Front. Neural Circuits 10*, 95. doi: 10.3389/fncir.2016.00095.

Kulik, A., Haentzsch, A., Lückermann, M., Reichelt, W., and Ballanyi, K. (1999). Neuron-glia signaling via alpha(1) adrenoceptor-mediated Ca(2+) release in Bergmann glial cells in situ. *J. Neurosci. 19*, 8401-8408. doi: 10.1523/JNEUROSCI.19-19-08401.1999.

Lalo, U., Palygin, O., Rasooli-Nejad, S., Andrew, J., Haydon, P.G., and Pankratov, Y. (2014). Exocytosis of ATP from astrocytes modulates phasic and tonic inhibition in the neocortex. *PLoS Biol. 12*, 1001747. doi: 10.1371/journal.pbio.1001747.

Lim, T.K., and Ruthazer, E.S. (2021). Microglial trogocytosis and the complement system regulate axonal pruning in vivo. *Elife 10*, 62167. doi: 10.7554/eLife.62167.

Lines, J., Martin, E.D., Kofuji, P., Aguilar, J., and Araque, A. (2020). Astrocytes modulate sensory-evoked neuronal network activity. *Nat. Commun.* 11, 3689. doi: 10.1038/s41467-020-17536-3.

Liu, Z., Ciarleglio, C.M., Hamodi, A.S., Aizenman, C.D., and Pratt, K.G. (2016). A population of gap junction-coupled neurons drives recurrent network activity in a developing visual circuit. *J. Neurophysiol. 115*, 1477-1486. doi: 10.1152/jn.01046.2015.

Ma, Z., Stork, T., Bergles, D.E., and Freeman, M.R. (2016). Neuromodulators signal through astrocytes to alter neural circuit activity and behaviour. *Nature 539*, 428-432. doi: 10.1038/nature20145.

Marques, J.C., Li, M., Schaak, D., Robson, D.N., and Li, J.M. (2020). Internal state dynamics shape brainwide activity and foraging behaviour. *Nature 577*, 239-243. doi: 10.1038/s41586-019-1858-z.

Mathis, C., Savier, E., Bott, J.B., Clesse, D., Bevins, N., Sage-Ciocca, D., Geiger, K., Gillet, A., Laux-Biehlmann, A., Goumon, Y., Lacaud, A., Lelièvre, V., Kelche, C., Cassel, J.C., Pfrieger, F.W., and Reber, M. (2015). Defective response inhibition and collicular noradrenaline enrichment in mice with duplicated retinotopic map in the superior colliculus. *Brain Struct. Funct. 220*, 1573-84. doi: 10.1007/s00429-014-0745-5.

Meunier, C., Wang, N., Yi, C., Dallerac, G., Ezan, P., Koulakoff, A., Leybaert, L., and Giaume, C. (2017). Contribution of Astroglial Cx43 Hemichannels to the Modulation of Glutamatergic Currents by D-Serine in the Mouse Prefrontal Cortex. *J. Neurosci. 37*, 9064-9075. doi: 10.1523/JNEUROSCI.2204-16.2017.

Miraucourt, L.S., Silva, J.S., Burgos, K., Li, J., Abe, H., Ruthazer, E.S., and Cline, H.T. (2012). GABA expression and regulation by sensory experience in the developing visual system. *PLoS One 7*, 29086. doi: 10.1371/journal.pone.0029086.

Mu, Y., Bennett, D.V., Rubinov, M., Narayan, S., Yang, C.T., Tanimoto, M., Mensh, B.D., Looger, L.L., and Ahrens, M.B. (2019). Glia Accumulate Evidence that Actions Are Futile and Suppress Unsuccessful Behavior. *Cell 178*, 27-43 doi: 10.1016/j.cell.2019.05.050.

Nagai, J., Yu, X., Papouin, T., Cheong, E., Freeman, M.R., Monk, K.R., Hastings, M.H., Haydon, P.G., Rowitch, D., Shaham, S., and Khakh, B.S. (2021). Behaviorally consequential astrocytic regulation of neural circuits. *Neuron 109*, 576-596. doi: 10.1016/j.neuron.2020.12.008.

Ni, A.M., Bowes, B.S., Ruff, D.A., and Cohen, M.R. (2022). Methylphenidate as a causal test of translational and basic neural coding hypotheses. *Proc. Natl. Acad. Sci. U.S.A. 119*, 2120529119. doi: 10.1073/pnas.2120529119.

Nuriya, M., Morita, A., Shinotsuka, T., Yamada, T., and Yasui, M. (2018). Norepinephrine induces rapid and long-lasting phosphorylation and redistribution of connexin 43 in cortical astrocytes. *Biochem. Biophys. Res. Commun*. *504*, 690-697. doi: 10.1016/j.bbrc.2018.09.021.

Octeau, J.C., Gangwani, M.R., Allam, S.L., Tran, D., Huang, S., Hoang-Trong, T.M., Golshani, P., Rumbell, T.H., Kozloski, J.R., and Khakh, B.S. (2019). Transient, Consequential Increases in Extracellular Potassium Ions Accompany Channelrhodopsin2 Excitation. *Cell rep.* 27, 2249–2261 doi: 10.1016/j.celrep.2019.04.078.

Oe, Y., Wang, X., Patriarchi, T., Konno, A., Ozawa, K., Yahagi, K., Hirai, H., Tsuboi, T., Kitaguchi, T., Tian, L., McHugh, T.J., and Hirase, H. (2020). Distinct temporal integration of noradrenaline signaling by astrocytic second messengers during vigilance. *Nat. Commun*. *11*, 471. doi: 10.1038/s41467-020-14378-x.

Ohkita, M., Saito, S., Imagawa, T., Takahashi, K., Tominaga, M., and Ohta, T. (2012). Molecular cloning and functional characterization of Xenopus tropicalis frog transient receptor potential vanilloid 1 reveal its functional evolution for heat, acid, and capsaicin sensitivities in terrestrial vertebrates. *J. Biol. Chem*. *287*, 2388-2397. doi: 10.1074/jbc.M111.305698.

Orellana, J.A., and Stehberg, J. (2014). Hemichannels: new roles in astroglial function. *Front. Physiol. 5*, 193. doi: 10.3389/fphys.2014.00193.

Paukert, M., Agarwal, A., Cha, J., Doze, V.A., Kang, J.U., and Bergles, D.E. (2014). Norepinephrine controls astroglial responsiveness to local circuit activity. *Neuron 82*, 1263-1270. doi: 10.1016/j.neuron.2014.04.038.

Pang, R., Lansdell, B.J., and Fairhall, A.L. (2016). Dimensionality reduction in neuroscience. *Curr. Biol*. *26*, 656-660. doi: 10.1016/j.cub.2016.05.029.

Papouin, T., Dunphy, J.M., Tolman, M., Dineley, K.T., and Haydon, P.G. (2017). Septal Cholinergic Neuromodulation Tunes the Astrocyte-Dependent Gating of Hippocampal NMDA Receptors to Wakefulness. *Neuron 94*, 840-854. doi: 10.1016/j.neuron.2017.04.021.

Pascual, O., Casper, K.B., Kubera, C., Zhang, J., Revilla-Sanchez, R., Sul, J.Y., Takano, H., Moss, S.J., McCarthy, K., and Haydon, P.G. (2005). Astrocytic purinergic signaling coordinates synaptic networks. *Science 310*, 113-116. doi: 10.1126/science.1116916.

Perea, G., Yang, A., Boyden, E.S., and Sur, M. (2014). Optogenetic astrocyte activation modulates response selectivity of visual cortex neurons in vivo. *Nat. Commun. 5*, 3262. doi: 10.1038/ncomms4262.

Pérez-Fernández, J., Kardamakis, A.A., Suzuki, D.G., Robertson, B., and Grillner, S. (2017). Direct Dopaminergic Projections from the SNc Modulate Visuomotor Transformation in the Lamprey Tectum. *Neuron 96*, 910-924. doi: 10.1016/j.neuron.2017.09.051.

Poskanzer, K.E., and Yuste, R. (2016). Astrocytes regulate cortical state switching in vivo. *Proc. Natl. Acad. Sci. U.S.A. 113*, 2675-2684. doi: 10.1073/pnas.1520759113.

Ribot, J., Breton, R., Calvo, C.F., Moulard, J., Ezan, P., Zapata, J., Samama, K., Moreau, M., Bemelmans, A.P., Sabatet, V., Dingli, F., Loew, D., Milleret, C., Billuart, P., Dallérac, G., and Rouach, N. (2021). Astrocytes close the mouse critical period for visual plasticity. *Science 373*, 77-81. doi: 10.1126/science.abf5273.

Roux, L., Madar, A., Lacroix, M.M., Yi, C., Benchenane, K., and Giaume, C. (2015). Astroglial Connexin 43 Hemichannels Modulate Olfactory Bulb Slow Oscillations. *J. Neurosci. 35*, 15339-15352. doi: 10.1523/JNEUROSCI.0861-15.2015.

Rowe, S.J., Messenger, N.J., and Warner, A.E. (1993). The role of noradrenaline in the differentiation of amphibian embryonic neurons. *Development 119*, 1343-1357. doi: 10.1242/dev.119.4.1343.

Sharma, P., and Cline, H.T. (2010). Visual activity regulates neural progenitor cells in developing xenopus CNS through musashi1. *Neuron 68*, 442-455. doi: 10.1016/j.neuron.2010.09.028.

Sild, M., Van Horn, M.R., Schohl, A., Jia, D., and Ruthazer, E.S. (2016). Neural Activity-Dependent Regulation of Radial Glial Filopodial Motility Is Mediated by Glial cGMP-Dependent Protein Kinase 1 and Contributes to Synapse Maturation in the Developing Visual System. *J. Neurosci. 36*, 5279-88. doi: 10.1523/JNEUROSCI.3787-15.2016.

Slezak, M., Kandler, S., Van Veldhoven, P.P., Van den Haute, C., Bonin, V., and Holt, M.G. (2019). Distinct Mechanisms for Visual and Motor-Related Astrocyte Responses in Mouse Visual Cortex. *Curr. Biol. 29*, 3120-3127. doi: 10.1016/j.cub.2019.07.078.

Stringer, C., Pachitariu, M., Steinmetz, N., Carandini, M., and Harris, K.D. (2019). High-dimensional geometry of population responses in visual cortex. *Nature 571*, 361-365. doi: 10.1038/s41586-019-1346-5.

Stringer, C., Pachitariu, M., Steinmetz, N., Reddy, C.B., Carandini, M., and Harris, K.D. (2019). Spontaneous behaviors drive multidimensional, brainwide activity. *Science* 2019 *364*, 255. doi: 10.1126/science.aav7893.

Takano, T., Wallace, J.T., Baldwin, K.T., Purkey, A.M., Uezu, A., Courtland, J.L., Soderblom, E.J., Shimogori, T., Maness, P.F., Eroglu, C., and Soderling, S.H. (2020). Chemico-genetic discovery of astrocytic control of inhibition in vivo. *Nature 588*, 296-302. doi: 10.1038/s41586-020-2926-0.

Tan, Z., Liu, Y., Xi, W., Lou, H.F., Zhu, L., Guo, Z., Mei, L., and Duan, S. (2017). Glia-derived ATP inversely regulates excitability of pyramidal and CCK-positive neurons. *Nat. Commun. 8*, 13772. doi: 10.1038/ncomms13772.

Temizer, I., Donovan, J.C., Baier, H., and Semmelhack, J.L. (2015). A Visual Pathway for Looming-Evoked Escape in Larval Zebrafish. *Curr. Biol. 25*, 1823-1834. doi: 10.1016/j.cub.2015.06.002.

Tremblay, M., Fugère, V., Tsui, J., Schohl, A., Tavakoli, A., Travençolo, B.A., Costa, L., and Ruthazer, E.S. (2009). Regulation of radial glial motility by visual experience. *J. Neurosci. 29*, 14066-14076. doi: 10.1523/JNEUROSCI.3542-09.2009.

Van Horn, M.R., Strasser, A., Miraucourt, L.S., Pollegioni, L., and Ruthazer, E.S. (2017). The Gliotransmitter d-Serine Promotes Synapse Maturation and Axonal Stabilization *In Vivo*. *J. Neurosci. 37*, 6277-6288. doi: 10.1523/JNEUROSCI.3158-16.2017.

Wahis, J., Baudon, A., Althammer, F., Kerspern, D., Goyon, S., Hagiwara, D., Lefevre, A., Barteczko, L., Boury-Jamot, B., Bellanger, B., Abatis, M., Da Silva, Gouveia, M., Benusiglio, D., Eliava, M., Rozov, A., Weinsanto, I., Knobloch-Bollmann, H.S., Kirchner, M.K., Roy, R.K., Wang, H., Pertin, M., Inquimbert, P., Pitzer, C., Siemens, J., Goumon, Y., Boutrel, B., Lamy, C.M., Decosterd, I., Chatton, J.Y., Rouach, N., Young, W.S., Stern, J.E., Poisbeau, P., Stoop, R., Darbon, P., Grinevich, V., and Charlet, A. (2021). Astrocytes mediate the effect of oxytocin in the central amygdala on neuronal activity and affective states in rodents. *Nat. Neurosci. 24*, 529-541. doi: 10.1038/s41593-021-00800-0.

Wahis, J., and Holt, M.G. (2021). Astrocytes, Noradrenaline, α1-Adrenoreceptors, and Neuromodulation: Evidence and Unanswered Questions. *Front. Cell. Neurosci. 15*, 645691. doi: 10.3389/fncel.2021.645691.

Weigel, S., and Luksch, H. Local cholinergic interneurons modulate GABAergic inhibition in the chicken optic tectum. *Eur. J. Neurosci. 9*, 730-737. doi: 10.1111/ejn.12438.

Woolrych, A., Vautrelle, N., Reynolds, J.N.J., and Parr-Brownlie, L.C. (2021). Throwing open the doors of perception: The role of dopamine in visual processing. *Eur. J. Neurosci. 54*, 6135-6146. doi: 10.1111/ejn.15408.

Wu, Z., He, K., Chen, Y., Li, H., Pan, S., Li, B., Liu, T., Xi, F., Deng, F., Wang, H., Du, J., Jing, M., and Li, Y. (2022). A sensitive GRAB sensor for detecting extracellular ATP in vitro and in vivo. *Neuron 110*, 770-782 doi: 10.1016/j.neuron.2021.11.027.

Ye, L., Orynbayev, M., Zhu, X., Lim, E.Y., Dereddi, R.R., Agarwal, A., Bergles, D.E., Bhat, M.A., and Paukert, M. (2020). Ethanol abolishes vigilance-dependent astroglia network activation in mice by inhibiting norepinephrine release. *Nat. Commun. 11*, 6157. doi: 10.1038/s41467-020-19475-5.

Supplementary Materials

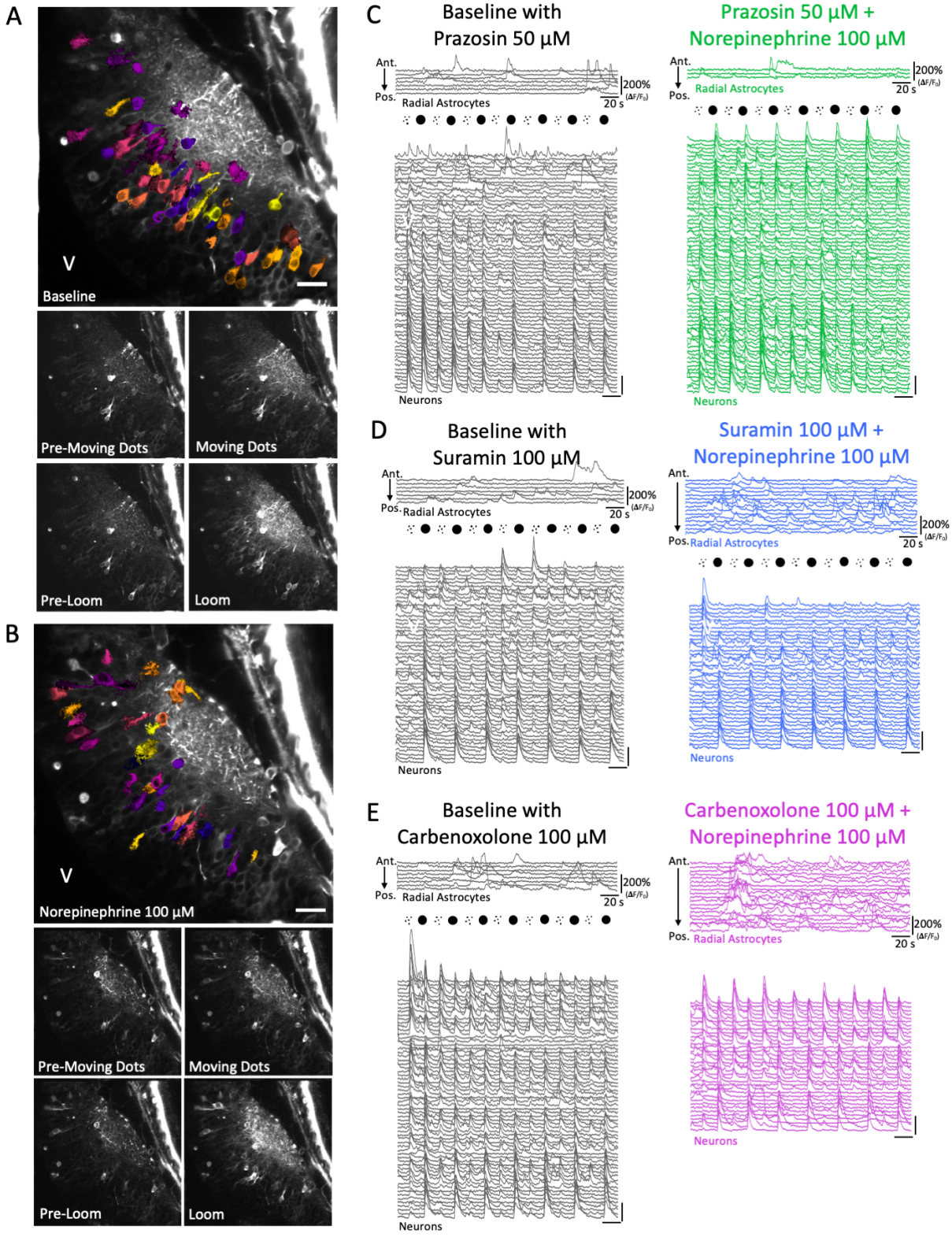

Figure. S1 related to Figures 2 and 3. Tectal responses to alternating presentation of moving dots and looming stimulus under various baseline and pharmacological manipulations

(A and B) Top panel: averaged projection of the calcium signal from a single optical section of the tectum across 300 s during baseline (A) stimulus presentation and during NE state (B) stimulus presentation. V: ventricle. Scale bar 25 μm. Subpanels: two time intervals showing the tectal calcium signal 5 s before each stimulus onset and 5 s following each stimulus onset. (C-E) Calcium traces of radial astrocytes sorted from anterior to posterior along the pial surface of the tectum and calcium traces of tectal neurons sorted by the first principal component showing responses to alternating moving dots and looming stimulus events during baseline (gray) and NE+pharmacology (green, blue, purple).

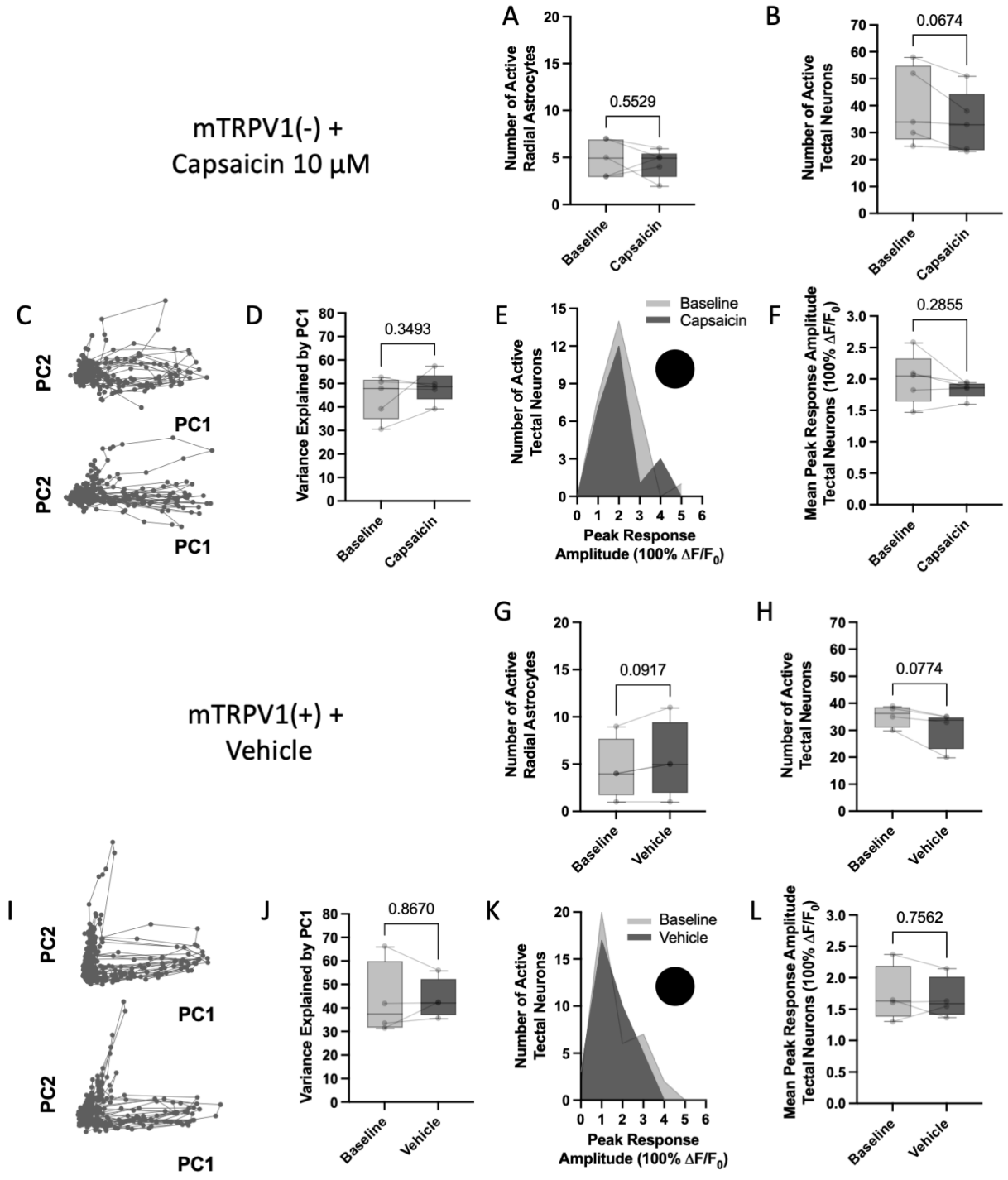
mTRPV1(-) +
Capsaicin 10 µM
A
Number of Active Radial Astrocytes
0.5529
Baseline
Capsaicin
B
Number of Active Tectal Neurons
0.0674
C
PC2
PC1
D
Variance Explained by PC1
0.3493
E
Baseline
Capsaicin
Number of Active Tectal Neurons
Peak Response Amplitude (100% ΔF/F0)
F
Mean Peak Response Amplitude Tectal Neurons (100% ΔF/F0)
0.2855
mTRPV1(+) +
Vehicle
G
Number of Active Radial Astrocytes
0.0917
Vehicle
H
Number of Active Tectal Neurons
0.0774
I
J
Variance Explained by PC1
0.8670
K
Baseline
Vehicle
Number of Active Tectal Neurons
Peak Response Amplitude (100% ΔF/F0)
L
Mean Peak Response Amplitude Tectal Neurons (100% ΔF/F0)
0.7562

Figure S2 related to Figure 5. Control experiments for chemogenetic activation of radial astrocytes in the optic tectum

(A and B) Number of active cells during baseline and following treatment with capsaicin in mTRPV1(-) animals. Paired t tests (n=5 animals): $p_{\text{Radial Astrocytes}}=0.5529$, $p_{\text{Neurons}}=0.0674$.
(C and D) (C) PCA plots showing the network activity during baseline and following capsaicin treatment, and (D), the percentage of the variance in the network activity explained by the first principal component in each state. Paired t test (n=5 animals): p=0.3493.
(E and F) (E) Histogram showing the peak looming stimulus response amplitudes of all active tectal neurons during both baseline (light gray) and following capsaicin treatment (dark gray), and (G), the mean peak looming stimulus response amplitudes of all active tectal neurons during each state. Paired t tests (n=5 animals): p=0.2855.
(G and H) Number of active cells during baseline and following treatment with vehicle in mTRPV1(+) animals. Paired t tests (n=4 animals): $p_{\text{Radial Astrocytes}}=0.0917$, $p_{\text{Neurons}}=0.0774$.
(I and J) (I) PCA plots showing the network activity during baseline and following vehicle treatment, and (J), the percentage of the variance in the network activity explained by the first principal component in each state. Paired t test (n=4 animals): p=0.8670.
(K and L) (K) Histogram showing the peak looming stimulus response amplitudes of all active tectal neurons during both baseline (light gray) and following vehicle treatment (dark gray), and (K), the mean peak looming stimulus response amplitudes of all active tectal neurons during each state. Paired t tests (n=5 animals): p=0.7562.

Author Contributions For Chapter 4

This chapter was written by Nicholas Benfey and edited by Edward Ruthazer.

Preface To Chapter 4: Comprehensive Discussion

This final chapter provides an overarching discussion of what I have come to understand of the functional properties of radial astrocytes in the developing optic tectum and how their activation influences visual function. This discussion will contextualize my findings related to NCX in the light of complementary new data that has emerged and extend upon the information presented in chapter 3 to highlight further nuances beyond the current scope of the manuscript presented in that chapter. I will also discuss numerous interesting observations I had while carrying out pharmacological manipulations of the optic tectum that weren't presented in either of my manuscripts. The mechanisms of neuron-glia communication in the optic tectum that weren't explored in my studies which likely remain relevant to understanding the overall function of the system will also be discussed. I will touch on what my observations suggest in terms of the functional heterogeneity of radial astrocytes in the tectum as well. I will finish by presenting what I view to be some of the important future directions for this work and discuss what implications my research is likely to have for our understanding of neurodevelopment and the functional roles of astrocytes in the visual system.

Comprehensive Discussion

Taken as a whole, my thesis reviews what is currently known about the functional roles of glial cells, predominantly astrocytes, throughout the vertebrate visual system and characterizes the signaling pathways mediating neuron to glia and glia to neuron signaling in the developing optic tectum of *Xenopus laevis*. Similarly to astroglia in other systems, radial astrocytes in the optic tectum also reliably detect sensory-evoked neuronal activity as well as the release of neuromodulators such as norepinephrine suggesting that their effects on local circuit function are likely to be influenced by the overall arousal state of the animal. These observations complement the existing literature on the functional properties of astrocytes in circuits of the visual system *in vivo* and are likely to be relevant to neuron-glia signaling in other circuits as well. While my experimental characterization of the functional properties of radial astrocytes was extensive, it was not exhaustive, and important questions remain to be discussed about the ways in which these cells can sense and respond to neuronal activity.

Despite demonstrating that radial astrocytes detect visual events through glutamate reuptake and the reversal of sodium-calcium exchangers, and NE through alpha-1-adrenergic receptors, it remains quite likely that other signaling pathways also contribute to their activation in this system. Future studies should investigate what potential roles radial astrocytes play in the reuptake of GABA and NE given that the reuptake of either is likely to trigger reversal of NCX similarly to the reuptake of glutamate. The activation of alpha-2-receptors on cultured astrocytes has also been shown to increase their calcium levels and so may also be relevant to the observations we have reported in chapter 3 (Gaidin et al., 2020).

My experiments using glutamate receptor agonists to activate radial astrocytes in the optic tectum strongly suggest indirect actions of these drugs on the calcium activity of radial astrocytes in this system. Researchers using such pharmacological manipulations in their systems should characterize any possible temporal delays between the activation of neurons and glia by these compounds when it is possible to do so. My observations of a temporal delay between the activation of neighboring tectal neurons and radial astrocytes are consistent with the release of diffusible signals following postsynaptic depolarization and suggests a possible role for either nitric oxide and/or endocannabinoids, among other compounds, in mediating this delayed recruitment of tectal radial astrocytes. Astrocytes are known to express CB1Rs and exhibit calcium increases following either activation *in vivo*, and nitric oxide has been implicated in calcium signaling in radial astrocytes by previous work in our lab as well as more recent work investigating the regulation NE release and the recruitment of astrocytes in primary visual cortex (Navarrete et al., 2014; Tremblay et al., 2009; Gray et al., 2021). Curiously, in my preliminary unpublished experiments using the nitric oxide synthase inhibitor L-NMMA to prevent NO release during visual stimulation, I did not observe a consistent effect on glial calcium signaling in the few animals I tested. While I have no doubt that NO is likely to be implicated in regulating the activity of radial astrocytes in the tectum, I suspect it may be playing more of a permissive role under specific conditions, perhaps regulating the sensitivity of radial astrocytes to visual stimulation, rather than acting as a primary signal activating these cells.

Recent work has characterized a novel form of neuron-glia communication which is complementary to my findings involving EAATs and NCX presented in chapter 2 (Armbruster et

al., 2022). Using new genetically encoded voltage indicators, the authors demonstrated that the fine processes of astrocytes exhibit significant alterations in membrane voltage as a result of activity-dependent potassium efflux and glutamate reuptake which modulate synaptic strength by regulating the rate of glutamate clearance. They observed that potassium efflux inhibits glutamate reuptake during periods of neuronal activity, and that these microdomain changes in voltage were influenced by extracellular calcium. Together this suggests that the seconds long delay we and others have observed between the activation of neurons and astrocytes in the visual system may be a result of the inhibited glutamate reuptake during neuronal activity preventing the reversal of NCX and thus preventing visually-evoked calcium events in astrocytes during the neuronal response to the visual stimulus. It will be important to investigate the role of NCX in mediating sensory-evoked calcium events in mammalian astrocytes *in vivo* to determine whether this is a conserved mechanism across vertebrates.

Next I will discuss some of the results of my analysis of the data presented in chapter 3 which supplement the findings but were not included in the draft of the manuscript at the time of its writing. Perhaps notably absent from my discussion of the material presented in chapter 3 is the role of adenosine release from radial astrocytes following their activation by NE and its effects on neuronal activity in the optic tectum. There is a considerable amount of literature demonstrating that the activation of astrocytes leads to the release of both ATP and adenosine and that the activation of presynaptic adenosine receptors, particularly the type 1 adenosine receptor (A1), plays an important role in the modulation of neural circuits by astrocytes (Pascual et al., 2005; Tan et al., 2017; Covelo and Araque, 2018; Corkrum et al., 2020; Agostinho et al., 2020). I performed a number of experiments assessing the role of A1 in mediating the effects of

NE in the tectum using the A1 receptor antagonist DPCPX and the A1 receptor agonist N^6cyclopentyladenosine.

Similarly to what we observed following the blockade of either P2 receptors or gap junctions/hemichannels, the blockade of A1 receptors with DPCPX also prevented the shift in the dimensionality of tectal network activity that we normally observed following the application of NE. Curiously, DPCPX also had no clear effect on the large inhibition of tectal neurons we also observed. Despite the preliminary evidence that A1 receptors are likely to play a role in the effects of NE, a couple of things led us not to include the findings in the initial draft of the manuscript and will be discussed below.

Firstly, when assessing the difference between the recruitment of, and increased calcium in, radial astrocytes, in DPCPX and non-DPCPX treated groups, we observed a reduction in both measures of glial activity in the DPCPX treated group following the application of NE which was suggestive of adenosine contributing to the sustained activation of radial astrocytes by NE. This was further confirmed using the A1 specific agonist N^6cyclopentyladenosine which we found to be a potent activator of calcium signaling in radial astrocytes in the optic tectum, similar to NE. This alone is of considerable interest given that A1 activation is classically associated with alterations in cyclic AMP and not calcium, and there remains little knowledge of the roles of A1 receptors on astrocytes. Additionally, when comparing the final levels of neuronal activity and the variance explained by the first principal component following application of NE between DPCPX and non-DPCPX treated groups, the levels were similar despite a reduction in within-group effects of NE in the DPCPX treated group suggesting that the two groups had meaningful

differences at baseline which complicate analysis. These observations made any interpretation of the cause of the effects of blocking A1 on tectal function ambiguous without further knowledge as to the specific patterns of A1 expression throughout the tectum. The results are consistent with both activation of presynaptic A1 receptors on RGCs (and perhaps NE releasing axons) and on radial astrocytes as being important to the network alterations induced by NE. Further experimentation will be necessary to validate the roles of adenosine in the tectum. Of particular interest is the possibility that radial astrocytes in the visual system track adenosine levels and alter visual processing in a circadian fashion as has been observed to be the case for astrocytes in other systems.

One significant limitation of my experimental work with NE in the optic tectum remains that I do not demonstrate under what context the release of endogenous NE occurs and what perhaps more nuanced effects such endogenous release of NE has on tectal function. Most relevant to filling this gap will be the implementation of genetically-encoded fluorescent indicators for measuring NE release *in vivo*. Such tools have been implemented in other systems including in zebrafish where single looming stimuli have been shown to induce the release of endogenous NE in the optic tectum (Feng et al., 2019). Using these new imaging tools along with the presentation of a wide variety of visual stimuli will be particularly instructive moving forward. Although I decided not to include it in the draft of the manuscript in chapter 3, I did perform preliminary experiments with the alpha-2-adrenergic receptor antagonist yohimbine which is known to elevate endogenous NE levels by preventing the desensitization of NE release from axonal terminals following the autocrine activation of presynaptic alpha-2 receptors. I monitored resting state calcium activity in both tectal neurons and radial astrocytes following the application of

yohimbine to the optic tectum and observed increases in glial calcium levels and decreases in the number of active neurons within minutes of its application in most animals that were qualitatively similar to those induced by the exogenous application of NE. While not conclusive and demanding more validation before drawing any firm conclusions, I believe these preliminary observations are consistent with there being tonic release of NE in the optic tectum during the developmental stages in which we are experimenting. NE is known to be released endogenously in *Xenopus* during early development, regulating the proliferation of new neurons through the activation of alpha-1-adrenergic receptors (Rowe et al., 1993). This is consistent with our observations and the presence of an endogenous mechanism which mediates the effects of NE we have characterized so far.

Several observations lead me to believe that high frequency looming stimulation may be the best driver of endogenous NE release in the optic tectum. During my experiments for the NCX manuscript presented in chapter 2, I used a relatively high looming stimulus frequency of once every 6 seconds and observed that the activation of radial astrocytes was more robust than when I used the lower frequency looming stimulus of once every 20 seconds for the experiments in chapter 3. A lower stimulus frequency was used for these experiments to prevent the habituation of the visual responses which occurs at higher stimulus frequencies. This high frequency looming stimulus would occasionally evoke wide scale activation of radial astrocytes in a way which was qualitatively similar to that induced by the application of NE. Calcium signals would sometimes propagate to the cell bodies of the radial astrocytes under these stimulus conditions, something I only observed following the application of NE, ATP, or N^6cyclopentyladenosine to the tectum. Consistent with this possibility is that in the hindbrain of zebrafish, radial astrocytes

have been shown to sum NE release events across time and trigger a behavioral state change only once a threshold of NE release has been crossed (Mu et al., 2019). Given that looming stimuli evoke NE release in the tectum of zebrafish, it's intriguing to speculate as to whether a rapid succession of looming stimuli, something likely to occur during a predation attempt, may induce a similar change in state to what we have seen following the application of NE to the tectum through the triggering of a similar threshold in radial astrocytes. I have observed preliminary evidence for such a threshold effect in my data as under baseline conditions higher levels of visually-evoked neuronal activity correlate with higher levels of glial activation, while under NE conditions, I see an inverse relationship between glial activation and neuronal activity. This also suggests that low levels and high levels of NE release in the tectum may play different roles in the system. Low levels may enhance neuronal function, possibly through the release of the NMDAR co-agonist D-serine, a gliotransmitter known to be present in the *Xenopus laevis* optic tectum, while high levels may trigger a rapid inhibition of the tectum to enhance signal to noise ratios for a particularly salient stimulus (Van Horn et al., 2017; Covelo and Araque, 2018). I believe experimental work attempting to address this speculation will be very informative for helping to understand what role NE plays in modulating visual function in freely behaving animals.

In other systems, it's rapidly becoming apparent that astrocytes do not form one homogenous population of cells and exhibit considerable levels of cellular heterogeneity both within and between different regions of the brain including the visual system (Batiuk et al., 2020; Bayraktar et al., 2020). Perhaps largely implicit in my experimental results are observations related to the heterogeneity of the radial astrocytes populating the optic tectum. While I largely treat the radial

astrocytes as a mostly homogenous population for the sake of parsimony in our experiments to date, I have multiple reasons to believe this is unlikely to represent the true reality of the full complexity of the system.

Firstly, when I apply NE to the optic tectum, I often see only a proportion of the radial astrocytes there show sustained calcium elevations while many of the radial astrocytes are only transiently activated by NE. Speaking from a purely qualitative standpoint, it appears to me as though the radial astrocytes in the more central regions of the tectal neuropil are more robustly activated by NE and that as you move out from the center of the neuropil, in both the anterior and posterior directions, there is often a decay in the strength of glial activation by NE. This could be consistent with a gradient of regional expression of adrenergic receptors on the radial astrocytes that may reflect the innervation patterns of noradrenergic axons into the tectum. It also suggests that there may be a population of radial astrocytes which act as the primary NE detectors and which then transiently propagate their activated state to other radial astrocytes through the release of ATP/ADO or calcium through gap junctions. I believe the release of ATP/ADO to be more consistent with my observations given that neighboring radial astrocytes rarely had highly similar calcium responses to NE which is what I would have expected should calcium be propagating through gap junctions between cells.

Additionally, in my experiments for the NCX paper, not all radial astrocytes exhibited responses to the visual stimuli I presented, and when we prevent visually-evoked responses in radial astrocytes by blocking EAATs or NCX, we still observe a subset of radial astrocytes with continued spontaneous activity. We know that this spontaneous activity is mediated by neuronal

activity given it is largely abolished in animals pretreated with TTX. While these spontaneous calcium events did not correlate with visually-evoked activity in the tectum, it remains important to understand the full breadth of signaling mechanisms mediating their generation and what role they play, particularly during resting state function of the visual system. Interestingly, visual stimulation often caused astrocytes initially inactive in the baseline resting state to become active while some radial astrocytes which were active in the resting state became unresponsive during visual stimulation strongly suggesting that not all radial astrocytes contribute directly to visual processing. Whether distinct radial astrocytes are preferentially active during distinct states remains an interesting open question for future research to explore.

Summary and Conclusions

I'd now like to summarize everything I've observed about radial astrocytes throughout my Ph.D into a coherent narrative explaining my views on how radial astrocytes fit into the visual networks in the optic tectum. During resting state, and periods of visual stimulation, radial astrocytes in the optic tectum exhibit highly dynamic fluctuations in their calcium levels. During baseline these calcium events are largely uncorrelated with one another, although occasional pockets of correlated activity are observed, consistent with the topographic organization of retinal inputs into the tectum. These spontaneous calcium events are dependent on neuronal activity as blockade of neuronal spiking activity with TTX largely silences them. Whether this is a result of direct action of TTX on astrocyte NaVs, the reduced metabolic demand on neurons in the absence of neuronal spiking activity, the abrupt reduction in the release of neurotransmitters, or some combination between these and other factors, remains to be explored.

During periods of visual stimulation, some radial astrocytes exhibit robust calcium increases which are often more correlated with those in their nearest neighbors. These visually-evoked calcium increases occur with a delay of several seconds relative to those in tectal neurons, a phenomenon observed in various other circuits as well (Schummers et al., 2008; Lines et al., 2020). These calcium increases are sustained even during the blockade of all glutamate receptors in the optic tectum suggesting that radial astrocytes are preferentially responsive to presynaptic release of glutamate from RGCs rather than to retrograde signals released following depolarization of postsynaptic tectal neurons. Mechanistically these calcium events appear to occur following the reuptake of glutamate through EAATs and the reversal of NCX which causes calcium to rapidly enter the glial cell. High frequency visual stimulation (once every 6 seconds) appears to more robustly activate radial astrocytes compared to low frequency stimulation (once every 20 seconds), possibly due to the accumulation of glutamate and NE in the tectum. Should activity levels increase to the point where they cross a threshold, radial astrocytes appear to be globally, or at least regionally, activated leading to a significant decrease in the activity of tectal neurons. This activation of radial astrocytes by NE may enhance their ability to remove glutamate from the synaptic cleft leading to the preferential silencing of weakly innervated neurons, although this remains purely speculative at this time (Hansson and Rönnbäck, 1989; Fahrig, 1993).

Both high frequency stimulation and NE are likely to enhance the release of ATP/ADO by radial astrocytes, possibly through the calcium-dependent opening of glial hemichannels. This ATP release appears to serve multiple roles. Normally, calcium activity in radial astrocytes is largely

restricted to the neuropil segment of cell, ATP/ADO causes a back propagation of the glial calcium signals out of the neuropil segment and into their cell bodies which suggests it may serve a role in differentially regulating gene expression following a behavioral state change given that calcium activity and that activation of alpha-1-adrenergic receptors is known to induce neuronal proliferation in *Xenopus* (Rowe et al., 1993). This ATP/ADO release also shifts the encoding state of the optic tectum in such a way as to enhance the detection of looming stimuli. This likely occurs in part through the activation of postsynaptic P2 receptors, possibly on a subpopulation of strongly loom selective neurons, SINs and/or a subset neurons in the superficial layers of the optic tectum known to express gap junctions and regulate the excitability of deep layer tectal neurons known to be important for mediating escape behavior, are interesting potential candidates (Del Bene et al., 2010; Barker and Baier, 2013; Temizer et al., 2015; Jang et al., 2016; Liu et al., 2016; Dunn et al., 2016; Abbas et al., 2017; Barker et al., 2021). This shift in encoding is also likely to involve the breakdown of ATP to ADO which may act both to further propagate calcium signals through the network of radial astrocytes and to decrease presynaptic release of glutamate from RGCs. This complex sequence of intercellular signaling events rapidly shifts the optic tectum into a state where it is primed to detect visual information related to looming threats in the environment, greatly enhancing the detection of such stimuli by freely swimming animals. This places radial astrocytes in an important role in the tectum where they appear to operate as master regulators of tectal function capable of rapidly altering visual processing to focus the visual attention of the animal. This is likely to have many important implications for neurodevelopment and behavior which will be exciting to explore through future research.

While the majority of my experimental work focused on finding ways to drive increases in the activity of radial astrocytes, of equal importance will be experiments which are able to selectively decrease or inhibit the activity of radial astrocytes, ideally with both high spatial and temporal precision. Experiments employing genetically encoded calcium extruding pumps, or a number of calcium chelators will be particularly instructive (Lyon and Allen, 2022). Given that the selective activation of radial astrocytes in the optic tectum induces a state primed for looming stimulus detection at the expense of the detection of other salient stimuli such as small moving dots, whether the selective deactivation of radial astrocytes can induce a preference for prey detection remains an interesting possibility to explore. Equally important will be finding ways to precisely identify the specific tectal neurons mediating the changes in circuit function downstream of glial activation. Electrophysiological measurements in specific populations of genetically defined tectal neurons following the targeted (de)activation of radial astrocytes will be particularly illuminating in these regards.

My experimental findings are likely to have a number of important implications relevant to both neurodevelopment and sensory processing in healthy and disordered systems. My findings suggest that during the earliest stages of the activity-dependent refinement of sensory systems astrocytes are already primed to integrate complex information and mediate changes in behavior. My findings implicate NCX and alpha-1 adrenergic receptors, among others, as important contributors to glial calcium signaling in the retinotectal system during these stages. This suggests that any alteration in the function of adrenergic signaling or the membrane excitability of glial cells is likely to have important impacts on the development of, and information processing in, sensory systems when they are at their most plastic. Any such alterations could

have long lasting effects on attentional regulation as well as the general ability of glial cells to regulate the excitability of neural circuits and may have relevance towards understanding neurodevelopmental disorders such as ADHD, autism, and epilepsy. Finally, my experimental findings highlight the continued importance of including astrocytes within our network models, especially in neural circuits which are heavily innervated by neuromodulatory systems, as without doing so, we are unlikely to ever understand the full dynamic range of these systems.

Reference List

Abbas, F., Triplett, M.A., Goodhill, G.J., and Meyer, M.P. (2017). A Three-Layer Network Model of Direction Selective Circuits in the Optic Tectum. *Front. Neural Circuits 11*, 88. doi: 10.3389/fncir.2017.00088.

Agarwal, A., Wu, P.H., Hughes, E.G., Fukaya, M., Tischfield, M.A., Langseth, A.J., Wirtz, D., and Bergles, D.E. (2017). Transient Opening of the Mitochondrial Permeability Transition Pore Induces Microdomain Calcium Transients in Astrocyte Processes. *Neuron 93*(3), 587-605. doi: 10.1016/j.neuron.2016.12.034.

Agostinho, P., Madeira, D., Dias, L., Simões, A.P., Cunha, R.A., and Canas, P.M. (2020). Purinergic signaling orchestrating neuron-glia communication. *Pharmacol. Res. 162*, 105253. doi: 10.1016/j.phrs.2020.105253.

Agulhon, C., Platel, J.C., Kolomiets, B., Forster, V., Picaud, S., Brocard, J., Faure, P., and Brulet, P. (2007). Bioluminescent imaging of Ca2+ activity reveals spatiotemporal dynamics in glial networks of dark-adapted mouse retina. *J. Physiol. 583*(3), 945-958. doi: 10.1113/jphysiol.2007.135715.

Allen, N.J., and Lyons, D.A. (2018). Glia as architects of central nervous system formation and function. *Science 362*(6411), 181–185. doi: 10.1126/science.aat0473.

Anderson, S.R., Zhang, J., Steele, M.R., Romero, C.O., Kautzman, A.G., Schafer, D.P., and Vetter, M.L. (2019). Complement Targets Newborn Retinal Ganglion Cells for Phagocytic Elimination by Microglia. *J. Neurosci. 39*(11), 2025-2040. doi: 10.1523/JNEUROSCI.1854-18.2018.

Armbruster, M., Naskar, S., Garcia, J.P., Sommer, M., Kim, E., Adam, Y., Haydon, P.G., Boyden, E.S., Cohen, A.E., and Dulla, C.G. (2022). Neuronal activity drives pathway-specific depolarization of peripheral astrocyte processes. *Nat. Neurosci. 25*, 607–616. doi: 10.1038/s41593-022-01049-x.

Badimon, A., Strasburger, H.J., Ayata, P., Chen, X., Nair, A., Ikegami, A., Hwang, P., Chan, A.T., Graves, S.M., Uweru, J.O., Ledderose, C., Kutlu, M.G., Wheeler, M.A., Kahan, A., Ishikawa, M., Wang, Y.C., Loh, Y.E., Jiang, J.X., Surmeier, D.J., Robson, S.C., Junger, W.G., Sebra, R., Calipari, E.S., Kenny, P.J., Eyo, U.B., Colonna, M., Quintana, F.J., Wake, H., Gradinaru, V., and Schaefer, A. (2020). Negative feedback control of neuronal activity by microglia. *Nature 586*(7829), 417-423. doi: 10.1038/s41586-020-2777-8.

Baier, H., and Wullimann, M. F. (2021). Anatomy and function of retinorecipient arborization fields in zebrafish. *J. Comp. Neurol. 529*(15), 3454–3476. doi: 10.1002/cne.25204.

Barker, A.J., and Baier, H. (2013). SINs and SOMs: neural microcircuits for size tuning in the zebrafish and mouse visual pathway. *Front. Neural Circuits. 7*, 89. doi: 10.3389/fncir.2013.00089.

Barker, A.J., Helmbrecht, T.O., Grob, A.A., and Baier, H. (2021). Functional, molecular and morphological heterogeneity of superficial interneurons in the larval zebrafish tectum. *J. Comp. Neurol. 529*, 2159-2175. doi: 10.1002/cne.25082.

Batiuk, M.Y., Martirosyan, A., Wahis, J., de Vin, F., Marneffe, C., Kusserow, C., Koeppen, J., Viana, J.F., Oliveira, J.F., Voet, T., Ponting, C.P., Belgard, T.G., and Holt, M.G. (2020). Identification of region-specific astrocyte subtypes at single cell resolution. *Nat. Commun. 11*(1), 1220. doi: 10.1038/s41467-019-14198-8.

Bayraktar, O.A., Bartels, T., Holmqvist, S., Kleshchevnikov, V., Martirosyan, A., Polioudakis, D., Ben Haim, L., Young, A., Batiuk, M.Y., Prakash, K., Brown, A., Roberts, K., Paredes, M.F., Kawaguchi, R., Stockley, J.H., Sabeur, K., Chang, S.M., Huang, E., Hutchinson, P., Ullian, E.M., Hemberg, M., Coppola, G., Holt, M.G., Geschwind, D.H., and Rowitch, D.H. (2020). Astrocyte layers in the mammalian cerebral cortex revealed by a single-cell in situ transcriptomic map. *Nat. Neurosci. 23*(4), 500–509. doi: 10.1038/s41593-020-0602-1.

Bazargani, N., and Attwell, D. (2016). Astrocyte calcium signaling: the third wave. *Nat. Neurosci. 19*(2), 182-189. doi: 10.1038/nn.4201.

Bear, M.F., and Singer, W. (1986). Modulation of visual cortical plasticity by acetylcholine and noradrenaline. *Nature 320*(6058), 172-176. doi: 10.1038/320172a0.

Benfey, N.J., Li, V.J., Schohl, A., and Ruthazer, E.S. (2021). Sodium-calcium exchanger mediates sensory-evoked glial calcium transients in the developing retinotectal system. *Cell Rep*. *37*(1), 109791. doi: 10.1016/j.celrep.2021.109791.

Berson, D. M., Dunn, F. A., and Takao, M. (2002). Phototransduction by retinal ganglion cells that set the circadian clock. *Science 295*(5557), 1070–1073. doi: 10.1126/science.1067262.

Bernardos, R.L., Barthel, L.K., Meyers, J.R., and Raymond, P.A. (2007). Late-stage neuronal progenitors in the retina are radial Müller glia that function as retinal stem cells. *J. Neurosci. 27*(26), 7028-7040. doi: 10.1523/JNEUROSCI.1624-07.2007.

Biesecker, K.R., Srienc, A.I., Shimoda, A.M., Agarwal, A., Bergles, D.E., Kofuji, P., and Newman, E.A. (2016). Glial Cell Calcium Signaling Mediates Capillary Regulation of Blood Flow in the Retina. *J. Neurosci. 36*(36), 9435-9445. doi: 10.1523/JNEUROSCI.1782-16.2016.

Bonder, D.E., and McCarthy, K.D. (2014). Astrocytic Gq-GPCR-linked IP3R-dependent Ca2+ signaling does not mediate neurovascular coupling in mouse visual cortex in vivo. *J. Neurosci. 34*(39), 13139-13150. doi: 10.1523/JNEUROSCI.2591-14.2014.

Campbell, W.A., Blum, S., Reske, A., Hoang, T., Blackshaw, S., and Fischer, A.J. (2021). Cannabinoid signaling promotes the de-differentiation and proliferation of Müller glia-derived progenitor cells. *Glia 69*(10), 2503-2521. doi: 10.1002/glia.24056.

Cheadle, L., Rivera, S.A., Phelps, J.S., Ennis, K.A., Stevens, B., Burkly, L.C., Lee, W.A., and Greenberg, M.E. (2020). Sensory Experience Engages Microglia to Shape Neural Connectivity through a Non-Phagocytic Mechanism. *Neuron 108*(3), 451-468. doi: 10.1016/j.neuron.2020.08.002.

Chen, N., Sugihara, H., Sharma, J., Perea, G., Petravicz, J., Le, C., and Sur, M. (2012). Nucleus basalis-enabled stimulus-specific plasticity in the visual cortex is mediated by astrocytes. *Proc. Natl. Acad. Sci. U.S.A. 109*(41), 2832-2841. doi: 10.1073/pnas.1206557109.

Chorghay, Z., Li, V.J., Ghosh, A., Schohl, A., and Ruthazer, E.S. (2021). The effects of the NMDAR co-agonist D-serine on the structure and function of the optic tectum. *bioRxiv* 2021.08.25.457610. doi: 10.1101/2021.08.25.457610.

Christopherson, K.S., Ullian, E.M., Stokes, C.C., Mullowney, C.E., Hell, J.W., Agah, A., Lawler, J., Mosher, D.F., Bornstein, P., and Barres, B.A. (2005). Thrombospondins are astrocyte-secreted proteins that promote CNS synaptogenesis. *Cell 120*(3), 421-433. doi: 10.1016/j.cell.2004.12.020.

Chung, W.S., Clarke, L.E., Wang, G.X., Stafford, B.K., Sher, A., Chakraborty, C., Joung, J., Foo, L.C., Thompson, A., Chen, C., Smith, S.J., and Barres, B.A. (2013). Astrocytes mediate synapse elimination through MEGF10 and MERTK pathways. *Nature 504*(7480), 394-400. doi: 10.1038/nature12776.

Clark, B.D., Kurth-Nelson, Z.L., and Newman, E.A. (2009). Adenosine-evoked hyperpolarization of retinal ganglion cells is mediated by G-protein-coupled inwardly rectifying K+ and small conductance Ca2+-activated K+ channel activation. *J. Neurosci. 29*(36), 11237-11245. doi: 10.1523/JNEUROSCI.2836-09.2009.

Conedera, F.M., Pousa, A.M.Q., Mercader, N., Tschopp, M., and Enzmann, V. (2019). Retinal microglia signaling affects Müller cell behavior in the zebrafish following laser injury induction. *Glia 67*(6), 1150-1166. doi: 10.1002/glia.23601.

Corkrum, M., Covelo, A., Lines, J., Bellocchio, L., Pisansky, M., Loke, K., Quintana, R., Rothwell, P.E., Lujan, R., Marsicano, G., Martin, E.D., Thomas, M.J., Kofuji, P., and Araque, A. (2020). Dopamine-Evoked Synaptic Regulation in the Nucleus Accumbens Requires Astrocyte Activity. *Neuron 105*(6), 1036-1047. doi: 10.1016/j.neuron.2019.12.026.

Covelo, A., and Araque, A. (2018). Neuronal activity determines distinct gliotransmitter release from a single astrocyte. *Elife 7*, e32237. doi: 10.7554/eLife.32237.

Del Bene, F., Wyart, C., Robles, E., Tran, A., Looger, L., Scott, E.K., Isacoff, E.Y., and Baier, H. (2010). Filtering of visual information in the tectum by an identified neural circuit. *Science 330*,
669-673. doi: 10.1126/science.1192949.

Dixon, M.A., Greferath, U., Fletcher, E.L., and Jobling, A.I. (2021). The Contribution of Microglia to the Development and Maturation of the Visual System. *Front. Cell. Neurosci. 15*, 659843. doi: 10.3389/fncel.2021.659843.

Dunn, T.W., Gebhardt, C., Naumann, E.A., Riegler, C., Ahrens, M.B., Engert, F., and Del Bene, F. (2016). Neural Circuits Underlying Visually Evoked Escapes in Larval Zebrafish. *Neuron 89*, 613-628. doi: 10.1016/j.neuron.2015.12.021.

Espinosa, J.S., and Stryker, M.P. (2012). Development and plasticity of the primary visual cortex. *Neuron*. *75*(2), 230-249. doi: 10.1016/j.neuron.2012.06.009.

Fahrig T. (1993). Receptor subtype involved and mechanism of norepinephrine-induced stimulation of glutamate uptake into primary cultures of rat brain astrocytes. *Glia 7*(3), 212-218. doi: 10.1002/glia.440070304.

Farhy-Tselnicker, I., Boisvert, M.M., Liu, H., Dowling, C., Erikson, G.A., Blanco-Suarez, E., Farhy, C., Shokhirev, M.N., Ecker, J.R., and Allen, N.J. (2021). Activity-dependent modulation of synapse-regulating genes in astrocytes. *Elife 10*, e70514. doi: 10.7554/eLife.70514.

Feng, J., Zhang, C., Lischinsky, J.E., Jing, M., Zhou, J., Wang, H., Zhang, Y., Dong, A., Wu, Z., Wu, H., Chen, W., Zhang, P., Zou, J., Hires, S.A., Zhu, J.J., Cui, G., Lin, D., Du, J., and Li, Y. (2019). A Genetically Encoded Fluorescent Sensor for Rapid and Specific In Vivo Detection of Norepinephrine. *Neuron 102*(4), 745-761. doi: 10.1016/j.neuron.2019.02.037.

Fischer, A.J., Zelinka, C., Gallina, D., Scott, M.A., and Todd, L. (2014). Reactive microglia and macrophage facilitate the formation of Müller glia-derived retinal progenitors. *Glia 62*(10), 1608-1628. doi: 10.1002/glia.22703.

Franze, K., Grosche, J., Skatchkov, S.N., Schinkinger, S., Foja, C., Schild, D., Uckermann, O., Travis, K., Reichenbach, A., and Guck, J. (2007). Müller cells are living optical fibers in the vertebrate retina. *Proc. Natl. Acad. Sci. U.S.A. 104*(20), 8287-8292. doi: 10.1073/pnas.0611180104.

Gaidin, S.G., Zinchenko, V.P., Sergeev, A.I., Teplov, I.Y., Maltseva, V.N., and Kosenkov, A.M. (2020). Activation of alpha-2 adrenergic receptors stimulates GABA release by astrocytes. *Glia 68*, 1114-1130. doi: 10.1002/glia.23763.

Gray, S.R., Ye, L., Ye, J.Y., and Paukert, M. (2021). Noradrenergic terminal short-term potentiation enables modality-selective integration of sensory input and vigilance state. *Sci. Adv. 7*(51), eabk1378. doi: 10.1126/sciadv.abk1378.

Guido, W. (2008). Refinement of the retinogeniculate pathway. *J. Physiol.* 586(18), 4357-4362. doi: 10.1113/jphysiol.2008.157115.

Hansson, E., and Rönnbäck, L. (1989). Regulation of glutamate and GABA transport by adrenoceptors in primary astroglial cell cultures. *Life Sci. 44*(1), 27-34. doi: 10.1016/0024-3205(89)90214-2.

Harada, T., Harada, C., Watanabe, M., Inoue, Y., Sakagawa, T., Nakayama, N., Sasaki, S., Okuyama, S., Watase, K., Wada, K., and Tanaka, K. (1998). Functions of the two glutamate transporters GLAST and GLT-1 in the retina. *Proc. Natl. Acad. Sci. U.S.A. 95*(8), 4663-4666. doi: 10.1073/pnas.95.8.4663.

Hattar, S., Liao, H.W., Takao, M., Berson, D.M., and Yau, K.W. (2002) Melanopsin-containing retinal ganglion cells: architecture, projections, and intrinsic photosensitivity. *Science 295*(5557), 1065-70. doi: 10.1126/science.1069609.

Henneberger, C., Papouin, T., Oliet, S. H., and Rusakov, D. A. (2010). Long-term potentiation depends on release of D-serine from astrocytes. *Nature*, *463*(7278), 232–236. doi: 10.1038/nature08673.

Hennes, M., Lombaert, N., Wahis, J., Van den Haute, C., Holt, M.G., and Arckens, L. (2020). Astrocytes shape the plastic response of adult cortical neurons to vision loss. *Glia 68*(10), 2102-2118. doi: 10.1002/glia.23830.

Hooks, B.M., and Chen, C. (2020). Circuitry Underlying Experience-Dependent Plasticity in the Mouse Visual System. *Neuron 106*(1), 21-36. doi: 10.1016/j.neuron.2020.01.031.

Isa, T., Marquez-Legorreta, E., Grillner, S., and Scott, E.K. (2021). The tectum/superior colliculus as the vertebrate solution for spatial sensory integration and action. *Curr. Biol. 31*(11), 741-762. doi: 10.1016/j.cub.2021.04.001.

Ito, S., and Feldheim, D.A. (2018). The Mouse Superior Colliculus: An Emerging Model for Studying Circuit Formation and Function. *Front. Neural Circuits 12*, 10. doi: 10.3389/fncir.2018.00010.

Jang, E.V., Ramirez-Vizcarrondo, C., Aizenman, C.D., and Khakhalin, A.S. (2016). Emergence of Selectivity to Looming Stimuli in a Spiking Network Model of the Optic Tectum. *Front. Neural Circuits 10*, 95. doi: 10.3389/fncir.2016.00095.

Jobling, A.I., Waugh, M., Vessey, K.A., Phipps, J.A., Trogrlic, L., Greferath, U., Mills, S.A., Tan, Z.L., Ward, M.M., and Fletcher, E.L. (2018). The Role of the Microglial Cx3cr1 Pathway in the Postnatal Maturation of Retinal Photoreceptors. *J. Neurosci. 38*(20), 4708-4723. doi: 10.1523/JNEUROSCI.2368-17.2018.

Karl, M.O., Hayes, S., Nelson, B.R., Tan, K., Buckingham, B., and Reh, T.A. (2008). Stimulation of neural regeneration in the mouse retina. *Proc. Natl. Acad. Sci. U.S.A. 105*(49), 19507-19513. doi: 10.1073/pnas.0807453105.

Kerschensteiner, D., and Guido, W. (2017). Visual thalamus, "it's complicated". *Vis. Neurosci*. *34*, E018. doi: 10.1017/S0952523817000311.

Kolodziejczak, M., Béchade, C., Gervasi, N., Irinopoulou, T., Banas, S.M., Cordier, C., Rebsam, A., Roumier, A., and Maroteaux, L. (2015). Serotonin Modulates Developmental Microglia via 5-HT2B Receptors: Potential Implication during Synaptic Refinement of Retinogeniculate Projections. *ACS Chem. Neurosci. 6*(7), 1219-1230. doi: 10.1021/cn5003489.

Kurth-Nelson, Z.L., Mishra, A., and Newman, E.A. (2009). Spontaneous glial calcium waves in the retina develop over early adulthood. *J. Neurosci. 29*(36), 11339-11346. doi: 10.1523/JNEUROSCI.2493-09.2009.

Labin, A.M., Safuri, S.K., Ribak, E.N., and Perlman, I. (2014). Müller cells separate between wavelengths to improve day vision with minimal effect upon night vision. *Nat. Commun. 5*, 4319. doi: 10.1038/ncomms5319.

Lazzerini Ospri, L., Prusky, G., and Hattar, S. (2017). Mood, the Circadian System, and Melanopsin Retinal Ganglion Cells. *Annu. Rev. Neurosci. 40*, 539–556. doi: 10.1146/annurev-neuro-072116-031324.

Lim, T.K., and Ruthazer, E.S. (2021). Microglial trogocytosis and the complement system regulate axonal pruning in vivo. *Elife 10*, e62167. doi: 10.7554/eLife.62167.

Lines, J., Martin, E.D., Kofuji, P., Aguilar, J., and Araque, A. (2020). Astrocytes modulate sensory-evoked neuronal network activity. Nat. Commun. *11*, 3689. doi: 10.1038/s41467-020-17536-3.

Liu, Y.J., Spangenberg, E.E., Tang, B., Holmes, T.C., Green, K.N., and Xu, X. (2021). Microglia Elimination Increases Neural Circuit Connectivity and Activity in Adult Mouse Cortex. *J. Neurosci. 41*(6). 1274-1287. doi: 10.1523/JNEUROSCI.2140-20.2020.

Liu, Z., Ciarleglio, C.M., Hamodi, A.S., Aizenman, C.D., and Pratt, K.G. (2016). A population of gap junction-coupled neurons drives recurrent network activity in a developing visual circuit. *J. Neurophysiol. 115*, 1477-1486. doi: 10.1152/jn.01046.2015.

López-Hidalgo, M., Hoover, W.B., and Schummers, J. (2016). Spatial organization of astrocytes in ferret visual cortex. *J. Comp. Neurol. 524*(17), 3561-3576. doi: 10.1002/cne.24015.

Lowery, R.L., Tremblay, M.E., Hopkins, B.E., and Majewska, A.K. (2017). The microglial fractalkine receptor is not required for activity-dependent plasticity in the mouse visual system. *Glia 65*(11), 1744-1761. doi: 10.1002/glia.23192.

Lyon, K.A., and Allen, N.J. (2022). From Synapses to Circuits, Astrocytes Regulate Behavior. *Front. Neural Circuits 15*, 786293. https://doi.org/10.3389/fncir.2021.786293.

Masland R.H. (2012). The neuronal organization of the retina. *Neuron 76*(2), 266-280. doi:10.1016/j.neuron.2012.10.002.

Mu, Y., Bennett, D.V., Rubinov, M., Narayan, S., Yang, C.T., Tanimoto, M., Mensh, B.D., Looger, L.L., and Ahrens, M.B. (2019). Glia Accumulate Evidence that Actions Are Futile and Suppress Unsuccessful Behavior. *Cell 178*(1), 27-43. doi: 10.1016/j.cell.2019.05.050.

Müller, C.M., and Best, J. (1989). Ocular dominance plasticity in adult cat visual cortex after transplantation of cultured astrocytes. *Nature 342*(6248), 427-430. doi: 10.1038/342427a0.

Müller, C.M. (1990). Dark-rearing retards the maturation of astrocytes in restricted layers of cat visual cortex. *Glia 3*(6), 487-494. doi: 10.1002/glia.440030607.

Nagai, J., Yu, X., Papouin, T., Cheong, E., Freeman, M.R., Monk, K.R., Hastings, M.H., Haydon, P.G., Rowitch, D., Shaham, S., and Khakh, B.S. (2021). Behaviorally consequential astrocytic regulation of neural circuits. *Neuron 109*(4), 576–596. doi: 10.1016/j.neuron.2020.12.008.

Nakadate, K., Imamura, K., and Watanabe, Y. (2001). Effects of monocular deprivation on the expression pattern of alpha-1 and beta-1 adrenergic receptors in the kitten visual cortex. *Neurosci. Res. 40*(2), 155-162. doi: 10.1016/s0168-0102(01)00224-3.

Nakadate, K., Imamura, K., and Watanabe, Y. (2006). Cellular and subcellular localization of alpha-1 adrenoceptors in the rat visual cortex. *Neuroscience 141*(4), 1783-1792. doi: 10.1016/j.neuroscience.2006.05.031.

Navarrete, M., Díez, A., and Araque, A. (2014). Astrocytes in endocannabinoid signalling. *Philos. Trans. R. Soc. Lond., B, Biol. Sci. 369*(1654), 20130599. doi: 10.1098/rstb.2013.0599

Newman, E.A. (2001). Propagation of intercellular calcium waves in retinal astrocytes and Müller cells. *J. Neurosci. 21*(7), 2215-2223. doi: 10.1523/JNEUROSCI.21-07-02215.2001.

Newman, E.A. (2005). Calcium increases in retinal glial cells evoked by light-induced neuronal activity. *J. Neurosci. 25*(23), 5502-5510. doi: 10.1523/JNEUROSCI.1354-05.2005.

Oe, Y., Wang, X., Patriarchi, T., Konno, A., Ozawa, K., Yahagi, K., Hirai, H., Tsuboi, T., Kitaguchi, T., Tian, L., McHugh, T.J., and Hirase, H. (2020). Distinct temporal integration of noradrenaline signaling by astrocytic second messengers during vigilance. *Nat. Commun*. *11*(1), 471. doi: 10.1038/s41467-020-14378-x.

Parnavelas, J.G., Luder, R., Pollard, S.G., Sullivan, K., and Lieberman, A.R. (1983). A qualitative and quantitative ultrastructural study of glial cells in the developing visual cortex of the rat. *Philos. Trans. R. Soc. Lond. B. Biol. Sci*. *301*(1103), 55-84. doi: 10.1098/rstb.1983.0022.

Pascual, O., Casper, K.B., Kubera, C., Zhang, J., Revilla-Sanchez, R., Sul, J.Y., Takano, H., Moss, S.J., McCarthy, K., and Haydon, P.G. (2005). Astrocytic purinergic signaling coordinates synaptic networks. *Science 310*(5745), 113-116. doi: 10.1126/science.1116916.

Paukert, M., Agarwal, A., Cha, J., Doze, V.A., Kang, J.U., and Bergles, D.E. (2014). Norepinephrine controls astroglial responsiveness to local circuit activity. *Neuron 82*(6), 1263-1270. doi: 10.1016/j.neuron.2014.04.038.

Perea, G., Yang, A., Boyden, E.S., and Sur, M. (2014). Optogenetic astrocyte activation modulates response selectivity of visual cortex neurons in vivo. *Nat. Commun. 5*, 3262. doi: 10.1038/ncomms4262.

Philips, R.T., Sur, M., and Chakravarthy, V.S. (2017). The influence of astrocytes on the width of orientation hypercolumns in visual cortex: A computational perspective. *PLoS Comput. Biol. 13*(10), e1005785. doi: 10.1371/journal.pcbi.1005785.

Pratt, K. G., Hiramoto, M., and Cline, H. T. (2016). An Evolutionarily Conserved Mechanism for Activity-Dependent Visual Circuit Development. *Front. Neural Circuits 10*, 79. doi: 10.3389/fncir.2016.00079.

Ribot, J., Breton, R., Calvo, C.F., Moulard, J., Ezan, P., Zapata, J., Samama, K., Moreau, M., Bemelmans, A.P., Sabatet, V., Dingli, F., Loew, D., Milleret, C., Billuart, P., Dallérac, G., and

Rouach, N. (2021). Astrocytes close the mouse critical period for visual plasticity. *Science 373*(6550), 77-81. doi: 10.1126/science.abf5273.

Rosa, J.M., Bos, R., Sack, G.S., Fortuny, C., Agarwal, A., Bergles, D.E., Flannery, J.G., and Feller, M.B. (2015). Neuron-glia signaling in developing retina mediated by neurotransmitter spillover. *Elife 4*, e09590. doi: 10.7554/eLife.09590.

Rowe, S.J., Messenger, N.J., and Warner, A.E. (1993). The role of noradrenaline in the differentiation of amphibian embryonic neurons. *Development 119*(4), 1343-1357. doi: 10.1242/dev.119.4.1343.

Ryczko, D., Hanini-Daoud, M., Condamine, S., Bréant, B.J.B., Fougère, M., Araya, R., and Kolta, A. (2021). S100β-mediated astroglial control of firing and input processing in layer 5 pyramidal neurons of the mouse visual cortex. *J. Physiol. 599*(2), 677-707. doi: 10.1113/JP280501.

Schecter, R.W., Maher, E.E., Welsh, C.A., Stevens, B., Erisir, A., and Bear, M.F. (2017). Experience-Dependent Synaptic Plasticity in V1 Occurs without Microglial CX3CR1. *J. Neurosci. 37*(44), 10541-10553. doi: 10.1523/JNEUROSCI.2679-16.2017.

Schummers, J., Yu, H., and Sur, M. (2008). Tuned responses of astrocytes and their influence on hemodynamic signals in the visual cortex. *Science 320*(5884), 1638-1643. doi: 10.1126/science.1156120.

Sharma, P., and Cline, H.T. (2010). Visual Activity Regulates Neural Progenitor Cells in Developing Xenopus CNS through Musashi1. *Neuron 68*(3), 442-455. doi: 10.1016/j.neuron.2010.09.028.

Sild, M., Van Horn, M.R., Schohl, A., Jia, D., and Ruthazer, E.S. (2016). Neural activity-dependent regulation of radial glial filopodial motility is mediated by glial cGMp-dependent protein kinase 1 and contributes to synapse maturation in the developing visual system. *J. Neurosci. 36*(19), 5279-5288. doi: 10.1523/JNEUROSCI.3787-15.2016.

Singh, S.K., Stogsdill, J.A., Pulimood, N.S., Dingsdale, H., Kim, Y.H., Pilaz, L.J., Kim, I.H., Manhaes, A.C., Rodrigues, W.S. Jr., Pamukcu, A., Enustun, E., Ertuz, Z., Scheiffele, P., Soderling, S.H., Silver, D.L., Ji, R.R., Medina, A.E., and Eroglu, C. (2016). Astrocytes Assemble Thalamocortical Synapses by Bridging NRX1α and NL1 via Hevin. *Cell 164*(1-2), 183-196. doi: 10.1016/j.cell.2015.11.034.

Sipe, G.O., Lowery, R.L., Tremblay, M.È., Kelly, E.A., Lamantia, C.E., and Majewska, A.K. (2016). Microglial P2Y12 is necessary for synaptic plasticity in mouse visual cortex. *Nat. Commun. 7*, 10905. doi: 10.1038/ncomms10905.

Sipe, G.O., Petravicz, J., Rikhye, R.V., Garcia, R., Mellios, N., and Sur, M. (2021). Astrocyte glutamate uptake coordinates experience-dependent, eye-specific refinement in developing visual cortex. *Glia 69*(7), 1723-1735. doi: 10.1002/glia.23987.

Slezak, M., Grosche, A., Niemiec, A., Tanimoto, N., Pannicke, T., Münch, T.A., Crocker, B., Isope, P., Härtig, W., Beck, S.C., Huber, G., Ferracci, G., Perraut, M., Reber, M., Miehe, M., Demais, V., Lévêque, C., Metzger, D., Szklarczyk, K., Przewlocki, R., Seeliger, M.W., Sage-Ciocca, D., Hirrlinger, J., Reichenbach, A., Reibel, S., and Pfrieger, F.W. (2012). Relevance of exocytotic glutamate release from retinal glia. *Neuron 74*(3), 504-516. doi: 10.1016/j.neuron.2012.03.027.

Slezak, M., Kandler, S., Van Veldhoven, P.P., Van den Haute, C., Bonin, V., Holt, M.G. (2019). Distinct mechanisms for visual and motor-related astrocyte responses in mouse visual cortex. *Curr. Biol. 29*(18), 3120-3127. doi: 10.1016/j.cub.2019.07.078.

Somaiya, R.D., Huebschman, N.A., Chaunsali, L., Sabbagh, U., Carrillo, G.L., Tewari, B.P., and Fox, M.A. (2021). Development of astrocyte morphology and function in mouse visual thalamus. *J. Comp. Neurol. 530*(7), 945-962. doi: 10.1002/cne.25261.

Sonoda, K., Matsui, T., Bito, H., and Ohki, K. (2018). Astrocytes in the mouse visual cortex reliably respond to visual stimulation. *Biochem. Biophys. Res. Commun. 505*(4), 1216-1222. doi: 10.1016/j.bbrc.2018.10.027.

Stevens, B., Allen, N.J., Vazquez, L.E., Howell, G.R., Christopherson, K.S., Nouri, N., Micheva, K.D., Mehalow, A.K., Huberman, A.D., Stafford, B., Sher, A., Litke, A.M., Lambris, J.D.,

Smith, S.J., John, S.W., and Barres, B.A. (2007). The classical complement cascade mediates CNS synapse elimination. *Cell 131*(6), 1164-1178. doi: 10.1016/j.cell.2007.10.036.

Stobart, J.L., Ferrari, K.D., Barrett, M.J.P., Glück, C., Stobart, M.J., Zuend, M., and Weber, B. (2018). Cortical Circuit Activity Evokes Rapid Astrocyte Calcium Signals on a Similar Timescale to Neurons. *Neuron 98*(4), 726-735. doi: 10.1016/j.neuron.2018.03.050.

Stowell, R.D., Sipe, G.O., Dawes, R.P., Batchelor, H.N., Lordy, K.A., Whitelaw, B.S., Stoessel, M.B., Bidlack, J.M., Brown, E., Sur, M., and Majewska, A.K. (2019). Noradrenergic signaling in the wakeful state inhibits microglial surveillance and synaptic plasticity in the mouse visual cortex. *Nat. Neurosci. 22*(11), 1782-1792. doi: 10.1038/s41593-019-0514-0.

Su, J., Charalambakis, N.E., Sabbagh, U., Somaiya, R.D., Monavarfeshani, A., Guido, W., and Fox, M.A. (2020). Retinal inputs signal astrocytes to recruit interneurons into visual thalamus. *Proc. Natl. Acad. Sci. U.S.A. 117*(5), 2671-2682. doi: 10.1073/pnas.1913053117.

Tan, Z., Liu, Y., Xi, W., Lou, H.F., Zhu, L., Guo, Z., Mei, L., and Duan, S. (2017). Glia-derived ATP inversely regulates excitability of pyramidal and CCK-positive neurons. *Nat. Commun. 8*, 13772. doi: 10.1038/ncomms13772.

Temizer, I., Donovan, J.C., Baier, H., and Semmelhack, J.L. (2015). A Visual Pathway for Looming-Evoked Escape in Larval Zebrafish. *Curr. Biol. 25*, 1823-1834. doi: 10.1016/j.cub.2015.06.002.

Tremblay, M., Fugère, V., Tsui, J., Schohl, A., Tavakoli, A., Travençolo, B.A., Costa Lda, F., and Ruthazer, E.S. (2009). Regulation of radial glial motility by visual experience. *J. Neurosci. 29*(45), 14066-14076. doi: 10.1523/JNEUROSCI.3542-09.2009.

Tremblay, M.È., Lowery, R.L., Majewska, A.K. (2010). Microglial interactions with synapses are modulated by visual experience. *PLoS Biol. 8*(11), e1000527. doi: 10.1371/journal.pbio.1000527.

Tremblay, M.È., Zettel, M.L., Ison, J.R., Allen, P.D., and Majewska, A.K. (2012). Effects of aging and sensory loss on glial cells in mouse visual and auditory cortices. *Glia 60*(4), 541-558. doi: 10.1002/glia.22287.

Tworig, J.M., Coate, C., and Feller, M.B. (2021). Excitatory neurotransmission activates compartmentalized calcium transients in Müller glia without affecting lateral process motility. *Elife 10*, e73202. doi: 10.1101/2021.09.02.458760.

Ullian, E.M., Sapperstein, S.K., Christopherson, K.S., and Barres, B.A. (2001). Control of synapse number by glia. *Science 291*(5504), 657-661. doi: 10.1126/science.291.5504.657.

Van Horn, M. R., Benfey, N. J., Shikany, C., Severs, L. J., and Deemyad, T. (2021). Neuron-astrocyte networking: astrocytes orchestrate and respond to changes in neuronal network activity across brain states and behaviors. *J. Neurophysiol. 126*(2), 627–636. doi: 10.1152/jn.00062.2021.

Van Horn, M.R., Strasser, A., Miraucourt, L.S., Pollegioni, L., and Ruthazer, E.S. (2017). The Gliotransmitter D-Serine Promotes Synapse Maturation and Axonal Stabilization In Vivo. *J. Neurosci. 37*(26), 6277-6288. doi: 10.1523/JNEUROSCI.3158-16.2017.

Wang, J., O'Sullivan, M.L., Mukherjee, D., Puñal, V.M., Farsiu, S., and Kay, J.N. (2017). Anatomy and spatial organization of Müller glia in mouse retina. *J. Comp. Neurol. 525*(8), 1759-1777. doi: 10.1002/cne.24153.

Wang, L.L., Xu, D., Luo, Y., Li, X., Gu, Y., and Wang, L. (2021). Homeostatic Regulation of Astrocytes by Visual Experience in the Developing Primary Visual Cortex. *Cereb. Cortex 32*(5), 970-986. doi: 10.1093/cercor/bhab259.

Wang, X., Zhao, L., Zhang, J., Fariss, R.N., Ma, W., Kretschmer, F., Wang, M., Qian, H.H., Badea, T.C., Diamond, J.S., Gan, W.B., Roger, J.E., and Wong, W.T. (2016). Requirement for Microglia for the Maintenance of Synaptic Function and Integrity in the Mature Retina. *J. Neurosci. 36*(9), 2827-2842. doi: 10.1523/JNEUROSCI.3575-15.2016.

Wu, G. Y., and Cline, H. T. (1998). Stabilization of dendritic arbor structure in vivo by CaMKII. *Science*, *279*(5348), 222–226. doi: 10.1126/science.279.5348.222

Zhang, R.W., Du, W.J., Prober, D.A., and Du, JL. (2019). Müller Glial Cells Participate in Retinal Waves via Glutamate Transporters and AMPA Receptors. *Cell Rep. 27*(10), 2871-2880. doi: 10.1016/j.celrep.2019.05.011.

Zhang, X., Zhaoping, L., Zhou, T., and Fang, F. (2012). Neural activities in v1 create a bottom-up saliency map. *Neuron 73*(1), 183-192. doi: 10.1016/j.neuron.2011.10.035.

Zhang, Y., Zhao, L., Wang, X., Ma, W., Lazere, A., Qian, H.H., Zhang, J., Abu-Asab, M., Fariss, R.N., Roger, J.E., and Wong, W.T. (2018). Repopulating retinal microglia restore endogenous organization and function under CX3CL1-CX3CR1 regulation. *Sci. Adv. 4*(3), eaap8492. doi: 10.1126/sciadv.aap8492.

Copyright Statements